

High Mountain Echiniscid (Heterotardigrada) Fauna of Taiwan

Piotr Gąsiorek^{1,*}, Katarzyna Vončina¹, Reinhardt Møbjerg Kristensen², and Łukasz Michalczyk¹

¹Department of Invertebrate Evolution, Institute of Zoology and Biomedical Research, Faculty of Biology, Jagiellonian University, Gronostajowa 9, 30-387 Kraków, Poland. *Correspondence: E-mail: piotr.lukas.gasiorek@gmail.com (Gąsiorek).

E-mail: kat.von@onet.eu (Vončina); lm@tardigrada.net (Michalczyk)

²Natural History Museum of Denmark, University of Copenhagen, Universitetsparken 15, DK-2100 Copenhagen, Denmark.
E-mail: rmkristensen@snm.ku.dk (Kristensen)

Received 3 August 2021 / Accepted 13 September 2021 / Published 13 December 2021
Communicated by Daniel Stec

Taiwan lies at the transitional zone between the East Palaearctic and Oriental regions, which translates into both Palaearctic and Indomalayan taxa being present on the island. Furthermore, large habitat heterogeneity and high mountains contributed to the rise of conditions favouring allopatric speciation and the emergence of endemic species. The tardigrade fauna of Taiwan is poorly studied, and the aim of this contribution is to provide new data on the members of the family Echiniscidae, the largest limno-terrestrial group of the class Heterotardigrada, found at high elevations in central Taiwan. We report 11 species grouped in 5 genera: *Claxtonia* (1 species), *Echiniscus* (3 species), *Hypechiniscus* (1 species), *Nebularmis* (2 species), and *Pseudechiniscus* (4 species). All are new to Taiwan, including 5 species that are new to science, 4 of which are described herein by means of integrative taxonomy: *Hypechiniscus crassus* sp. nov. (the *exarmatus* morphogroup), *Pseudechiniscus (Meridioniscus) dreyeri* sp. nov., *Pseudechiniscus (Pseudechiniscus) formosus* sp. nov., and *Pseudechiniscus (Pseudechiniscus) totoro* sp. nov. The new findings also help to clarify the description of *Echiniscus clevelandi* Beasley, 1999, and supplement the phylogenies of the *Echiniscus virginicus* complex and of the genera *Hypechiniscus*, *Nebularmis* and *Pseudechiniscus*.

Key words: Biogeography, Endemism, Integrative taxonomy, Oriental, Palaearctic, Phylogeny.

BACKGROUND

Taiwan is a large continental island separated from mainland Asia by the Taiwan Strait. The biogeographic history of Taiwan has been a subject of intense research because of the transitional character of its fauna, which comprises both East Palaearctic and Oriental (Indomalayan) taxa (Päckert et al. 2012; He et al. 2018). The mixed origin of the Taiwanese fauna, coupled with numerous isolated habitats in Taiwanese mountains that favoured speciation (Shih et al. 2006), led to the emergence of endemic biota (e.g., Yu 1995).

Considering the potential significance in

unravelling biodiversity and biogeographic patterns, not enough attention has been paid to the tardigrade fauna of Taiwan. There are only three reports from the 20th century (Mathews 1936–37; Ito 1990; Séméria 1994), followed by four works from the current century (Li and Li 2008; Yin and Li 2011; Gąsiorek et al. 2019a b). Out of the eight Taiwanese echiniscid records, only four can be considered trustworthy: *Echiniscus lineatus* Pilato et al., 2008a, *Kristenseniscus tessellatus* (Murray, 1910), *Stellariscus pseudelegans* (Séméria, 1994), and *Viridiscus perviridis* (Ramazzotti, 1959). The remaining four records are most likely misidentifications in the light of present taxonomic knowledge: *Pseudechiniscus*

(*P. facettalis* Petersen, 1951 and *Pseudechiniscus* (*P.*) *suillus* (Ehrenberg, 1853) (see the criticism of their historical records in Grobys et al. 2020), *Echiniscus spinulosus* (Doyère, 1840) (this West Palaearctic species represents a species complex and it also exhibits one of the most common chaetotaxy morphotypes within *Echiniscus*, making the verification of older records virtually impossible), and *Viridiscus viridis* (Murray, 1910) (see the criticism of its historical records in Pilato et al. 2008b). Such a low reported species richness signifies that a large fraction of Taiwanese echiniscid species diversity remains unknown.

Therefore, in order to widen our knowledge on the tardigrade fauna of this biogeographically important region, we analysed mixed moss and lichen samples collected at high elevations in Taiwanese mountains. The material contained numerous echiniscid species, including species new to science. All taxa were analysed under phase contrast microscope (PCM) and, if found in sufficiently high numbers, sequenced (DNA barcoding of five genetic markers). Some of them were additionally observed with a scanning electron

microscope (SEM). The genetic data were used in new phylogeny reconstructions of the *Echiniscus virginicus* group, and of the genera *Hypechiniscus*, *Nebularmis* and *Pseudechiniscus*. Our analyses contribute to a better understanding of Taiwanese tardigrade fauna and the biogeographic origin of some of its representatives.

MATERIALS AND METHODS

Sample collection, animal preparation and microscopy

Animals were extracted from seven Taiwanese moss samples (collected by Niklas Dreyer) and an additional Japanese (collected by Szymon Bacher) moss sample (Table 1) according to standard protocols (Dastyk 1980; Stec et al. 2015). Isolated specimens were used for the following analyses: (I) imaging in phase contrast microscopy – PCM (morphology and morphometry), (II) imaging in scanning electron microscopy – SEM (ultrastructure), and (III) DNA

Table 1. List of examined samples and identified tardigrade species

Sample code	Coordinates and altitude	Locality	Species	Collection date
JP.009	35°24'27"N 139°09'56"E 338 m asl	Japan, Kanagawa Prefecture, Tanzawa Mountains, Tanodotoke trail	<i>Echiniscus hoonsooi</i>	17.12.2017
TW.004	24°23'00"N 121°13'48"E 3 000 m asl	Taiwan, Snow Mountain (Xueshan)	EMPTY	17.01.2019
TW.005	24°23'18"N 121°15'39"E 3 200 m asl	Taiwan, Snow Mountain (Xueshan), East Peak	<i>Echiniscus clevelandi</i> <i>Hypechiniscus crassus</i> sp. nov. <i>Pseudechiniscus dreyeri</i> sp. nov. <i>Pseudechiniscus totoro</i> sp. nov.	10.02.2020
TW.006	24°23'18"N 121°15'39"E 3 200 m asl	Taiwan, Snow Mountain (Xueshan), East Peak	<i>Echiniscus clevelandi</i> <i>Hypechiniscus crassus</i> sp. nov.	10.02.2020
TW.007	24°23'51"N 121°14'04"E 3 700 m asl	Taiwan, Snow Mountain (Xueshan), North Peak	<i>Claxtonia</i> sp. nov. <i>Echiniscus blumi</i> <i>Echiniscus clevelandi</i> <i>Nebularmis reticulatus</i> <i>Pseudechiniscus formosus</i> sp. nov.	10.02.2020
TW.008	24°23'51"N 121°14'04"E 3 700 m asl	Taiwan, Snow Mountain (Xueshan), North Peak	<i>Echiniscus clevelandi</i> <i>Hypechiniscus crassus</i> sp. nov. <i>Nebularmis crebraclava</i> <i>Pseudechiniscus dreyeri</i> sp. nov.	10.02.2020
TW.009	24°23'51"N 121°14'04"E 3 700 m asl	Taiwan, Snow Mountain (Xueshan), North Peak	<i>Echiniscus blumi</i> <i>Echiniscus semifoveolatus</i> <i>Nebularmis reticulatus</i>	10.02.2020
TW.010	24°10'51"N 121°18'36"E 2°500 m asl	Taiwan, Joy Mountain (Hehuanshan)	<i>Pseudechiniscus ehrenbergi</i>	31.12.2020

sequencing. Specimens for PCM were mounted on microscope slides in Hoyer's medium and secured with cover slips. Slides were examined under an Olympus BX53 PCM associated with an Olympus DP74 digital camera. Specimens for SEM were processed in accordance with the protocol from Stec et al. (2015) and examined under high vacuum in a Versa 3D DualBeam SEM at the ATOMIN facility of the Jagiellonian University. All figures were assembled in Corel Photo-Paint X8. A stack of 2–10 images were taken with an equidistance of ca. 0.1 μm for some structures and assembled manually into a single deep-focus image in Corel.

Morphometry and terminology

All measurements were made under $\times 1000$ magnification with immersion oil and are given either in micrometres (μm) or as relative values presented in the text in italics (*sp* – the ratio between a length of a given structure and the scapular plate length; Dastych 1999). Structures were measured only if suitably oriented, undamaged and untwisted. Body length was measured from the anterior extremity to the end of the body, excluding the hind legs. Morphological terminology follows Kristensen (1987) with subsequent modifications introduced in Gąsiorek et al. (2019a 2021a b c). Body appendages are all appendages in lateral, dorsolateral and dorsal positions (*i.e.*, *A*, *B*, *C*, *D* and *E*), whereas trunk appendages exclude appendages *A*, which are situated at the border of head and trunk. Morphometric data were handled using the “Echiniscoidea” ver. 1.4 template available from the Tardigrada Register (Michalczyk and Kaczmarek 2013). Raw morphometric data for analysed species are provided as supplementary materials (SM.1–5) and in the Tardigrada Register. Tardigrade taxonomy is presented in accordance with the latest edition of the checklist by Degma et al. (2021).

Genotyping

Individual DNA extractions were made from animals and cysts following a protocol by Casquet et al. (2012) modified in Stec et al. (2020). Hologenophores (Pleijel et al. 2008) were mounted on permanent slides for *post-hoc* observations. Five DNA fragments were sequenced: the small ribosome subunit (18S rRNA, nDNA), the large ribosome subunit (28S rRNA, nDNA), the internal transcribed spacers (ITS-1 and ITS-2, nDNA), and the cytochrome oxidase subunit I (*COI*, mtDNA). All fragments were amplified using the primers and PCR programmes listed in SM.6. Sequencing products were read with the ABI 3130xl

sequencer at the Molecular Ecology Lab, Institute of Environmental Sciences of the Jagiellonian University. Sequences were processed in BioEdit ver. 7.2.5 (Hall 1999) and submitted to GenBank (for the accession numbers please see RESULTS).

Phylogenetics

The sequences were aligned using the default settings of BioEdit (in the case of ITS and *COI*) and the Q-INS-I method (in the case of ribosomal markers: 18S rRNA, 28S rRNA) of MAFFT7 (Katoh et al. 2002; Katoh and Toh 2008) and manually checked against non-conservative alignments in BioEdit. All *COI* sequences were translated into protein sequences in MEGA7 (Kumar et al. 2016) to check against pseudogenes. Concatenation was done in SequenceMatrix (Vaidya et al. 2011). Details on the phylogenetic reconstructions for each specific dataset are provided below.

The *Echiniscus virginicus* complex

A dataset of ITS-1, ITS-2 and *COI* from Gąsiorek et al. (2020) was used. The final alignment length was 1725 bp. Using PartitionFinder v.2.1.1 (Lanfear et al. 2017) under the Bayesian information criterion (BIC), the best scheme of partitioning and substitution models for posterior phylogenetic analysis were chosen. The analysis was run to test all possible models implemented in MrBayes. As *COI* is a protein-coding gene, before partitioning, we divided our alignments of this marker into three data blocks constituting three separate codon positions. GTR+G was inferred to be the best-fit model for the first coding site of *COI* and a joined ITS-1+ITS-2 partition, GTR+I – for the second coding site of *COI*, and HKY+G – for the third coding site of *COI*. Bayesian inference (BI) marginal posterior probabilities were calculated using MrBayes v.3.2 (Ronquist and Huelsenbeck 2003). Random starting trees were used and the analysis was run for ten million generations, sampling the Markov chain every thousand generations. An average standard deviation of split frequencies of < 0.01 was used as a guide to ensure the two independent analyses had converged. The program Tracer v.1.6 (Rambaut et al. 2014) was then used to ensure that Markov chains had reached stationarity and to determine the correct ‘burn-in’ for the analysis, which was the first 10% of generations. The ESS values were greater than 200 and a consensus tree was obtained after summarizing the resulting topologies and discarding the ‘burn-in’. All final consensus trees were visualised by FigTree v.1.4.3, available from <http://tree.bio.ed.ac.uk/software/figtree>. The parameters and programmes were

identical in the latter datasets if not specified otherwise.

Hypechiniscus phylogeny

A dataset of 18S rRNA, 28S rRNA and ITS-1 from Gąsiorek et al. (2021a) was used. The final alignment length was 2363 bp. PartitionFinder indicated the following models for predefined partitions: TRN+I+G (18S rRNA), GTR+G (28S rRNA) and TVM+I (ITS-1). These models were used in BI reconstructions in MrBayes. ModelFinder (Kalyaanamoorthy et al. 2017) was used to choose the best-fit models for Maximum Likelihood (ML) analyses—K2P+I+G4 (18S rRNA), TVMe+G4 (28S rRNA) and K3Pu+F+I (ITS-1)—according to the Bayesian information criterion. W-IQ-TREE was used for ML reconstruction (Nguyen et al. 2015; Trifinopoulos et al. 2016). One thousand ultrafast bootstrap (UFBoot) replicates were applied to provide support values for branches (Hoang et al. 2018).

Nebularmis phylogeny and biogeography

A dataset of 18S rRNA, 28S rRNA, ITS-1 and ITS-2 from Gąsiorek et al. (2021b) was used. The final alignment length was 2825 bp. PartitionFinder indicated GTR+I+G for two separate partitions (18S rRNA + 28S rRNA and ITS-1 + ITS-2). The original concatenated matrix was analysed using BEAST (Drummond and Rambaut 2007). Four combinations of clock and tree priors were chosen and run in parallel, analogously to the analyses from Gąsiorek et al. (2021b): (a) a random local clock (Drummond and Suchard 2010) with the coalescent tree prior, (b) a random local clock with speciation: Yule process as the tree prior, (c) a strict clock (Ferreira and Suchard 2008) with the coalescent tree prior, and (d) a strict clock with speciation: Yule process as the tree prior. Tree searches were run for 10 million generations, sampling the tree every 1000 steps. The trees were summarized with TREEANNOTATOR software (distributed with BEAST), with the first 1000 trees removed. Tracer was then used to check the stationarity of Markov chains and determine the ‘burn-in’.

Consensus trees constructed from all datasets shared identical topologies (consistent with the variant b from Gąsiorek et al. 2021b). Consequently, the first 9000 trees were removed from the set of trees b, and the remaining 1000 trees were used in independent statistical dispersal-vicariance analyses (S-DIVA; Ronquist 1997; Yu et al. 2015), implemented in RASP (Yu et al. 2020), with phylogenetic uncertainty considered in the calculations. *Nebularmis* records were assigned to the zoogeographic realms (Ficetola et al. 2017) and records of *N. reticulatus* (Murray, 1905)

outside the Palaearctic were discarded as unreliable (Gąsiorek et al. 2019c 2021b). The maximum number of areas at a node was set to 3.

Pseudechiniscus phylogeny

A dataset of 18S rRNA, 28S rRNA and ITS-1 from Gąsiorek et al. (2021c) was used. The final alignment length was 2307 bp. PartitionFinder indicated GTR+I+G for all three partitions treated separately. These models were used in BI reconstructions in MrBayes. ModelFinder indicated the following models: SYM+I+G4 (18S rRNA), SYM+G4 (28S rRNA) and GTR+F+G4 (ITS-1). They were applied in ML reconstruction in W-IQ-TREE.

RESULTS

Taxonomic account

Phylum: Tardigrada Doyère, 1840
Class: Heterotardigrada Marcus, 1927
Order: Echiniscoidea Richters, 1926
Family: Echiniscidae Thulin, 1928
Genus: *Claxtonia* Gąsiorek & Michalczyk, 2019
in Gąsiorek et al. 2019a

***Claxtonia* sp. nov.**

(Fig. 1)

Material examined: One adult male (slide TW.007.21) with evident U-shaped, granulated subcephalic plates.

Remarks: The scarce material and the lack of DNA data prevent a formal description of this new species, most closely resembling the following *Claxtonia* species: *C. wendti* (Richters, 1903), *C. pardalis* (Degma & Schill, 2015), and *C. goni* Degma et al., 2021. However, in none of the aforementioned echiniscids were males recorded, and the new species differs from these species by minute differences in dorsal plate sculpturing. In the light of this discovery, the record of *C. wendti* from Hainan (Li et al. 2008), another continental island nearby the East Asian coast, is more likely to represent the new *Claxtonia* species than *C. wendti*.

Genus: *Echiniscus* C.A.S. Schultz, 1840
***Echiniscus blumi* Richters, 1903 sensu lato**

Material examined: 18 adult females on slides TW.007.20, TW.009.02–5. Three specimens from each sample were preserved for further molecular analyses.

Remarks: A cold stenothermic species, thus it is common in the Arctic, often inhabiting lower

elevations (< 1000 m asl) in the temperate zone, but in the tropical and subtropical zone found only at high altitudes (McInnes 1994). The still unsolved species discrimination within the *Echiniscus blumi-canadensis* complex (Guil and Giribet 2009) makes this a *sensu lato* record.

***Echiniscus clevelandi* Beasley, 1999**

(Figs. 2–9, Tables 2–4)

Material examined: 23 adult females, 15 adult males, and three juveniles on slides TW.005.06–7, TW.006.06, TW.007.19, TW.008.02–7, 12. Four specimens on SEM stub 21.07. Four specimens from the sample TW.008 were used for DNA sequencing, including two retrieved as hologenophores.

Amended description: Females (i.e., from the third instar onwards; measurements and statistics in Table 2): Body cylindrical to plump (Figs. 2, 4), orange to red with dark red eyes; body colour and eyes disappear soon after mounting in Hoyer's medium. *Echiniscus*-type cephalic papillae (secondary clavae) and (primary) clavae; cirri growing out from bulbous cirrophores (Fig. 8D). The body appendage configuration is *A-B-C-D-E*, with all trunk appendages formed as short and relatively thick, smooth cirri. Instances of asymmetry in chaetotaxy frequent (Fig. 2B), but only rarely are more than one appendage absent.

Dorsal plates with the mixed type of sculpturing typical for the *Echiniscus virginicus* complex, comprising an evident layer of large polygonal

endocuticular pillars visible as black dots under PCM (Figs. 2, 6), and a layer of dark uniform epicuticular matrix (Figs. 2A–B, 6A) pierced with large, often irregularly shaped pores (Figs. 2, 6). Epicuticle and pores are typically well-developed and identifiable in SEM (Figs. 4, 8A–C). Rarely, the pores are small and scarce (Figs. 2C, 5A, 6B, 8C). The cephalic plate is narrow and separated from the cervical (neck) plate by smooth cuticle. The cervical plate visible as a dark belt of minute pillars clearly distinct from the scapular plate. The scapular plate clearly smaller than the caudal (terminal) plate, with additional lateral sutures separating narrow trapezoidal lateral portions devoid of pores (Figs. 2, 6). Paired segmental plates divided into a smaller, much narrower anterior and a dominant posterior part by a smooth transverse stripe. Epicuticular ornamentation better developed in the central plate portions compared to the lateral parts. The caudal plate with short incisions and fully developed epicuticle. Median plates 1, 3 unipartite, whereas median plate 2 bipartite, its anterior portion is narrow, but with identical sculpturing as the posterior part. Ventral cuticle with minute endocuticular pillars covering the entire venter; a pair of subcephalic swellings (likely rudimentary plates, Fig. 8D) and a pair of rectangular genital plates present. Sexpartite gonopore placed between genital plates, and a trilobed anus between legs IV.

Pedal plates I–III extremely reduced and only rarely identifiable as aggregations of pillars in central leg portions (Fig. 6B), pedal plate IV developed as a sculptured cushion bearing a dentate collar with

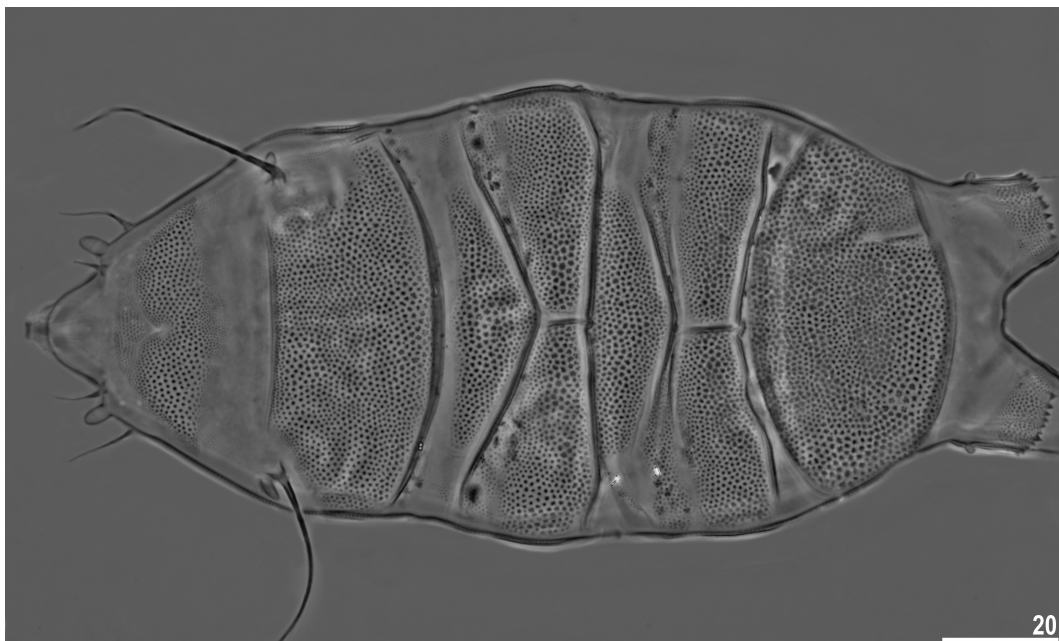


Fig. 1. Habitus of a male of a new, undescribed species of *Claxtonia* (PCM, dorsal view). Scale bar in μm .

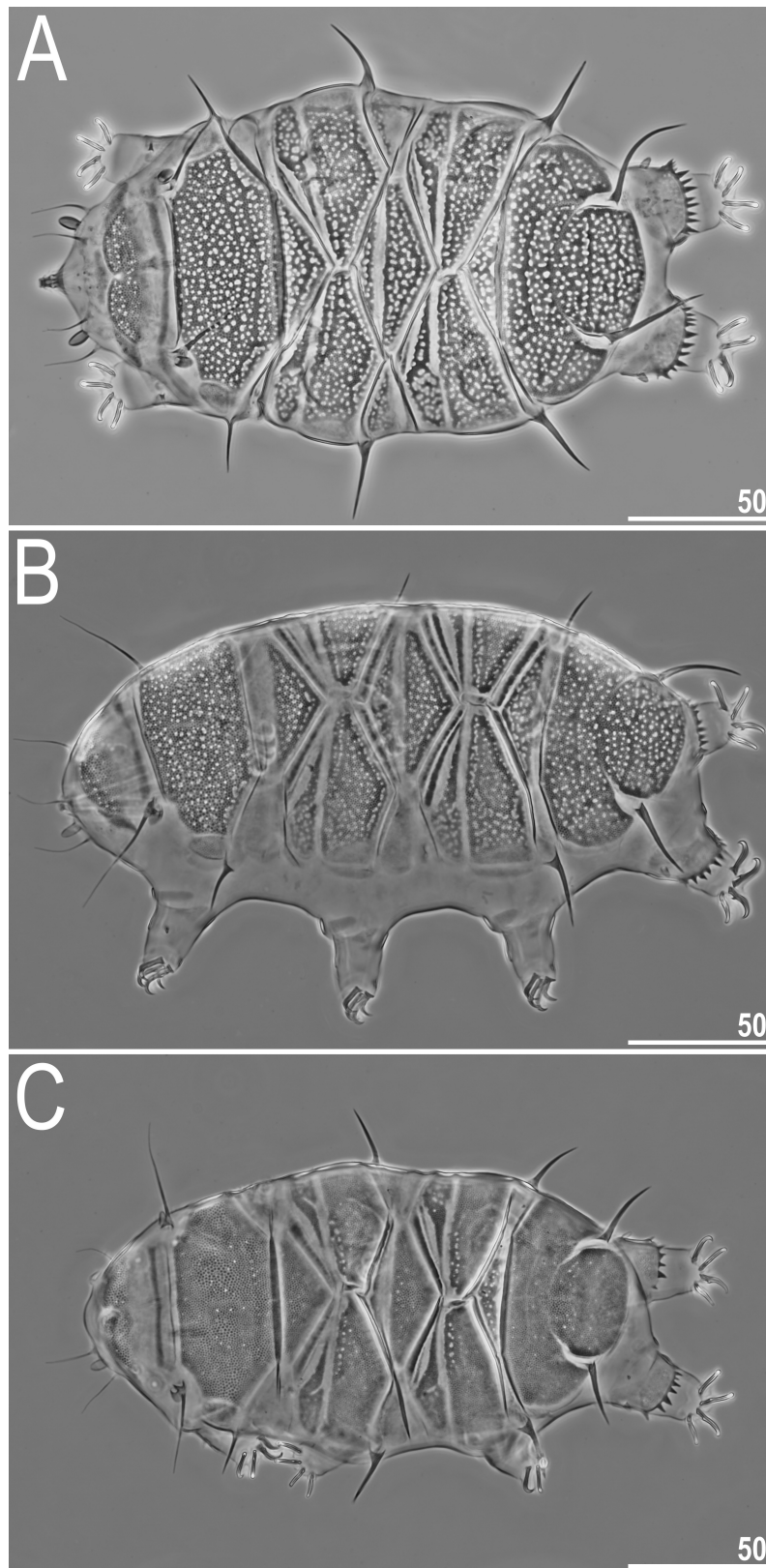


Fig. 2. Habitus of females of *Echiniscus clevelandi* (PCM): A, fully developed sculpturing and chaetotaxy (dorsal view); B, typical sculpturing and asymmetric lack of spine C (dorsolateral view); C, atypical sculpturing with poorly developed pores and full chaetotaxy (dorsal view). Scale bars in µm.

numerous teeth (Figs. 4, 6A, 8F). Pulvini present, but weakly visible (Fig. 2B). A small spine on leg I (Fig. 6) and a papilla on leg IV. Internal claws with identical large spurs on all legs (Figs. 8E–F, 9). Claws IV clearly higher than claws I–III (Table 2).

Buccal apparatus short, with a rigid, stout tube and a spherical pharynx. Stylet supports absent.

Males (i.e., from the third instar onwards; measurements and statistics in table 3): Sexual dimorphism poorly marked. Circular gonopore. Fully falling in the range of morphometric variability of females. Usually slightly slimmer than females (Fig. 3) and with fewer epicuticular pores (Figs. 3B, 5B, 7).

Juveniles (i.e., the second instar; measurements

and statistics in table 4): Gonopore absent. Smaller than sexually mature specimens of both sexes. Morphometric differences evident also in cephalic appendages and claw heights. Body appendage configuration *A-C-E*. Dorsal cuticle lacks epicuticular ornamentation.

Larvae: Not found.

Eggs: Two to three orange eggs per exuvia were found.

Molecular markers and phylogenetic position: Single haplotype was found in 18S rRNA (OK048609–10), ITS-1 (OK048639–40) and *COI* (OK047271–2), but two haplotypes were revealed in 28S rRNA (OK048627–8) and ITS-2 (OK048620–1), with minor intra-population *p*-distances (0.1–0.2%). We acquired

Table 2. Measurements [in μm] of selected morphological structures of the adult females of *E. clevelandi* mounted in Hoyer’s medium. N, number of specimens/structures measured; Range, refers to the smallest and the largest structure among all measured specimens; SD, standard deviation; *sp*, the proportion between the length of a given structure and the length of the scapular plate

Character	N	Range		Mean		SD	
		μm	<i>sp</i>	μm	<i>sp</i>	μm	<i>sp</i>
Body length	16	145–228	445–583	185	496	22	33
Scapular plate length	16	32.2–43.7	–	37.3	–	3.2	–
Head appendage lengths							
<i>Cirrus internus</i>	13	14.4–21.3	36.8–59.6	17.1	45.5	2.2	6.3
Cephalic papilla	16	6.5–8.6	16.7–23.9	7.3	19.7	0.7	2.1
<i>Cirrus externus</i>	15	15.0–23.1	40.5–63.0	18.3	49.3	2.1	5.9
Clava	15	4.7–6.8	14.4–18.2	5.9	15.9	0.5	1.1
<i>Cirrus A</i>	12	32.8–48.3	89.6–122.2	38.9	103.3	4.9	10.5
<i>Cirrus A</i> /Body length ratio	12	17%–24%	–	21%	–	2%	–
Body appendage lengths							
<i>Cirrus B</i>	16	11.9–21.4	31.6–53.8	17.0	45.5	2.9	6.8
<i>Cirrus C</i>	16	20.5–37.7	54.4–94.7	27.0	72.5	4.5	10.4
<i>Cirrus D</i>	16	21.9–35.3	57.0–88.7	26.3	70.5	3.6	9.0
<i>Cirrus E</i>	16	23.7–41.6	60.0–109.9	32.3	86.9	5.1	14.1
Spine on leg I length	16	2.4–4.5	7.3–11.5	3.2	8.6	0.5	1.2
Papilla on leg IV length	16	3.9–5.6	10.0–14.6	4.6	12.5	0.5	1.4
Number of teeth on the collar	15	5–15	–	10.4	–	2.4	–
Claw I heights							
Branch	16	8.8–11.7	23.8–31.1	10.1	27.1	0.7	2.2
Spur	13	1.9–2.4	4.6–7.5	2.1	5.7	0.2	0.7
Spur/branch height ratio	13	19%–24%	–	21%	–	2%	–
Claw II heights							
Branch	16	8.6–10.9	22.9–30.4	9.8	26.3	0.6	1.9
Spur	16	1.6–2.9	4.8–7.3	2.0	5.4	0.3	0.6
Spur/branch height ratio	16	18%–27%	–	21%	–	2%	–
Claw III heights							
Branch	16	8.8–11.1	23.8–29.2	9.9	26.5	0.7	1.7
Spur	14	1.6–3.0	4.6–7.5	2.1	5.5	0.3	0.8
Spur/branch height ratio	14	17%–27%	–	21%	–	2%	–
Claw IV heights							
Branch	15	10.9–13.4	28.6–38.8	12.1	32.5	0.8	2.6
Spur	4	2.4–3.7	6.4–9.3	3.0	8.1	0.6	1.2
Spur/branch height ratio	4	21%–29%	–	25%	–	3%	–

a set of all five markers (18S rRNA: OK048611, 28S rRNA: OK048629, ITS-1: OK048641, ITS-2: OK048622, *COI*: OK047273) also for one specimen of *E. hoonsooi* Moon & Kim, 1990, a species of similar phenotype (Fig. 10), previously reported from

Japan (Abe et al. 2000). The BI tree indicates that *E. clevelandi* and *E. hoonsooi* are sister species, and constitute a sister clade to the *E. lineatus* + *E. virginicus* Riggan, 1962 clade (Fig. 11; see also Gąsiorek et al. 2020).

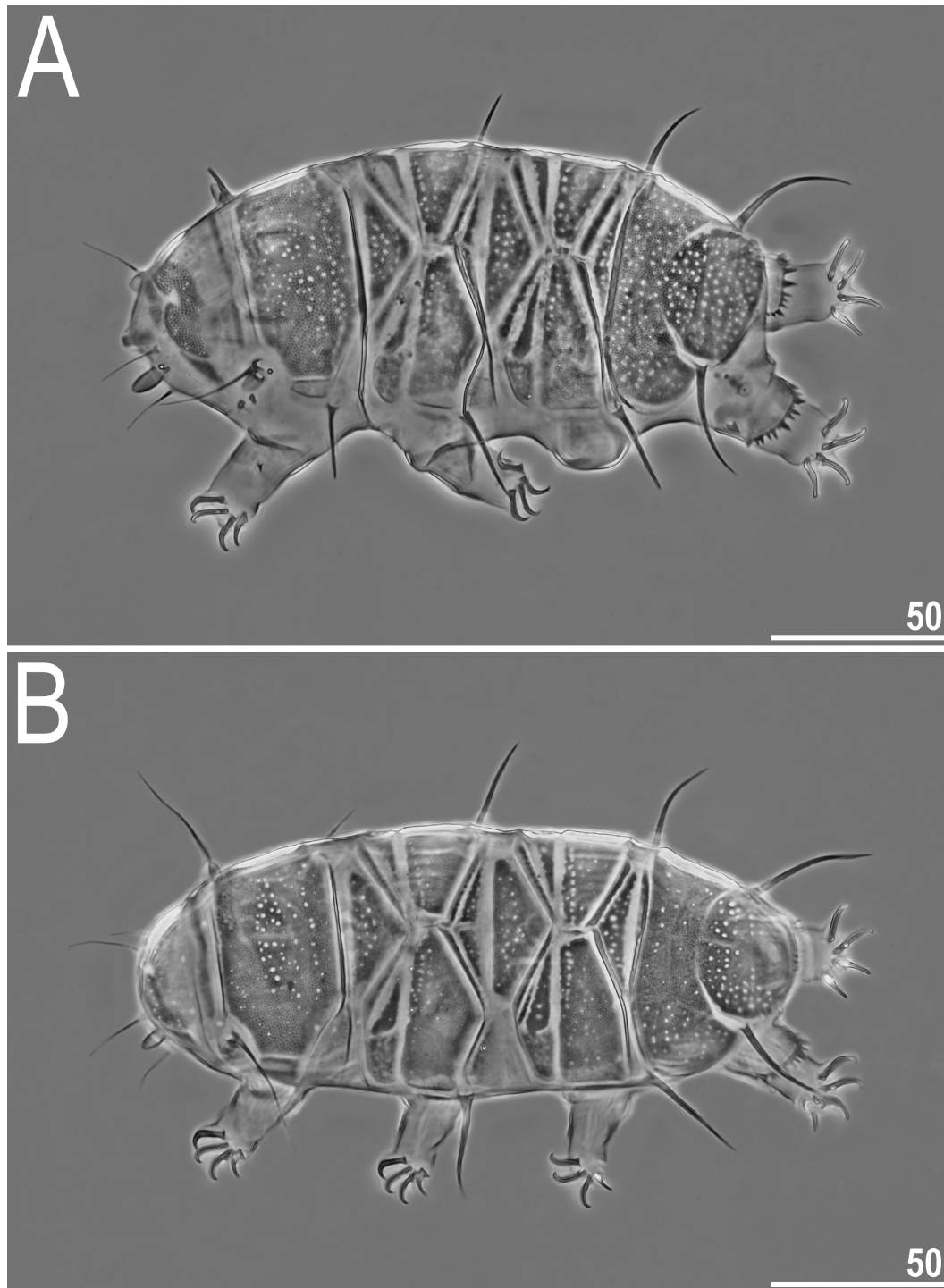


Fig. 3. Habitus of males of *Echiniscus clevelandi* (PCM): A, typical sculpturing (dorsolateral view); B, atypical sculpturing with poorly developed pores and asymmetric lack of spine B (dorsolateral view). Scale bars in µm.

Remarks: Taxonomy of the *virginicus* complex is scrutinised in table 5. The Taiwanese populations greatly broadened the range of intraspecific variability of *E. clevelandi* presented in the original description. Although Beasley (1999) specified that some type specimens lack dorsal appendages, this variant of chaetotaxy seems to be dominant in Taiwan. Therefore, the body appendage formula for the species is *A-B-C-(C^d)-D-(D^d)-E*. Moreover, the porosity of dorsal plates varies greatly between specimens, from highly porous with irregularly shaped pores (see fig. 4 in Beasley 1999 and Figs. 2–8C herein), through moderately porous with mostly round pores (Figs. 2–8C) to almost completely smooth plates with few small pores (Fig. 5A). If found

separately, these morphotypes could be identified as separate taxa, which underlines the importance of integrative analyses carried out on a considerable number of specimens in order to reduce the risk of taxonomic inflation.

Echiniscus semifoveolatus Ito, 1993

Material examined: One adult female on slide TW.009.01.

Remarks: A likely East Asian endemic species (Qiao et al. 2013; Suzuki 2017); rarely encountered, always in mountain locales.

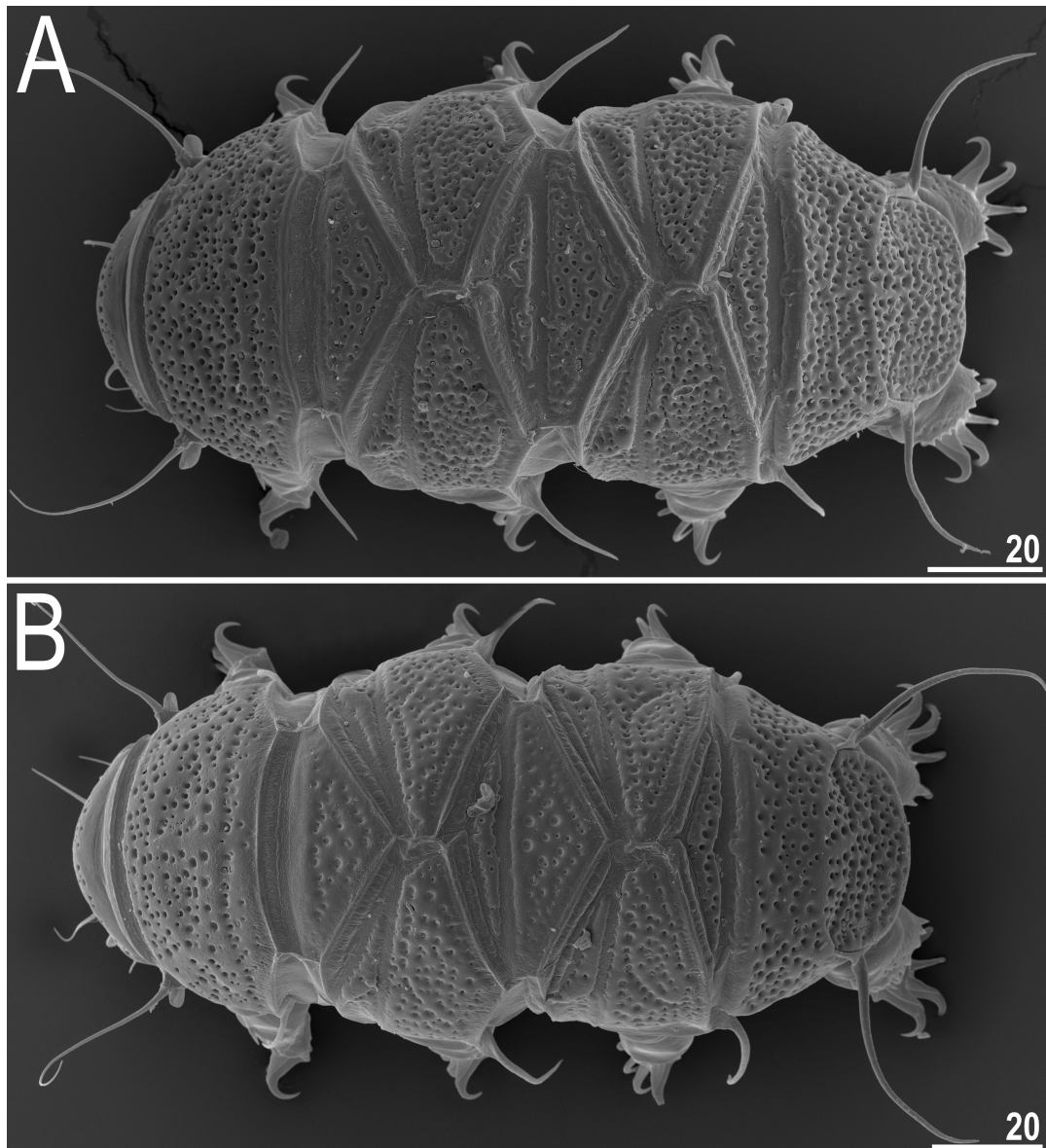


Fig. 4. Habitus of females of *Echiniscus clevelandi* with fully developed sculpturing (dorsal view, SEM). Scale bars in μm .

Genus: *Hypechiniscus* Thulin, 1928

***Hypechiniscus crassus* sp. nov.**

(Figs. 12–18, Tables 6–9)

urn:lsid:zoobank.org:act:F7750DD6-DE5C-4EFF-8EBB-4584FC140784

Tardigrada Register: www.tardigrada.net/register/0111.htm

Description: Females (i.e., from the third instar onwards; measurements and statistics in table 6): Body

plump (Figs. 12–13A, 14A), opalescent white before mounting in Hoyer’s medium. Large black eyes present (Fig. 12) but may dissolve during mounting (Fig. 13A). Dactyloid (elongated) clavae (Figs. 12, 15–16A); cephalic cirri with large cirrophores (Figs. 15–16A). *Cirrus dorsalis* absent.

Dorsal plate sculpturing of the *Pseudechiniscus* type, consisting of endocuticular pillars, which can be connected by *striae* in some plate portions (visible only under $\times 1000$ magnification, Figs. 15A, 16B). Epicuticular matrix forms ornamented pattern in

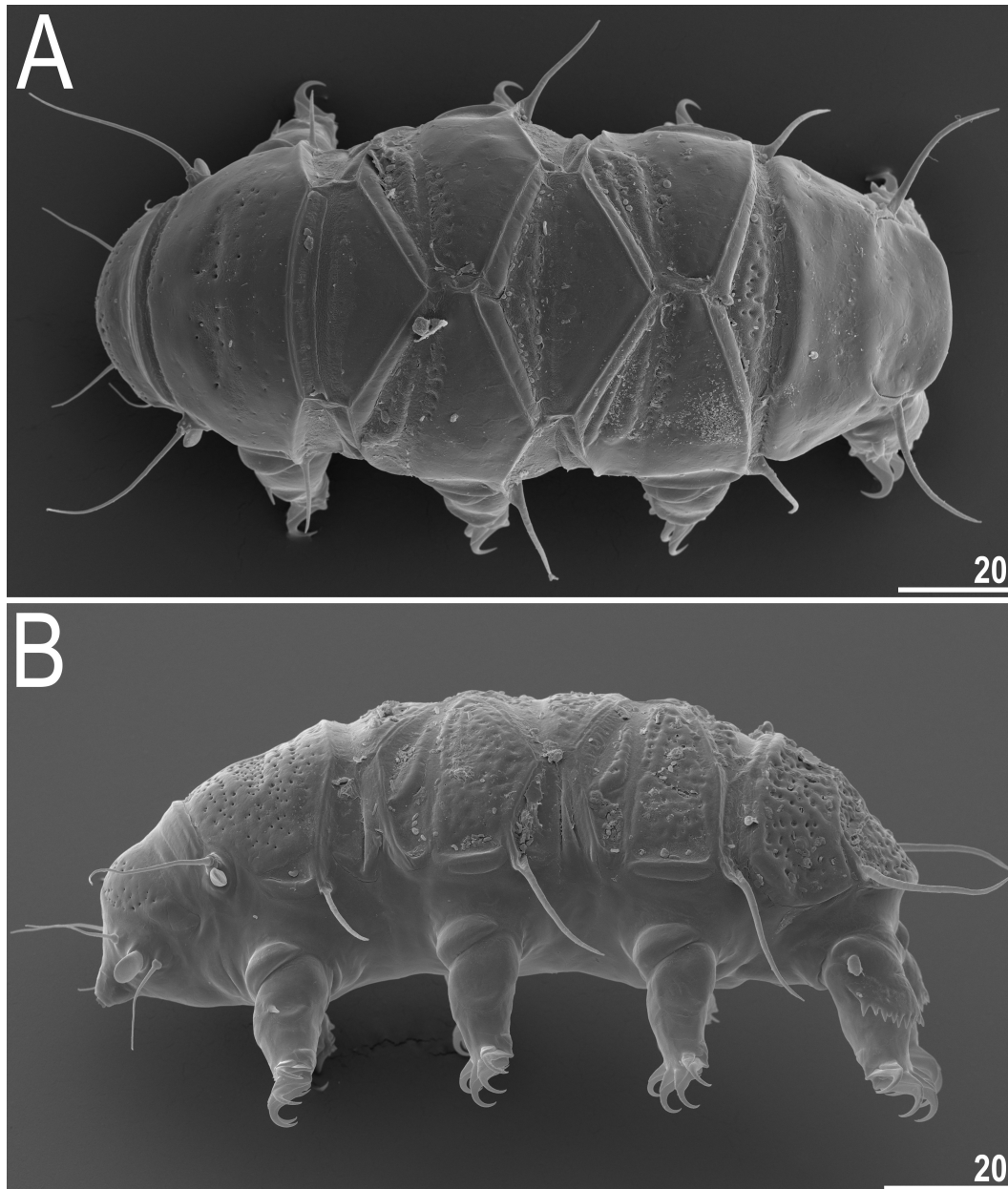


Fig. 5. Habitus of *Echiniscus clevelandi* (SEM): A, female with atypical sculpturing (dorsal view); B, male with poorly developed sculpturing (lateral view). Scale bars in μm .

all plates, overlapping with pillars. Cephalic plate hexapartite, with dominant trapezoidal posterolateral portions and a central rhomboidal portion; cervical plate adjacent to it and weakly delineated (Figs. 13A, 17A). Scapular plate divided in two portions by a central epicuticular ridge (Fig. 16B). Three median plates: m1–2 bipartite and m3 unipartite; m1 divided in two roughly similar portions by a transverse suture, identical suture divides m2, but its posterior portion is much reduced compared to the anterior, rhomboidal portion. Paired segmental plates I–II large, with no sutures or incisions. Five pairs of lateral supplementary plates

flanking the median plates (Fig. 17A). Caudal plate with two long, weakly sclerotised incisions (Figs. 13A, 14A, 15A, 17A).

Venter with evident species-specific sculpturing pattern (Figs. 15B, 17B) comprising overlapping belts of endocuticular pillars and epicuticular thickenings. Sexpartite gonopore placed between genital plates, and a trilobed anus between legs IV. Pedal plates in the form of aggregations of pillars in central leg portions (Fig. 15). Pulvini poorly delineated. Lacking papilla on leg I. Papilla IV small, but visible in PCM (Figs. 12, 14A, 15A). Curvature of claws typical for *Hypechiniscus*,

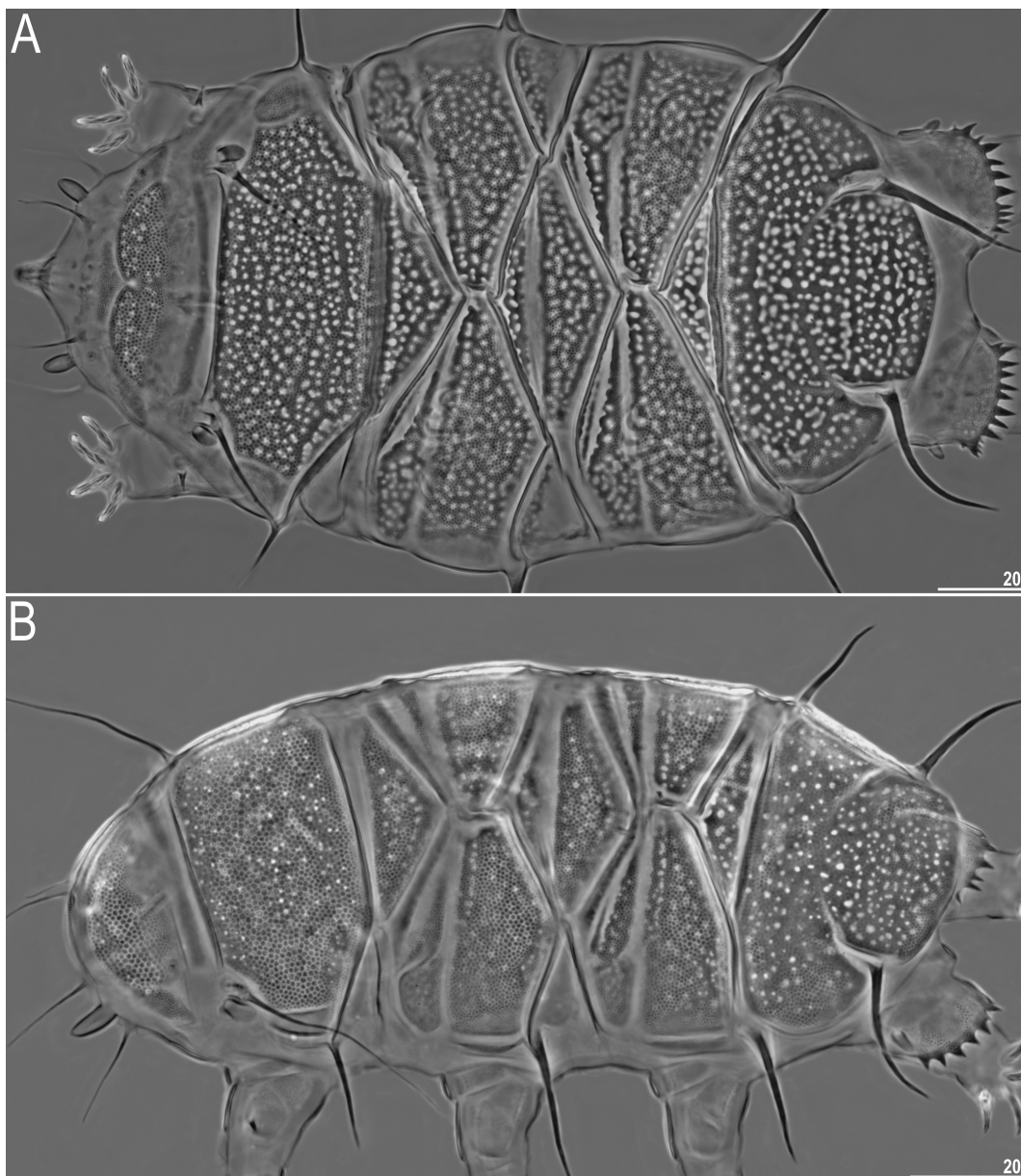


Fig. 6. Dorsal plate sculpturing of *Echiniscus clevelandi* (females, PCM). Scale bars in μm .

with strongly bent spurs on internal branches. Pseudoaccessory points present (Fig. 16C–D).

Males (*i.e.*, from the third instar onwards; measurements and statistics in table 7): Sexual dimorphism weakly marked. Males are only slightly slimmer (Figs. 13B, 14B) than large females. Qualitatively alike females, beside of the circular gonopore.

Juveniles (*i.e.*, the second instar; measurements and statistics in table 8): Qualitatively similar to adults. Gonopore absent. A clear morphometric gap between

juveniles and sexually mature individuals of both sexes.

Larvae (*i.e.*, the first instar; measurements and statistics in table 9): Gonopore and anus absent. Two-clawed individuals smaller than juveniles, but with a fully developed dorsal sculpturing and papilla IV visible in PCM (Fig. 18).

Eggs: Up to two pearly white eggs per exuvia were found.

Molecular markers and phylogenetic position: Single haplotype was found in 18S rRNA (OK048612–3) and 28S rRNA (OK048630–1) for both populations.

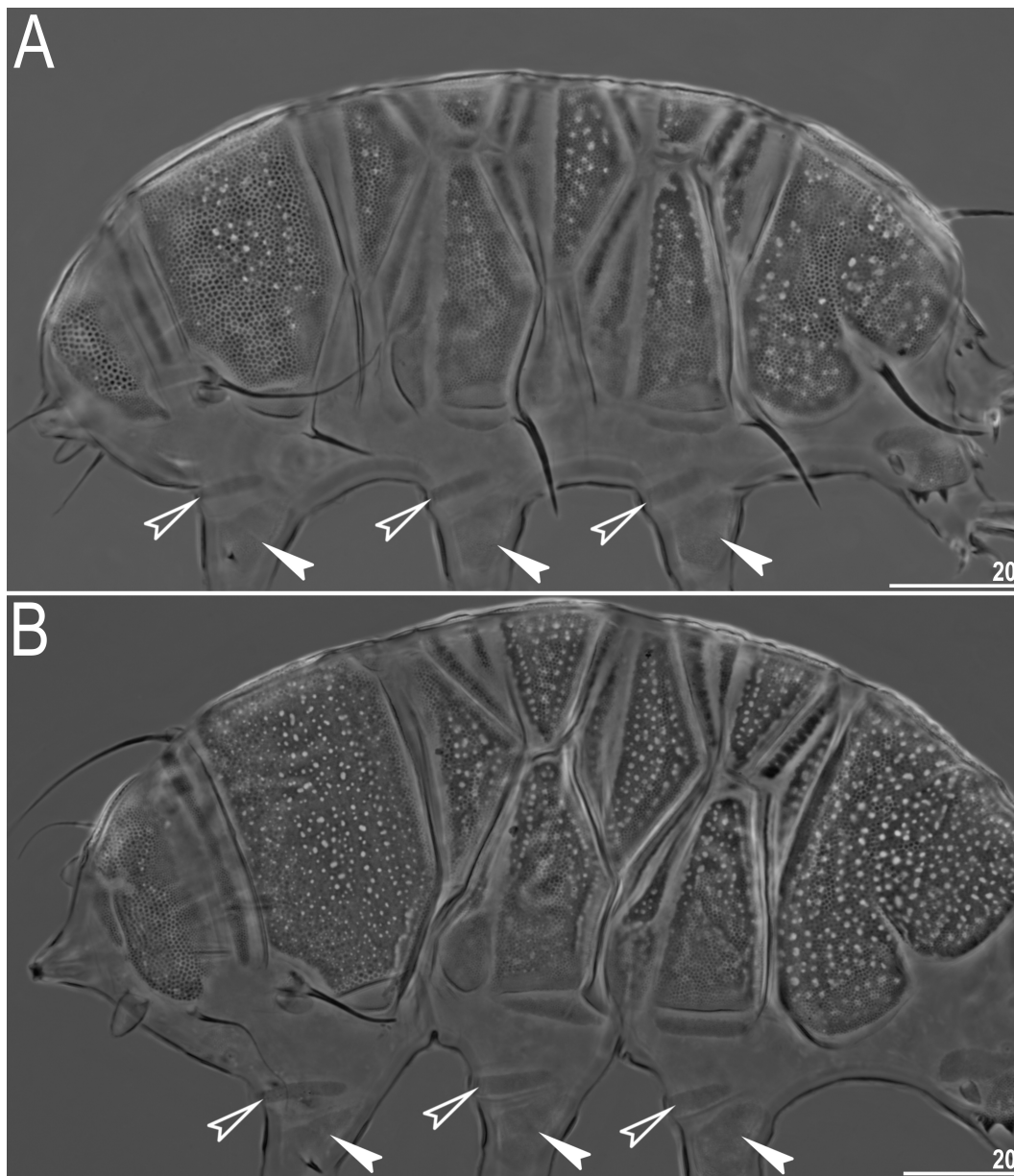


Fig. 7. Dorsal plate sculpturing of *Echiniscus clevelandi* (males, PCM). Empty arrowheads indicate pulvini, whereas white arrowheads – pedal plates. Scale bars in μm.

According to the updated phylogeny from Gąsiorek et al. (2021a), *H. crassus* sp. nov. is sister to the clade (*H. cataractus* Gąsiorek et al., 2021 + the *H. gladiator* group) (Fig. 19).

Type material: Holotype (adult female on the slide TW.006.04), allotype (adult male on slide TW.006.02), 23 paratypes: 13 adult females, 3 adult males, 4 juveniles, 3 larvae on slides TW.005.01–5, TW.006.01–5, TW.008.08–10, 13. Four females and one male on

SEM stub 21.08. Two specimens per samples TW.005–6 were used for DNA sequencing, including one retrieved as a hologenophore. Holotype (ASIZ01000036) deposited in the Biodiversity Research Center of Academia Sinica, one paratype (NHMD-915767) deposited in the Natural History Museum of Denmark, and the remaining material stored at the Jagiellonian University.

Type locality: 24°23'18"N, 121°15'39"E, 3 200 m

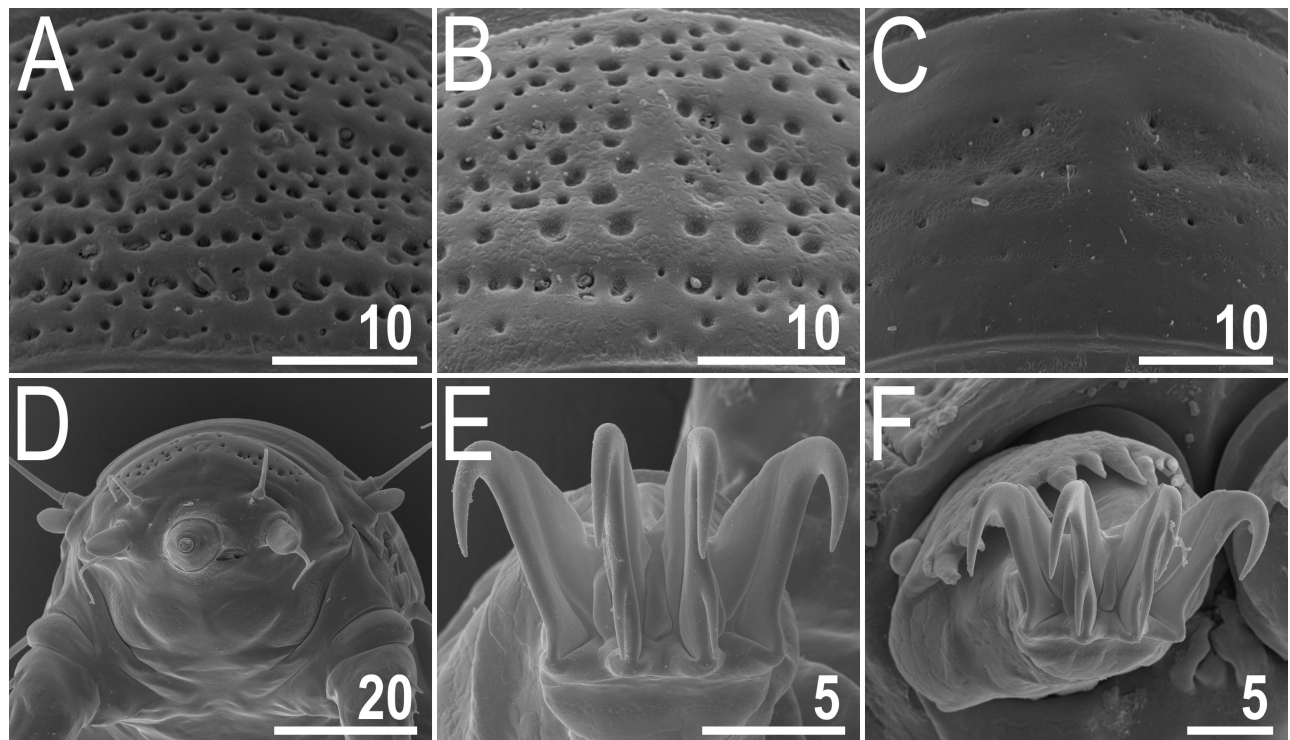


Fig. 8. Morphological details of *Echiniscus clevelandi* (SEM): A–C, varying levels of the sculpturing development of the scapular plate; D, cephalic region with peribuccal appendages and marked subcephalic swellings; E, claws II; F, claws IV. Scale bars in μm .

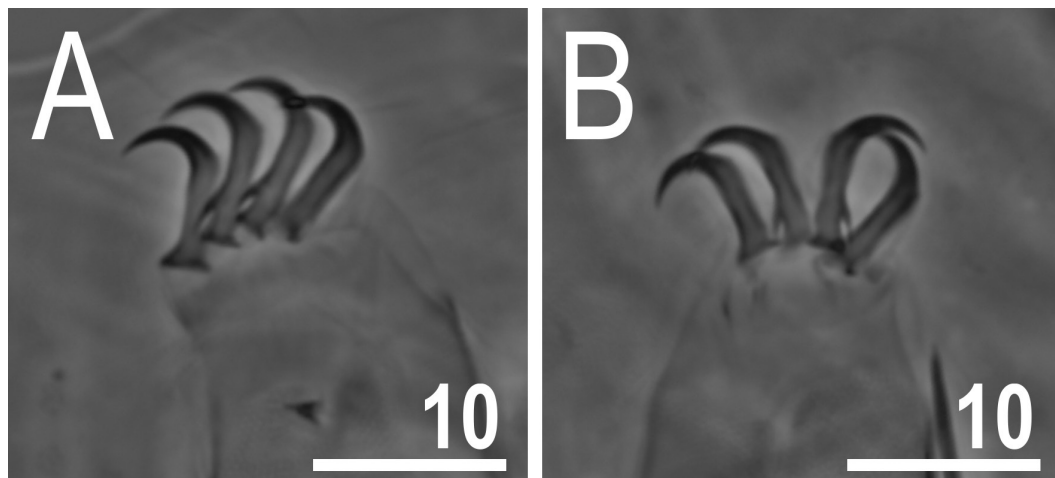


Fig. 9. Claws of *Echiniscus clevelandi* (PCM): A, claws I (female); B, claws III (female). Scale bars in μm .

asl: Taiwan, Snow Mountain (Xueshan), East Peak. Mosses on rocks exposed to sun.

Etymology: From Latin *crassus* = stout, plump; referring to the body proportions of both sexes. Adjective in the nominative singular.

Differential diagnosis: The new species differs from all representatives of the *gladiator* complex by the lack of *cirrus dorsalis*. It is also distinguishable from all members of the *exarmatus* morphogroup based on

the presence of *striae* in some plate portions (typically absent in *Hypechiniscus*, see Gąsiorek et al. 2021a) and in additional characters from:

H. cataractus, a Southeast Asian species, by the dorsal plate sculpturing (plates smooth in PCM in *H. cataractus* vs clear sculpturing in *H. crassus* sp. nov.) and ventral cuticle sculpturing (no epicuticular thickenings in *H. cataractus* vs epicuticular thickenings present and overlapping with belts of endocuticular

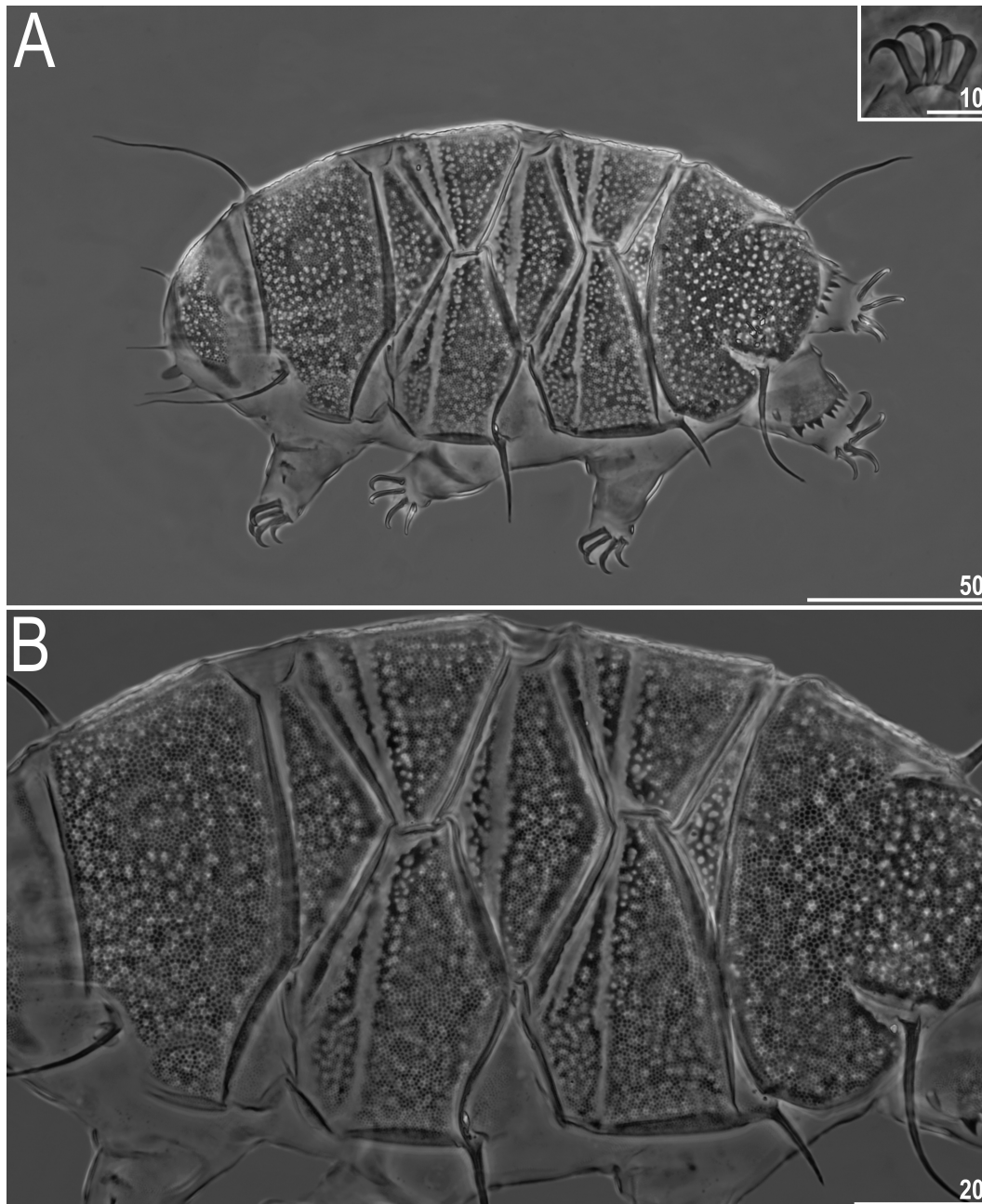


Fig. 10. Habitus of *Echiniscus hoonsooi* (PCM) from Japan: A, female (dorsolateral view, insert shows claws II); B, dorsal sculpturing in close-up. Scale bars in µm.

pillars in *H. crassus* sp. nov.).

H. exarmatus (Murray, 1907), a probable West Palaearctic element, exhibits no epicuticular ornamentation on dorsum and epicuticular thickenings on venter that do not overlap with belts of endocuticular pillars (both character states present in *H. crassus* sp. nov.).

H. flavus Gąsiorek et al., 2021, a likely Japanese endemic, by body colour (yellow in *H. flavus* vs opalescent white in *H. crassus* sp. nov.) and by the dorsal plate sculpturing (epicuticular thickenings in dorsal plates absent in *H. flavus* vs present in *H. crassus* sp. nov.).

Remarks: The presence of pseudoaccessory points on claws of *H. crassus* sp. nov. falsifies the hypothesis from Gąsiorek et al. (2021a) that these structures could constitute a synapomorphy of the *gladiator* clade.

Genus: *Nebularmis* Gąsiorek & Michalczyk, 2019 in Gąsiorek et al. 2019a
***Nebularmis crebraclava* (Sun, Li & Feng, 2014)**
 (Figs. 20–22, Table 10)

Material examined: Three adult females on the

slide TW.008.01. One specimen was used for DNA sequencing and retrieved as a hologenophore.

Amended description: Females (i.e., from the third instar onwards; measurements and statistics in table 10): Body massive and plump (Fig. 20), intensely red with dark red eyes; body colour and eyes dissolve in Hoyer’s medium. Large club-shaped cephalic papillae and elongated (primary) clavae (Figs. 20, 21A, 22A); only cirrus A present, embedded on a bulbous cirrophore (Fig. 20A).

Dorsal plate sculpturing with evident, numerous and widely spaced roundish or polygonal epicuticular granules connected by *striae* of various thicknesses (Figs. 20–21). Cephalic and cervical plates with minute granulation only (Fig. 21A). Large scapular plate with strongly sclerotised lateral sutures demarcating lateralmost portions characterised by minute granulation; micropores absent (Fig. 20). Two pairs of segmental plates I–II with weakly developed smooth transverse bands; m1–2 large and unipartite, m3 greatly reduced and formed as a narrow sculptured belt adjacent to the caudal plate (Fig. 21B–C). Caudal plate large, with short and weakly sclerotised incisions (Figs. 20, 21C).

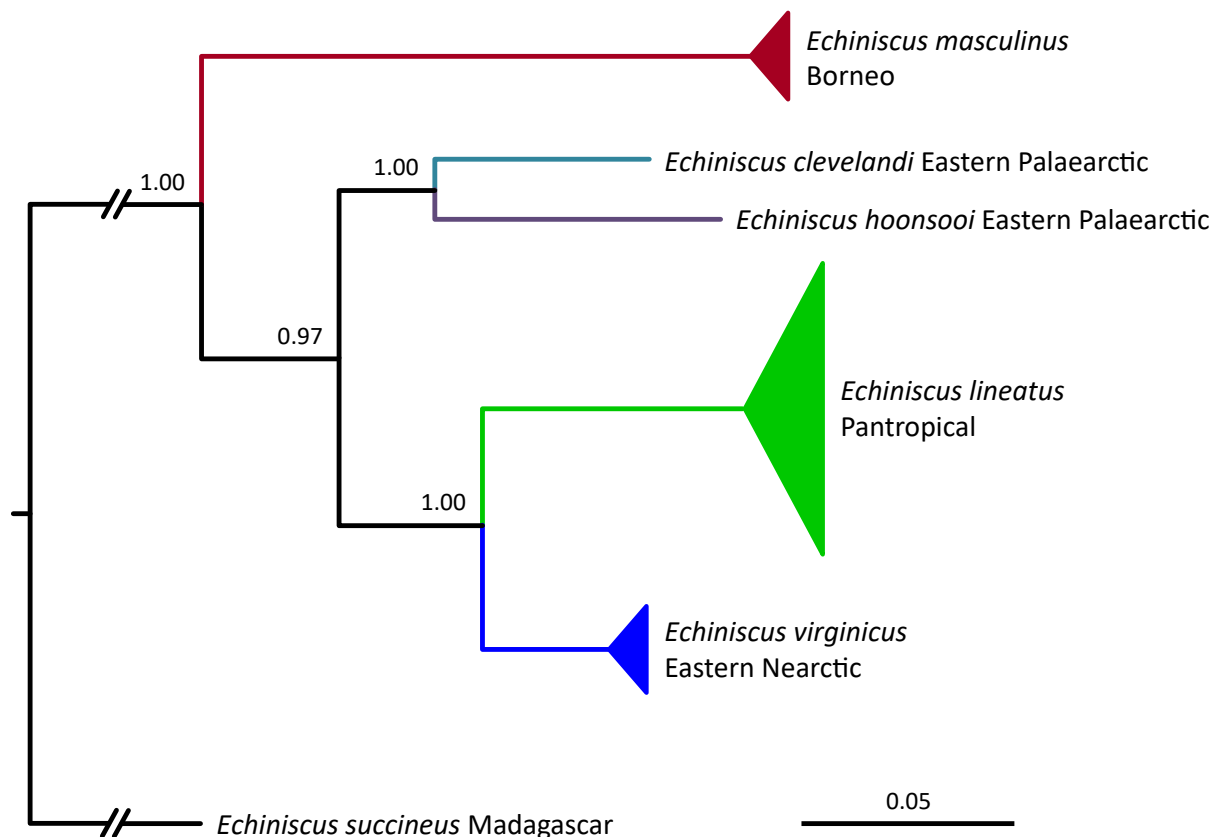


Fig. 11. Phylogenetic relationships within the *Echiniscus virginicus* complex based on concatenated ITS-1, ITS-2 and *COI* sequences as inferred in the Bayesian approach. *Echiniscus succineus* was used as an outgroup. Scale bar represents substitutions per site.

Venter weakly granulated and regularly wrinkled, as is typical for *Nebularmis* (Gąsiorek et al. 2021b); the only areas with evident endocuticular pillars are the pair of trapezoidal subcephalic plates (Fig. 22A–C) and the pair of wing-shaped genital plates (Fig. 22D). A sexpartite gonopore placed between genital plates, and a trilobed anus between legs IV. Pedal plates I–III formed as clear aggregations of pillars in central limb portions (Fig. 22B–C). Pedal plates IV strongly sculptured, with pillars present also on the dentate collar (Fig. 22D). Pulvini absent. Spine I triangular (Fig. 22B–C), papilla IV small and elongated (Figs. 20, 22D). Claws robust, isonych/homomorphic; primary spurs present on all

internal branches (Fig. 22C–D).

Males: Not found.

Juveniles, larvae and eggs: Not found.

Molecular markers and phylogenetic position:

All five gene fragments were sequenced: 18S rRNA (OK048614), 28S rRNA (OK048632), ITS-1 (OK048642), ITS-2 (OK048623) and *COI* (OK047274). The updated phylogeny from Gąsiorek et al. (2021b) indicates the presence of sister clades in *Nebularmis*: one of the Oriental origin, and the second of a mixed Palaearctic and Oriental origin (Fig. 23). *Nebularmis crebraclava* belongs to the latter clade, being the sister species of *N. reticulatus*.

Table 3. Measurements [in µm] of selected morphological structures of the adult males of *E. clevelandi* mounted in Hoyer’s medium. N, number of specimens/structures measured; Range, refers to the smallest and the largest structure among all measured specimens; SD, standard deviation; *sp*, the proportion between the length of a given structure and the length of the scapular plate

Character	N	Range		Mean		SD	
		µm	<i>sp</i>	µm	<i>sp</i>	µm	<i>sp</i>
Body length	11	145–192	475–598	169	522	17	33
Scapular plate length	11	28.6–37.5	–	32.5	–	3.0	–
Head appendage lengths							
<i>Cirrus internus</i>	10	13.8–20.2	42.7–59.2	17.3	53.7	1.9	5.7
Cephalic papilla	11	7.0–9.6	19.5–29.2	8.4	25.8	0.9	2.5
<i>Cirrus externus</i>	9	14.9–22.4	43.5–62.7	18.5	55.9	2.6	6.5
Clava	11	4.9–7.4	16.3–21.8	6.2	19.2	0.8	1.9
<i>Cirrus A</i>	10	29.7–45.2	92.0–131.2	35.9	111.7	4.3	13.3
<i>Cirrus A</i> /Body length ratio	10	18%–26%	–	22%	–	3%	–
Body appendage lengths							
<i>Cirrus B</i>	11	10.8–26.8	37.0–75.1	18.0	55.2	4.3	10.1
<i>Cirrus C</i>	11	16.9–37.9	57.9–106.2	27.3	83.9	5.7	13.7
<i>Cirrus D</i>	10	18.1–37.1	62.0–103.9	27.3	84.4	5.4	12.6
<i>Cirrus E</i>	10	21.2–38.1	72.6–106.7	29.8	91.8	5.6	10.8
Spine on leg I length	11	1.9–3.7	6.4–10.7	2.8	8.4	0.7	1.7
Papilla on leg IV length	11	3.5–5.7	12.0–16.5	4.6	14.0	0.7	1.5
Number of teeth on the collar	11	7–13	–	9.8	–	1.7	–
Claw I heights							
Branch	11	8.0–10.8	25.7–31.3	9.4	28.8	1.0	2.0
Spur	9	1.6–2.5	5.1–7.1	2.1	6.4	0.3	0.7
Spur/branch height ratio	9	18%–26%	–	23%	–	3%	–
Claw II heights							
Branch	11	7.4–10.1	24.6–28.9	8.8	27.2	0.9	1.7
Spur	11	1.7–2.2	4.8–6.4	1.9	5.9	0.2	0.6
Spur/branch height ratio	11	17%–25%	–	22%	–	2%	–
Claw III heights							
Branch	11	7.7–10.4	25.9–30.6	9.2	28.3	0.9	1.9
Spur	10	1.5–2.2	4.6–6.2	1.8	5.5	0.2	0.5
Spur/branch height ratio	10	16%–21%	–	19%	–	2%	–
Claw IV heights							
Branch	9	9.3–14.1	31.7–40.9	11.4	35.7	1.5	3.1
Spur	1	2.5–2.5	8.3–8.3	2.5	8.3	?	?
Spur/branch height ratio	1	22%–22%	–	22%	–	?	–

Table 4. Measurements [in μm] of selected morphological structures of the juveniles of *E. clevelandi* mounted in Hoyer’s medium. N, number of specimens/structures measured; Range, refers to the smallest and the largest structure among all measured specimens; SD, standard deviation; *sp*, the proportion between the length of a given structure and the length of the scapular plate

Character	N	Range		Mean		SD	
		μm	<i>sp</i>	μm	<i>sp</i>	μm	<i>sp</i>
Body length	3	121–139	481–495	129	487	9	7
Scapular plate length	3	25.0–28.1	–	26.6	–	1.6	–
Head appendage lengths							
Cirrus <i>internus</i>	3	8.8–11.4	33.1–42.9	9.8	37.1	1.4	5.1
Cephalic papilla	3	4.8–5.2	17.8–20.8	5.0	18.9	0.2	1.7
Cirrus <i>externus</i>	3	10.2–11.7	36.3–44.0	10.9	41.3	0.8	4.3
Clava	2	3.5–4.3	13.2–17.2	3.9	15.2	0.6	2.9
Cirrus <i>A</i>	3	22.3–27.1	81.1–101.9	24.1	90.7	2.6	10.5
Cirrus <i>A</i> /Body length ratio	3	16%–21%	–	19%	–	2%	–
Body appendage lengths							
Cirrus <i>C</i>	3	11.5–13.6	40.9–54.4	12.8	48.4	1.1	6.9
Cirrus <i>E</i>	3	14.1–19.4	56.2–72.9	16.4	61.9	2.7	9.6
Spine on leg I length	3	2.0–2.4	7.5–8.8	2.2	8.3	0.2	0.7
Papilla on leg IV length	2	2.8–3.5	10.0–14.0	3.2	12.0	0.5	2.9
Number of teeth on the collar	3	7–10	–	8.7	–	1.5	–
Claw I heights							
Branch	3	6.6–6.8	23.5–26.4	6.7	25.2	0.1	1.5
Spur	3	1.4–1.9	5.0–7.1	1.6	6.2	0.3	1.1
Spur/branch height ratio	3	21%–28%	–	24%	–	3%	–
Claw II heights							
Branch	3	6.3–6.5	22.8–25.2	6.4	24.1	0.1	1.2
Spur	3	1.3–1.5	4.6–6.0	1.4	5.3	0.1	0.7
Spur/branch height ratio	3	20%–24%	–	22%	–	2%	–
Claw III heights							
Branch	3	6.0–6.3	22.4–24.0	6.2	23.4	0.2	0.8
Spur	2	1.1–1.1	3.9–4.1	1.1	4.0	0.0	0.2
Spur/branch height ratio	2	17%–17%	–	17%	–	0%	–
Claw IV heights							
Branch	3	7.4–7.7	26.3–29.6	7.5	28.3	0.2	1.7
Spur	2	1.6–1.7	6.0–6.0	1.7	6.0	0.1	0.0
Spur/branch height ratio	2	21%–23%	–	22%	–	2%	–

Table 5. Comparison of morphological traits and reproductive modes between the *Echiniscus virginicus* complex species

Character	<i>E. cheonyoungi</i>	<i>E. clevelandi</i>	<i>E. hoonsooi</i>	<i>E. lineatus</i>	<i>E. masculinus</i>	<i>E. virginicus</i>
Chaetotaxy	<i>A-B-C-C^d-D-D^d-E</i>	<i>A-B-C-(C^d)-D-(D^d)-E</i>	<i>A-(C)-(D)-E</i>	<i>A-(B)-C-C^d-D-D^d-E</i>	<i>A-C-D-(D^d)-E</i>	<i>A-(B)-C-C^d-D-D^d-E</i>
Dorsal plates with pores	present, with both pillars and pores	present, only with pillars	pseudopores	pseudopores	pseudopores	pores
Pedal plate sculpturing	present, with both pillars and pores	present, only with pillars	absent	absent	absent	absent
Claws	homomorphic and spurless	homomorphic	heteromorphic	homomorphic	homomorphic	homomorphic
Males	never found*	present	never found	never found	present	never found

**E. cheonyoungi* is the only species for which ample population data are lacking, thus it is currently impossible to determine whether males are present in this species.

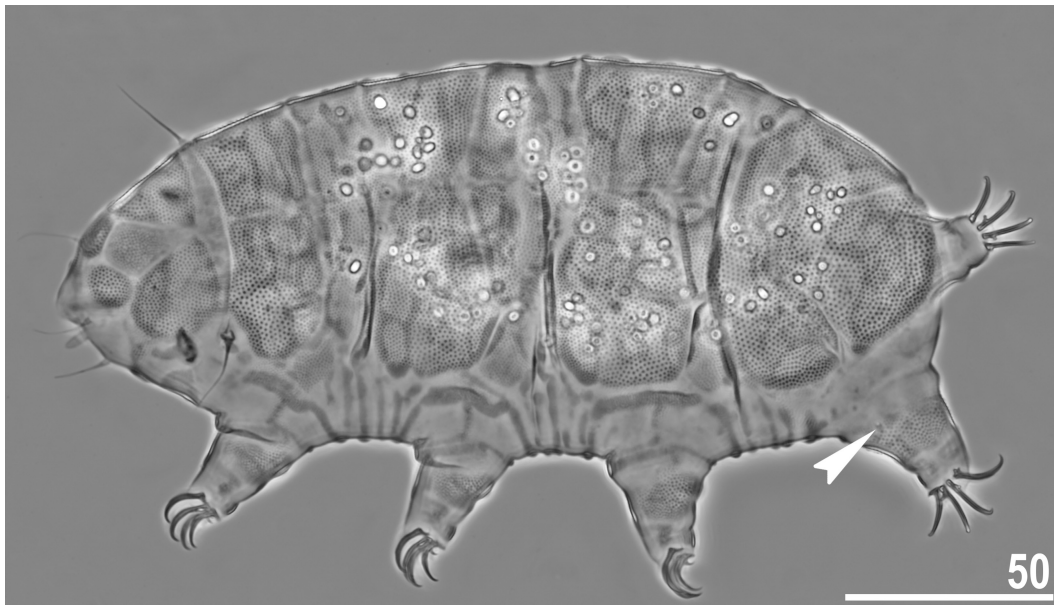


Fig. 12. Holotypic female of *Hypechiniscus crassus* sp. nov. (dorsolateral view, PCM). White arrowhead indicates papilla IV. Scale bar in μm .

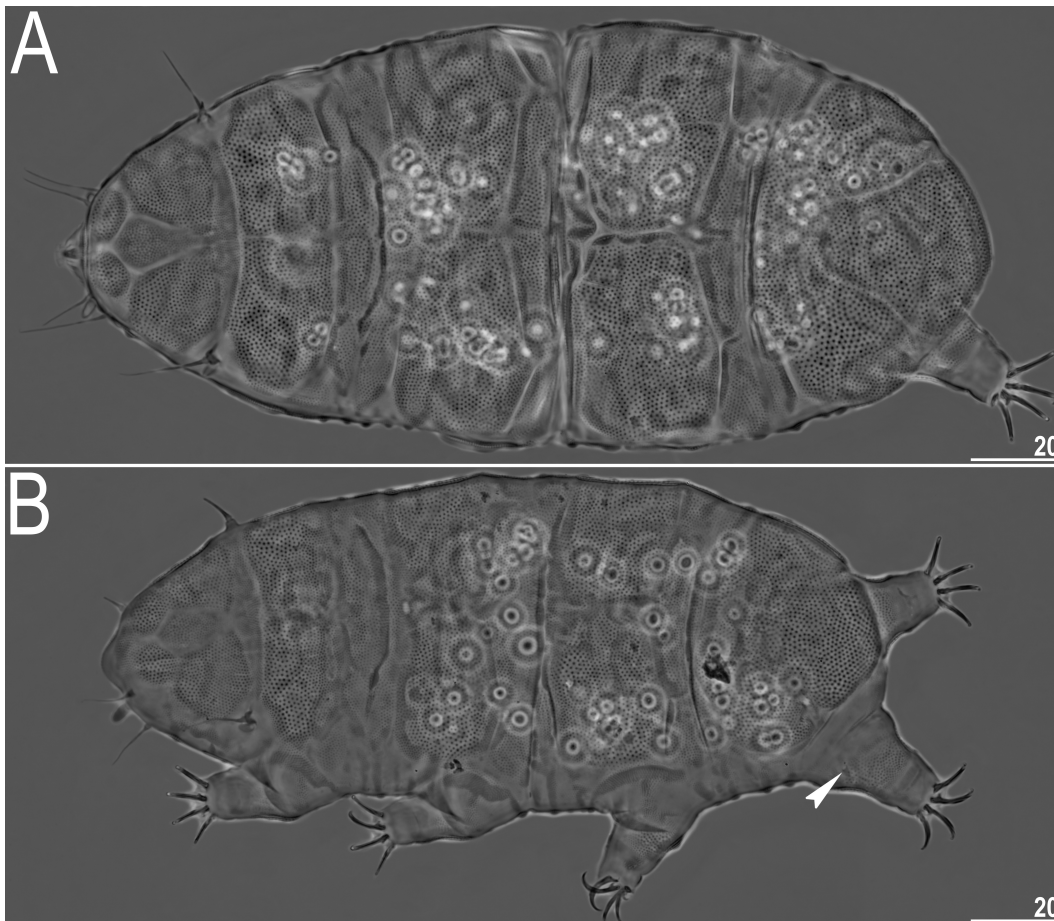


Fig. 13. Habitus of *Hypechiniscus crassus* sp. nov. (PCM): A, female (dorsal view); B, allotypic male (dorsolateral view). Arrowhead indicates papilla IV. Scale bars in μm .

Remarks: The newly found females supplement the original description which was based solely on males (Sun et al. 2014).

***Nebularmis reticulatus* (Murray, 1905)**

Material examined: 31 adult females, 29 juveniles, and 2 larvae on the slides TW.007.02–19, TW.009.06–8. Eight specimens on the SEM stubs 21.05–6. Four specimens per each of the two samples were used for DNA sequencing, including six retrieved as hologenophores.

Remarks: Numerous individuals exhibit large atypical granules (as depicted in fig. 5b in Gąsiorek et al. 2019c) on lateralmost portions of the scapular plate, and some of them also on other plates, e.g., on the caudal plate. However, the genetic distances with

respect to European populations (including the neotype population described in Gąsiorek et al. 2019c) are small and clearly fall under intraspecific variation: $p = 0.2\text{--}1.2\%$ in ITS-1 (a single new haplotype, OK048643–5), $0.2\text{--}3.3\%$ in ITS-2 (two new haplotypes, OK048624–6), $0.7\text{--}0.8\%$ in *COI* (a single new haplotype, OK047275–7).

Genus: *Pseudechiniscus* Thulin, 1911

Subgenus: *Meridioniscus* Gąsiorek et al., 2021
***Pseudechiniscus (Meridioniscus) dreyeri* sp. nov.**

(Figs. 24–25, Tables 11–12)

urn:lsid:zoobank.org:act:B38091F7-3B79-438B-A42A-A4E53C25C34B

Tardigrada Register: www.tardigrada.net/register/0112.htm

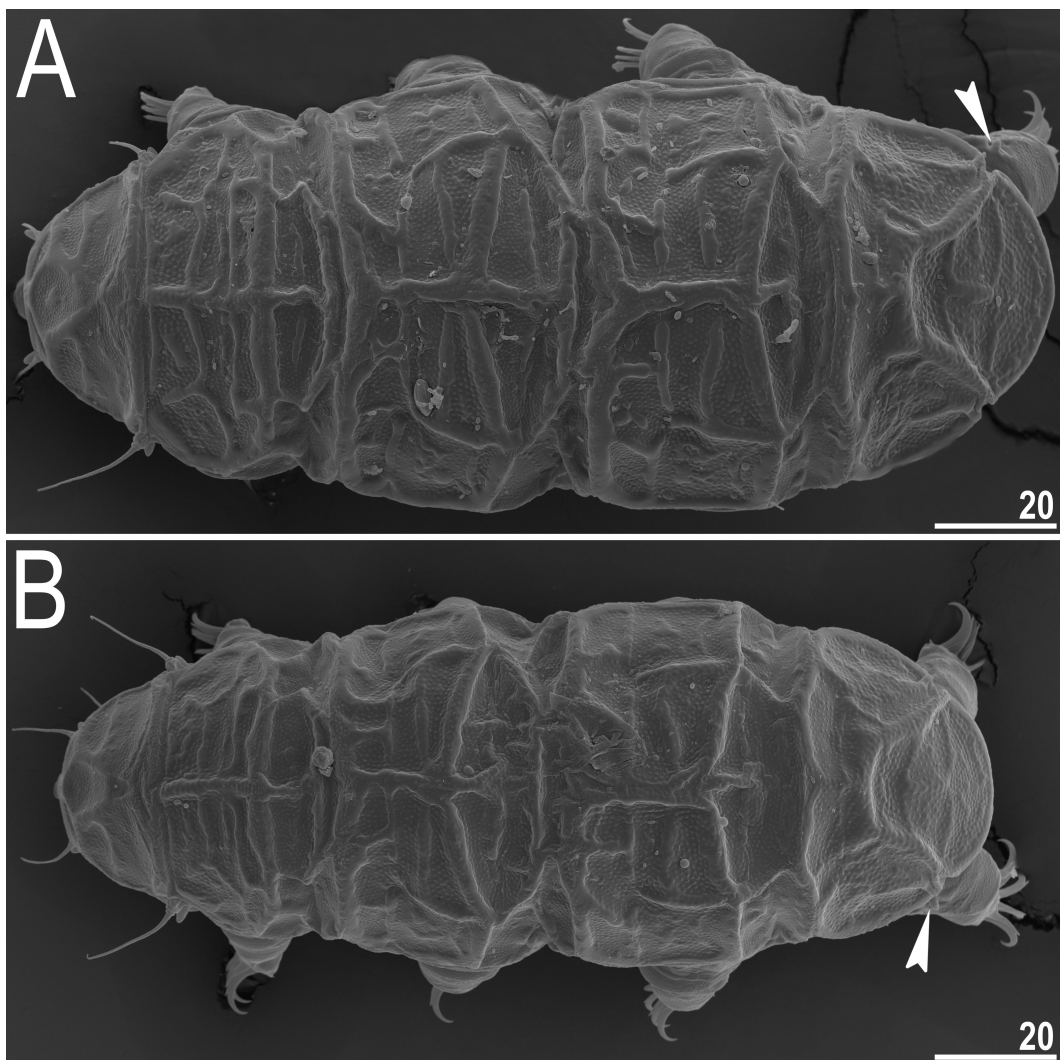


Fig. 14. Habitus of *Hypechiniscus crassus* sp. nov. (dorsal view, SEM): A, female; B, male. Arrowheads indicate papilla IV. Scale bars in μm .

Description: Females (i.e., from the third instar onwards; measurements and statistics in table 11): Body small and cylindrical (Fig. 24A), light orange with tiny crystalline eyes; body colour and eyes dissolve in Hoyer's medium. Clavae elongated (dactyloid); cirrophores of peribuccal cirri merged with *flagellum*, cirrophores *A* distinct (Fig. 24A–B).

Dorsal plate sculpturing of the *Pseudechiniscus* type, with rudimentary, faint *striae* present occasionally in central plate portions (Fig. 24B). Endocuticular pillars

of similar diameters throughout the dorsum. Pentapartite cephalic plate adjacent to the scapular plate; lacking cervical plate (Fig. 24A). Scapular plate divided by two weakly marked sutures: central longitudinal suture and transversal suture, thus delineating four plate portions: two large anterior ones and two posterior, more narrow and with poorly visible lateralmost subportions (Fig. 24B). Median plates *m1*, *m3* unipartite and large, a pair of lateral intersegmental plates flanking *m1* and two pairs of such plates flanking *m2*; *m2* bipartite, with

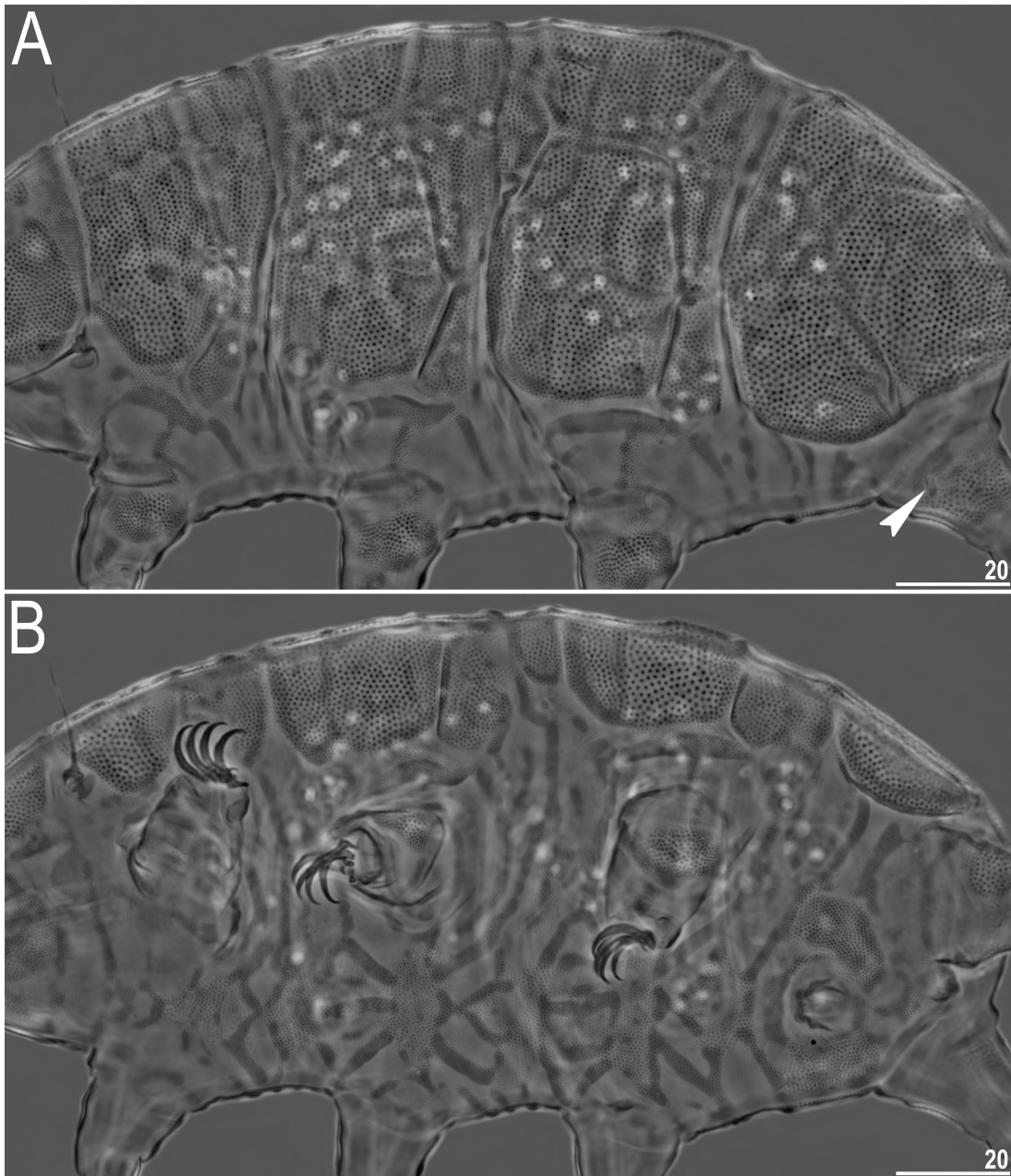


Fig. 15. Sculpturing of *Hypechiniscus crassus* sp. nov. (PCM): A, dorsal (female); B, ventral (female). Arrowhead indicates papilla IV. Scale bars in μm .

narrow triangular posterior part. Paired segmental plates I–II and paired pseudosegmental plate IV' present (Fig. 24B). Caudal plate with two slightly curved incisions (Fig. 24A).

Ventral sculpturing with well-developed and evident reticulum composed of endocuticular pillars solely (Figs. 24C–25). Single dense aggregation of pillars forming an aliform shape in the subcephalic region. Sexpartite gonopore placed between legs III–IV, and a trilobed anus between legs IV. Pedal plates formed as belts of pillars in central limb portions (Fig. 24A). Pulvini faint. Papillae or spines on legs I absent. Papilla IV small and tubby (Fig. 24A). Claws minute and isonych; internal claws with delicate primary spurs

positioned at ca. 20% of the branch height and closely adjacent to it (Fig. 24A, insert).

Males: Not found.

Juveniles (i.e., the second instar; measurements and statistics in table 12): Qualitatively identical to females, beside of the lack of gonopore. No morphometric gap with respect to adult females.

Larvae (i.e., the first instar): Cuticle sculpturing developed as in older instars. Gonopore and anus absent. Body length 94–100 μm , scapular plate length 14.4–14.7 μm ; cephalic appendages lengths: *cirri interni* 3.8–6.0 μm , cephalic papillae 2.8–3.0 μm , *cirri externi* 4.7–6.4 μm , (primary) clavae 3.0–3.1 μm , cirrus *A* 15.3–15.9 μm . Papilla IV length 1.4–1.6 μm . Claw

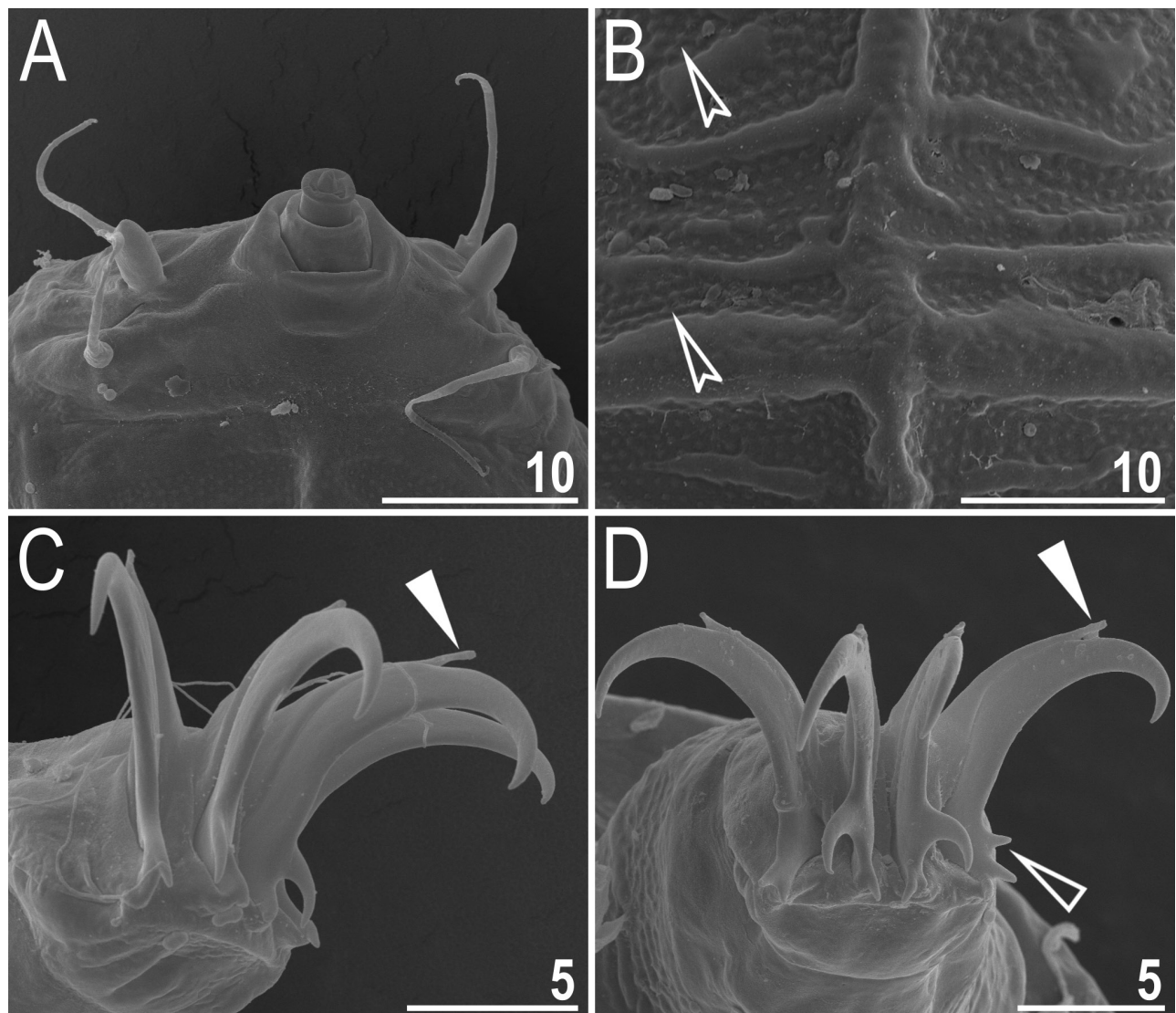


Fig. 16. Morphological details of *Hypechiniscus crassus* sp. nov. (SEM): A, cephalic region with peribuccal appendages; B, sculpturing of the scapular plate in close-up (empty incised arrowheads indicate rudimentary *striae*); C, claws I; D, claws IV. White arrowheads point out pseudoaccessory points, and empty arrowhead – aberrant secondary spur on external claw. Scale bars in μm .

branches 4.6–5.0 μm , spurs 1.4–1.8 μm .

Eggs: Up to two orange eggs per exuvia were found.

Molecular markers and phylogenetic position: Single haplotypes were found in all markers: 18S rRNA (OK048615), 28S rRNA (OK048633), ITS-1 (OK048646) and *COI* (OK047278). In the updated phylogeny from Gąsiorek et al. (2021c), the closest relative of *P. (M.) dreyeri* sp. nov. within the *Meridioniscus* clade is *P. (M.) cf. saltensis* from the Neotropics (Fig. 30).

Type material: Holotype (adult female on the slide TW.008.12), 32 paratypes: 18 adult females, 12 juveniles, and two larvae on the slides TW.005.11, 13, 15–16, TW.008.10–13. Four specimens were preserved for molecular analyses. Holotype deposited in the Biodiversity Research Center of the Academia Sinica

(ASIZ01000039), the one paratype (NHMD-915766) deposited in the Natural History Museum of Denmark, and remaining material stored at the Jagiellonian University.

Type locality: 24°23'51"N, 121°14'04"E, 3 700 m asl: Taiwan, Snow Mountain (Xueshan), North Peak. Mosses from rocks exposed to sun.

Etymology: Patronym honouring Niklas Dreyer, a carcinologist and the collector of the Taiwanese moss samples used in this study. Noun in the genitive singular.

Differential diagnosis: There are few *Meridioniscus* species with a smooth posterior margin of the pseudosegmental plate IV' (or with minute projections) and lacking lateral hemispherical projections. *Pseudechiniscus (M.) dreyeri* sp. nov. differs from:

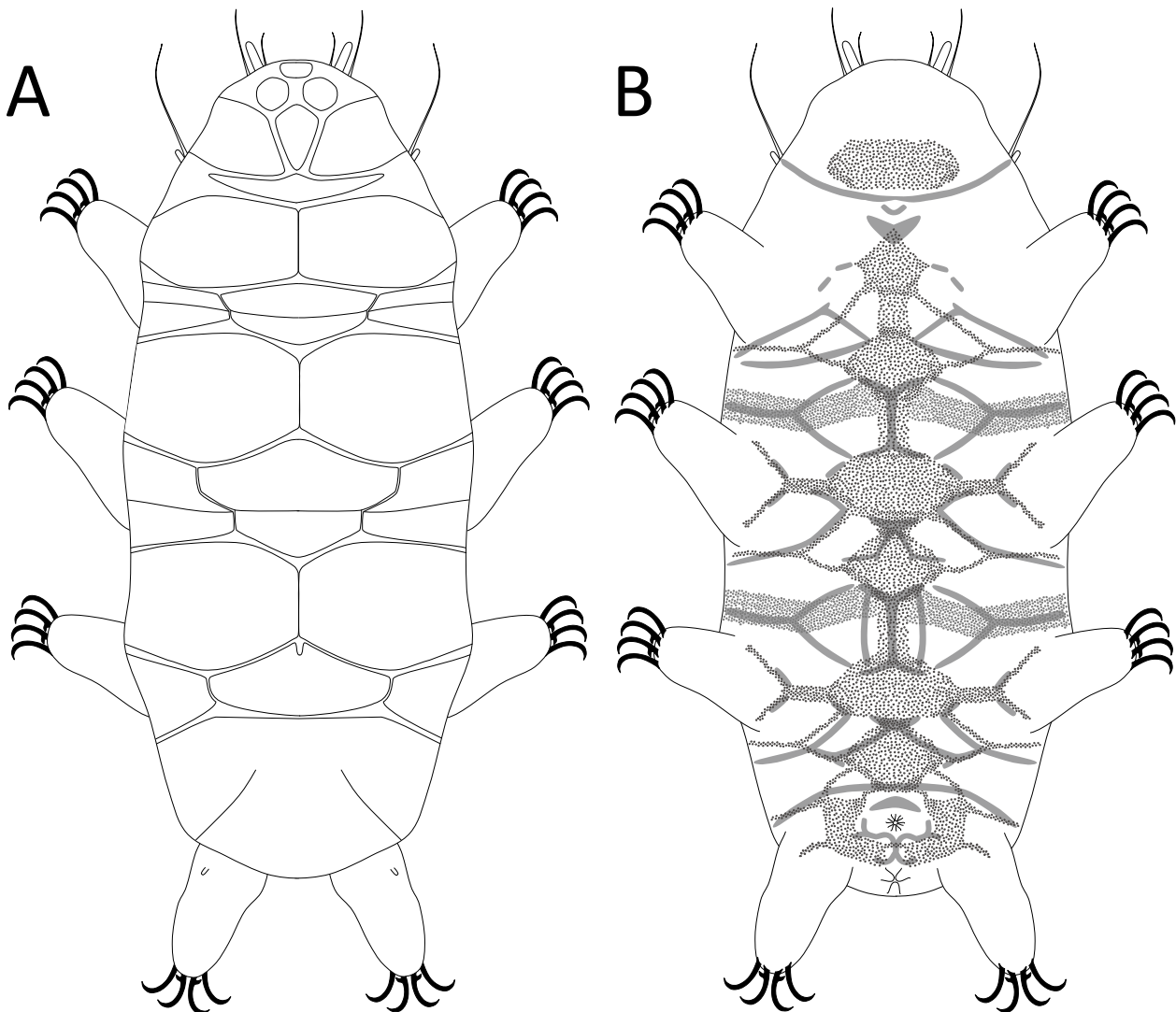


Fig. 17. Schematic depiction of female morphology of *Hypechiniscus crassus* sp. nov.: A, dorsum; B, venter.



Fig. 18. Larva of *Hypechiniscus crassus* sp. nov. Scale bar in μm . Arrowhead indicates papilla IV.

Table 6. Measurements [in μm] of selected morphological structures of the adult females of *H. crassus* sp. nov. mounted in Hoyer’s medium. N, number of specimens/structures measured; Range, refers to the smallest and the largest structure among all measured specimens; SD, standard deviation; *sp*, the proportion between the length of a given structure and the length of the scapular plate

Character	N	Range		Mean		SD		Holotype	
		μm	<i>sp</i>	μm	<i>sp</i>	μm	<i>sp</i>	μm	<i>sp</i>
Body length	11	186–220	888–1024	203	932	10	42	198	888
Scapular plate length	11	20.1	–	21.8	–	0.8	–	22.3	–
Head appendage lengths									
<i>Cirrus internus</i>	11	12.5–16.2	57.6–70.1	14.1	64.7	1.1	3.7	14.8	66.4
Cephalic papilla	10	4.8–5.8	21.8–26.4	5.4	24.6	0.3	1.2	5.7	25.6
<i>Cirrus externus</i>	11	16.9–21.7	79.0–94.6	18.9	86.7	1.5	5.6	19.6	87.9
Clava	11	3.8–5.6	17.5–25.1	4.7	21.6	0.4	1.9	4.7	21.1
<i>Cirrus A</i>	10	16.3–21.4	79.1–96.8	19.1	87.6	1.4	5.2	18.8	84.3
<i>Cirrus A</i> /Body length ratio	10	8%–10%	–	9%	–	1%	–	9%	–
Body appendage lengths									
Papilla on leg IV length	6	2.6–3.5	12.1–15.7	3.0	14.1	0.3	1.4	3.5	15.7
Claw I heights									
Branch	11	10.2–12.1	48.1–55.8	11.0	50.5	0.5	2.3	10.9	48.9
Spur	11	1.5–1.9	6.9–9.0	1.7	8.0	0.1	0.8	1.8	8.1
Spur/branch height ratio	11	14%–18%	–	16%	–	1%	–	17%	–
Claw II heights									
Branch	11	9.8–11.9	46.5–53.2	10.9	50.1	0.6	1.8	11.1	49.8
Spur	10	1.6–2.3	7.2–10.0	1.9	8.7	0.3	1.0	1.7	7.6
Spur/branch height ratio	10	14%–20%	–	17%	–	2%	–	15%	–
Claw III heights									
Branch	11	10.3–11.5	46.8–53.2	10.9	50.0	0.4	2.1	10.9	48.9
Spur	7	1.6–2.1	7.4–9.5	1.9	8.6	0.2	0.7	1.8	8.1
Spur/branch height ratio	7	14%–19%	–	17%	–	2%	–	17%	–
Claw IV heights									
Branch	11	11.6–13.0	52.9–60.7	12.2	56.0	0.5	2.3	12.1	54.3
Spur	2	2.0–2.4	9.7–10.8	2.2	10.2	0.3	0.7	2.4	10.8
Spur/branch height ratio	2	16%–20%	–	18%	–	3%	–	20%	–

P. (M.) angelusalas Roszkowska et al., 2020, described from Madagascar, by relative lengths of some of the cephalic appendages (*cirrus internus* 22.0–33.0, *cirrus A* 96.8–126.8 in *P. (M.) dreyeri* sp. nov. vs *cirrus internus* 34.4–36.6, *cirrus A* 129.2–152.2 in *P. (M.) angelusalas*).

P. (M.) dastychi Roszkowska et al., 2020, known from the maritime Antarctic, by adult female body size (body length 121–152 µm and scapular plate length 18.9–23.7 µm in *P. (M.) dreyeri* sp. nov. vs 167–202 µm and sc 27.5–33.0 µm in *P. (M.) dastychi*), lengths of cephalic appendages (*cirrus internus* 4.7–7.0 µm, *cirrus externus* 6.8–11.9 µm, *cirrus A* 21.0–27.0 µm [14–20% of the body length] in *P. (M.) dreyeri* sp. nov. vs *cirrus internus* 10.4–12.7 µm, *cirrus externus* 15.9–19.1 µm, *cirrus A* 40.0–45.0 µm [22–26% of the body length] in *P. (M.) dastychi*), and claw heights (5.0–8.1 µm in *P. (M.) dreyeri* sp. nov. vs 8.7–12.2 µm in *P. (M.) dastychi*).

P. (M.) indistinctus Roszkowska et al., 2020,

known from the Scandinavian Peninsula, by the morphology of dorsal pillars (homogeneous in size in *P. (M.) dreyeri* sp. nov. vs heterogeneous in size in *P. (M.) indistinctus*) and relatively shorter peribuccal cirri (*cirrus internus* 22.0–33.0, *cirrus externus* 31.9–52.2 in *P. (M.) dreyeri* sp. nov. vs *cirrus internus* 34.1–38.5, *cirrus externus* 54.3–59.3 in *P. (M.) indistinctus*).

P. (M.) mascarenensis Kiosya et al., 2021, known from Mauritius, by having smaller adult females (121–152 µm in *P. (M.) dreyeri* sp. nov. vs 151–177 µm in *P. (M.) mascarenensis*) and a relatively longer *cirrus A* (14–20% of the body length in *P. (M.) dreyeri* sp. nov. vs 9–13% in *P. (M.) mascarenensis*).

P. (M.) santomensis Fontoura et al., 2010, a São Tomé endemic, by a relatively longer *cirrus A* (14–20% of the body length in *P. (M.) dreyeri* sp. nov. vs 9–14% in *P. (M.) santomensis*) and dorsal plate sculpturing (*striae* rarely identifiable in *P. (M.) dreyeri* sp. nov. vs *striae* delicate and thin, but clear in all plates in *P. (M.)*

Table 7. Measurements [in µm] of selected morphological structures of the adult males of *H. crassus* sp. nov. mounted in Hoyer’s medium. N, number of specimens/structures measured; Range, refers to the smallest and the largest structure among all measured specimens; SD, standard deviation; *sp*, the proportion between the length of a given structure and the length of the scapular plate

Character	N	Range		Mean		SD		Allotype	
		µm	<i>sp</i>	µm	<i>sp</i>	µm	<i>sp</i>	µm	<i>sp</i>
Body length	4	178	909–1020	187	943	11	52	178	918
Scapular plate length	4	19.4–20.2	–	19.8	–	0.3	–	19.4	–
Head appendage lengths									
<i>Cirrus internus</i>	4	10.1–11.6	51.3–57.4	10.6	53.6	0.7	2.9	10.5	54.1
Cephalic papilla	4	4.4–5.3	21.8–27.3	4.9	24.7	0.5	2.8	5.3	27.3
<i>Cirrus externus</i>	4	14.8–15.9	75.1–79.8	15.4	78.0	0.5	2.0	15.2	78.4
Clava	4	3.7–4.5	18.8–23.2	4.2	21.3	0.4	2.1	4.5	23.2
<i>Cirrus A</i>	4	16.1–19.2	81.3–95.0	17.4	88.0	1.3	5.6	17.0	87.6
<i>Cirrus A</i> /Body length ratio	4	8%–10%	–	9%	–	1%	–	10%	–
Body appendage lengths									
Papilla on leg IV length	3	2.0–2.4	10.2–12.4	2.3	11.5	0.2	1.2	2.4	12.4
Claw I heights									
Branch	4	9.1–10.2	46.2–51.5	9.8	49.4	0.5	2.3	10.0	51.5
Spur	2	1.6–1.6	8.1–8.2	1.6	8.2	0.0	0.1	1.6	8.2
Spur/branch height ratio	2	16%–16%	–	16%	–	0%	–	16%	–
Claw II heights									
Branch	4	9.3–10.7	47.2–53.0	9.9	50.2	0.7	3.0	9.3	47.9
Spur	2	1.7–1.7	8.4–8.6	1.7	8.5	0.0	0.1	?	?
Spur/branch height ratio	2	16%–16%	–	16%	–	0%	–	?	–
Claw III heights									
Branch	4	9.2–10.0	46.5–50.5	9.7	48.8	0.3	1.7	9.8	50.5
Spur	0	?	?	?	?	?	?	?	?
Spur/branch height ratio	0	?	–	?	–	?	–	?	–
Claw IV heights									
Branch	4	9.6–11.2	48.7–56.6	10.7	54.1	0.7	3.7	10.9	56.2
Spur	1	2.1–2.1	10.6–10.6	2.1	10.6	?	?	?	?
Spur/branch height ratio	1	19%–19%	–	19%	–	?	–	?	–

santomensis).

Moreover, *P. (M.) dreyeri* sp. nov. is distinguishable from all abovementioned species by the ventral sculpturing pattern.

Subgenus: *Pseudechiniscus* Thulin, 1911
***Pseudechiniscus (Pseudechiniscus) ehrenbergi* Roszkowska et al., 2020**

Material examined: 37 adult females, eight adult males, and eight juveniles on slides TW.010.01–5. Ten specimens were used for DNA sequencing, including three retrieved as hologenophores.

Remarks: This is another record suggesting a wide geographic distribution of *P. (P.) ehrenbergi* (Cesari et al. 2020; Roszkowska et al. 2020; Gąsiorek et al. 2021c); however, there is a considerable variability in the ventral sculpturing between various populations (Gąsiorek et al. 2021c), thus the distribution and

intraspecific variation of the species require new, integrative analyses.

***Pseudechiniscus (Pseudechiniscus) formosus* sp. nov.**

(Figs. 26–27)

urn:lsid:zoobank.org:act:7FDACA7F-5E5F-4220-A668-DD8179BD04A6

Tardigrada Register: <http://www.tardigrada.net/register/0113.htm>

Description: Female (i.e., the third instar): Large (187 µm, sc = 24.9 µm) *Pseudechiniscus* with cylindrical body (Fig. 26A); pale yellow with black crystalline eyes, body colour disappears, but eyes persist after mounting in Hoyer’s medium. Pseudo-hemispherical cephalic papillae (3.9 µm) and elongated (primary) clavae (4.0 µm, Fig. 27); cirrophores of peribuccal

Table 8. Measurements [in µm] of selected morphological structures of the juveniles of *H. crassus* sp. nov. mounted in Hoyer’s medium. N, number of specimens/structures measured; Range, refers to the smallest and the largest structure among all measured specimens; SD, standard deviation; *sp*, the proportion between the length of a given structure and the length of the scapular plate

Character	N	Range		Mean		SD	
		µm	<i>sp</i>	µm	<i>sp</i>	µm	<i>sp</i>
Body length	4	150–172	896–980	162	927	9	38
Scapular plate length	4	15.3–19.2	–	17.6	–	1.6	–
Head appendage lengths							
<i>Cirrus internus</i>	4	8.1–10.6	46.0–60.1	9.2	52.5	1.1	6.4
Cephalic papilla	4	4.5–5.1	25.6–30.1	4.8	27.5	0.3	1.9
<i>Cirrus externus</i>	3	11.5–13.0	65.3–83.0	12.4	72.0	0.8	9.6
Clava	4	3.6–4.2	21.9–23.5	4.0	22.6	0.3	0.7
<i>Cirrus A</i>	4	12.8–15.0	70.7–94.1	14.1	80.6	0.9	9.8
<i>Cirrus A</i> /Body length ratio	4	8%–10%	–	9%	–	1%	–
Body appendage lengths							
Papilla on leg IV length	4	1.7–2.6	10.2–14.4	2.2	12.3	0.5	2.0
Claw I heights							
Branch	4	7.9–8.4	43.6–52.9	8.1	46.3	0.2	4.5
Spur	4	1.2–1.8	6.6–9.4	1.4	8.0	0.3	1.2
Spur/branch height ratio	4	15%–21%	–	17%	–	3%	–
Claw II heights							
Branch	4	7.5–9.1	41.4–53.6	8.1	46.5	0.7	5.3
Spur	4	1.3–1.5	7.2–8.5	1.4	7.7	0.1	0.6
Spur/branch height ratio	4	16%–17%	–	17%	–	1%	–
Claw III heights							
Branch	4	7.6–9.2	43.1–51.6	8.1	46.5	0.7	4.1
Spur	2	1.4–1.5	8.5–9.2	1.5	8.8	0.1	0.4
Spur/branch height ratio	2	18%–20%	–	19%	–	1%	–
Claw IV heights							
Branch	4	7.8–10.0	43.1–55.6	8.7	49.8	0.9	5.3
Spur	1	1.6–1.6	9.1–9.1	1.6	9.1	?	?
Spur/branch height ratio	1	19%–19%	–	19%	–	?	–

cirri (*cirrus internus* 9.3 μm, *cirrus externus* 16.6 μm) weakly outlined, cirrophore *A* tubular and distinct (Fig. 26A). Cirrus *A* short (32.1 μm).

Dorsal plate sculpturing of the *Pseudechiniscus* type, with large and hemispherical *capituli* of endocuticular pillars (Fig. 26B) not joined by *striae*. Pillars heterogeneous in size, their largest *capituli* present in centromedian plate portions of the scapular, paired segmental and pseudosegmental IV' plates (Fig. 26B). Cephalic plate pentapartite, lacking cervical plate (Fig. 26A). Scapular plate comprising the dominant anterior portion and four narrow posterior portions demarcated by weak sutures (Fig. 26A–B). All median plates large: m1–2 bipartite, with reduced posterior portions, m3 rhomboidal and unipartite. Four pairs of lateral intersegmental plates flanking borders of m1–2. Large paired segmental plates I–II and uniform pseudosegmental plate IV' with a sinusoidal posterior margin (Fig. 26B). Short and gently curved incisions on

the caudal plate (Fig. 26A).

Ventral sculpturing faint and poorly developed (Figs. 26C, 27), with larger accumulations of pillars only in the subcephalic and genital areas, and at the level of legs I–III. Sexpartite gonopore placed anteriorly to legs IV, and a trilobed anus between legs IV. Pedal plates formed as belts of large pillars in central portions of legs (Fig. 26A). Pulvini absent. Papillae or spines on legs I absent. Papilla IV present (3.8 μm). Claws minute (7.9–8.4 μm) and isonych; internal claws with robust primary spurs (2.0–2.4 μm) positioned at ca. 25% of the branch height and divergent from it.

Males, juveniles, larvae and eggs: Not found.

Molecular markers and phylogenetic position:

Two gene fragments were sequenced: 28S rRNA (OK048634) and ITS-1 (OK048647). In the updated phylogeny from Gąsiorek et al. (2021c), *P. formosus* sp. nov. is embedded in the subgenus *Pseudechiniscus* and it is sister to a subclade comprising six species,

Table 9. Measurements [in μm] of selected morphological structures of the larvae of *H. crassus* sp. nov. mounted in Hoyer's medium. N, number of specimens/structures measured; Range, refers to the smallest and the largest structure among all measured specimens; SD, standard deviation; *sp*, the proportion between the length of a given structure and the length of the scapular plate

Character	N	Range		Mean		SD	
		μm	<i>sp</i>	μm	<i>sp</i>	μm	<i>sp</i>
Body length	3	127–147	789–885	138	837	10	68
Scapular plate length	2	15.7–16.1	–	15.9	–	0.3	–
Head appendage lengths							
<i>Cirrus internus</i>	3	7.1–9.1	45.2–45.3	7.8	45.3	1.1	0.1
Cephalic papilla	3	3.4–4.5	21.1–26.1	4.0	23.6	0.6	3.5
<i>Cirrus externus</i>	2	10.6–11.1	67.5–67.5	10.9	67.5	0.4	?
Clava	3	3.4–4.0	21.1–22.3	3.6	21.7	0.3	0.8
Cirrus <i>A</i>	2	12.5–13.3	79.6–79.6	12.9	79.6	0.6	?
Cirrus <i>A</i> /Body length ratio	2	9%–9%	–	9%	–	0%	–
Body appendage lengths							
Papilla on leg IV length	2	1.9–2.1	12.1–12.1	2.0	12.1	0.1	?
Claw I heights							
Branch	3	7.5–7.9	46.6–50.3	7.7	48.5	0.2	2.6
Spur	3	1.4–1.5	8.7–9.6	1.5	9.1	0.1	0.6
Spur/branch height ratio	3	19%–19%	–	19%	–	0%	–
Claw II heights							
Branch	3	7.7–8.2	47.8–52.2	8.0	50.0	0.3	3.1
Spur	2	1.5–1.7	10.6–10.6	1.6	10.6	0.1	?
Spur/branch height ratio	2	19%–22%	–	20%	–	2%	–
Claw III heights							
Branch	3	7.3–8.3	45.3–52.9	7.7	49.1	0.6	5.3
Spur	2	1.2–1.3	8.1–8.1	1.3	8.1	0.1	?
Spur/branch height ratio	2	16%–18%	–	17%	–	1%	–
Claw IV heights							
Branch	3	8.3–8.5	52.8–53.5	8.4	53.1	0.1	0.5
Spur	2	1.7–1.8	11.5–11.5	1.8	11.5	0.1	?
Spur/branch height ratio	2	20%–21%	–	21%	–	1%	–

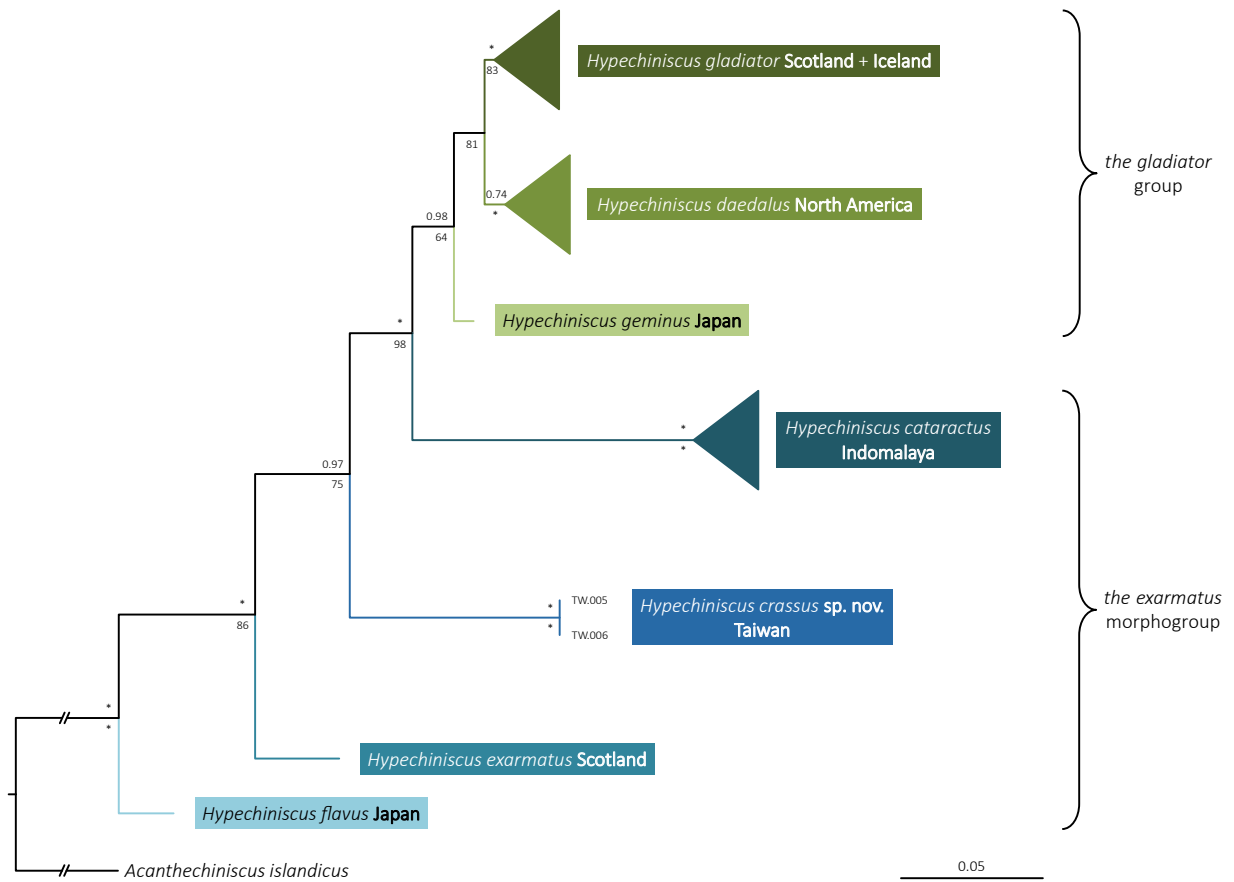


Fig. 19. The concatenated 18S rRNA+28S rRNA+ITS1 consensus Bayesian phylogenetic tree of *Hypechiniscus*, with *Acanthechiniscus islandicus* as the outgroup. Branch support is given as BI posterior probability values above branches and ML bootstrap values below branches. Maximum supports, *i.e.*, 1.00 for BI and 100 for ML, are indicated by asterisks (*). The ML and the BI tree had the same topology. Scale bar represents substitutions per site.

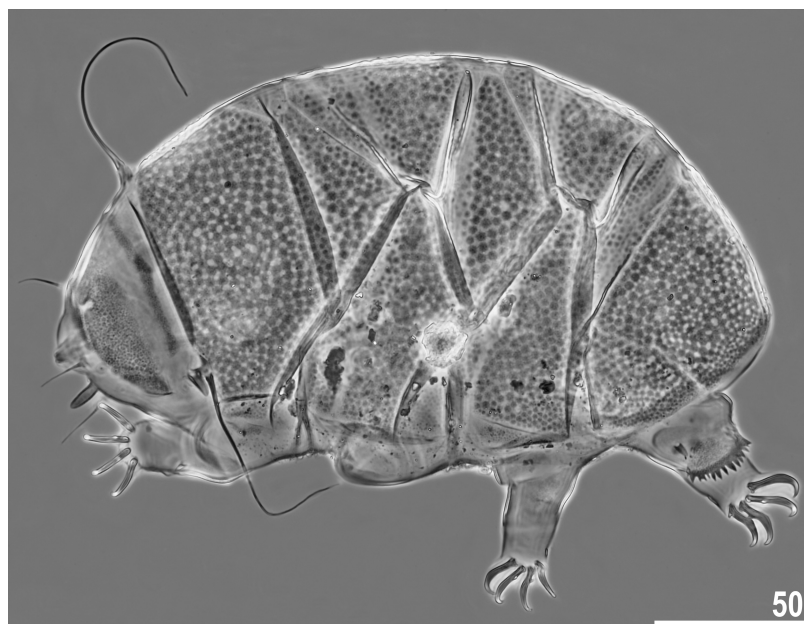


Fig. 20. Habitus of a female of *Nebularmis crebraclava* (PCM). Scale bar in μm .

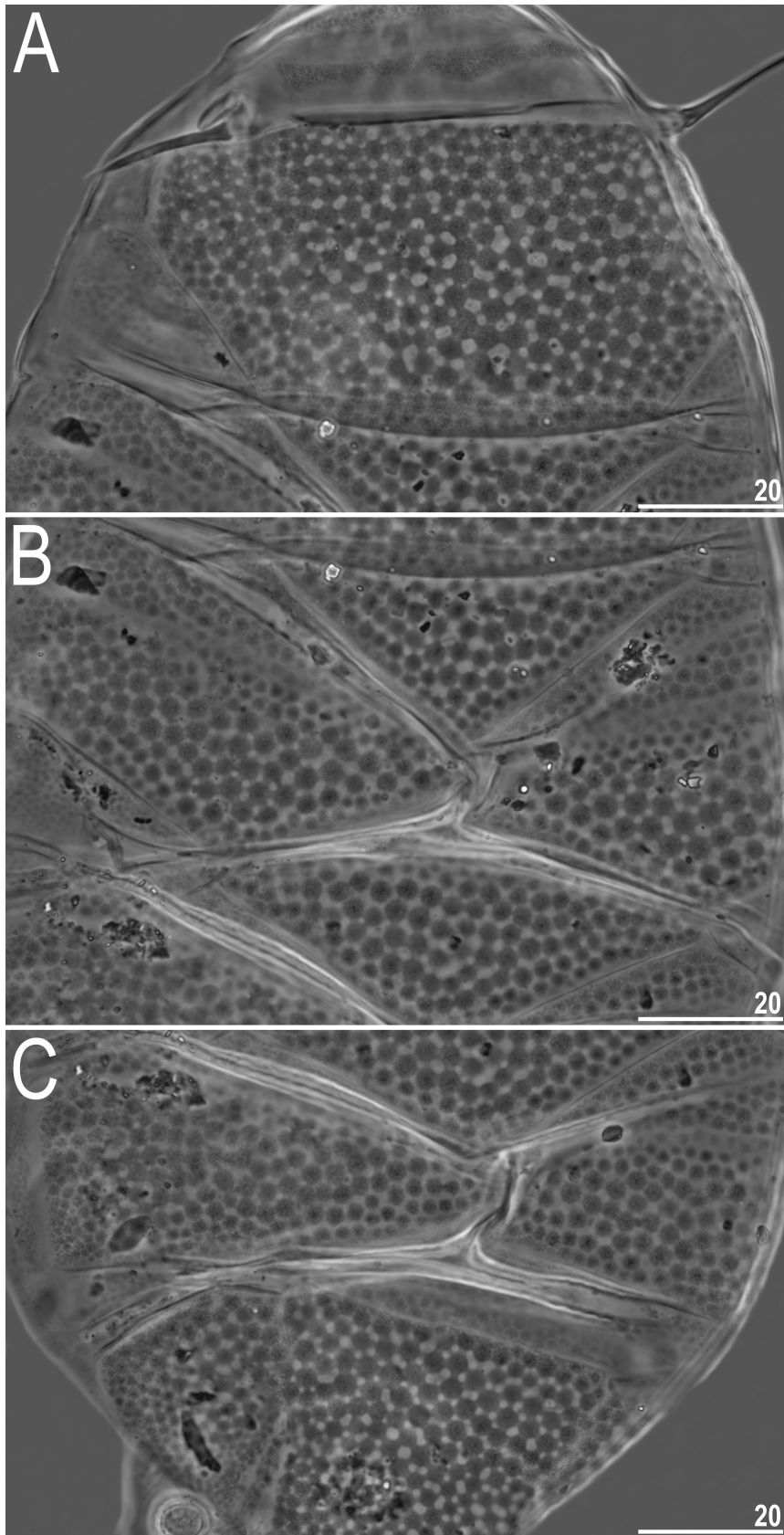


Fig. 21. Sculpturing of a female of *Nebularmis crebraclava* (PCM): A, cephalic region; B, central body portion; C, caudal region. Scale bars in μm .

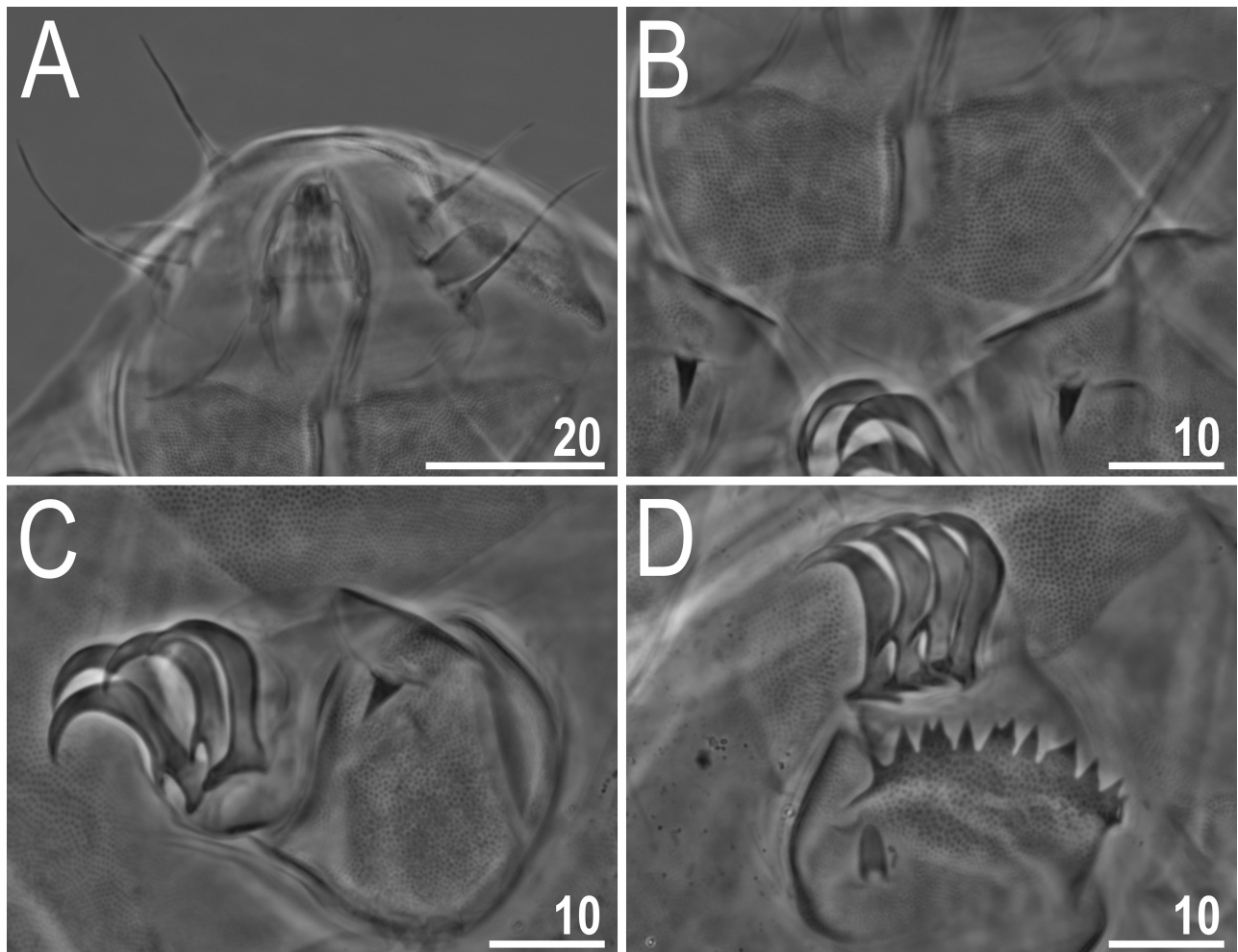


Fig. 22. Morphological details of females of *Nebularmis crebraclava* (PCM): A, cephalic region with peribuccal appendages; B, subcephalic plates and spines I; C, claws I; D, claws IV. Scale bars in μm .

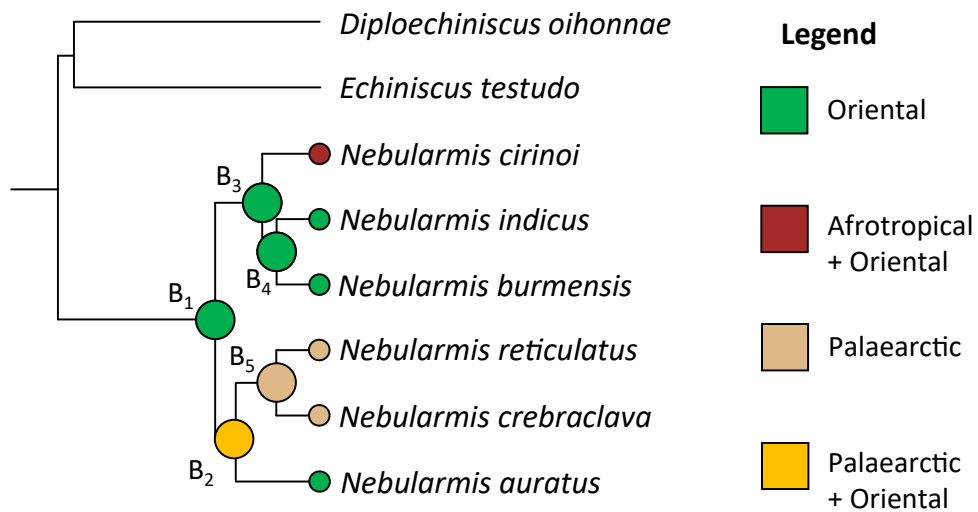


Fig. 23. Historical biogeography of the genus *Nebularmis* as inferred in the S-DIVA on the Bayesian phylogenetic tree under the random local clock with the speciation: Yule process as the tree prior. B1–B5 denote subsequent nodes, all but B2 (0.85) had maximal (1.00) support. *Echiniscus testudo* and *Diploechiniscus oihonnae* were used as outgroups.

including *P. (P.) asper*, *P. (P.)shintai*, and *P. (P.) totoro* sp. nov. (Fig. 30).

Type material: Holotype (adult female on slide TW.007.01) deposited in the Jagiellonian University. One specimen used for DNA sequencing.

Type locality: 24°23'51"N, 121°14'04"E, 3 700 m asl: Taiwan, Snow Mountain (Xueshan), North Peak. Mosses from rocks exposed to sun.

Etymology: The name has a twofold meaning, as in Latin *formosus* = beautiful, describing the dorsal plate sculpturing, and the former name of Taiwan, derived from Portuguese, was Formosa. Adjective in the nominative singular.

Differential diagnosis: Species representing the subgenus *Pseudechiniscus* are morphologically more similar to each other than species in the subgenus *Meridioniscus* (Gąsiorek et al. 2021c). There are several

species lacking appendages on the posterior margin of the pseudosegmental plate IV' (several species are considered dubious and/or indistinguishable from other congeners due to scarce descriptions and are therefore excluded from the list below, e.g., *P. (P.) clavatus* Mihelčič, 1955 and *P. (P.) megacephalus* Mihelčič, 1951; see Roszkowska et al. 2020, Tumanov 2020, and Gąsiorek et al. 2021c for details) that are differentiated from *P. formosus* sp. nov.:

P. (P.) beasleyi Li et al., 2007, described from the Qinling Mountains (Shaanxi, continental China), by body colour (pale yellow in *P. (P.) formosus* sp. nov. vs red in *P. (P.) beasleyi*) and shorter claws (7.9–8.4 μm in *P. (P.) formosus* sp. nov. vs 9.1–13.1 μm in *P. (P.) beasleyi*).

P. (P.) chengi Xue et al., 2017, also described from mainland China, by body colour (pale yellow in *P. (P.)*

Table 10. Measurements [in μm] of selected morphological structures of the adult females of *N. crebraclava* mounted in Hoyer's medium. N, number of specimens/structures measured; Range, refers to the smallest and the largest structure among all measured specimens; SD, standard deviation; *sp*, the proportion between the length of a given structure and the length of the scapular plate

Character	N	Range		Mean		SD	
		μm	<i>sp</i>	μm	<i>sp</i>	μm	<i>sp</i>
Body length	3	148–240	396–435	203	417	48	20
Scapular plate length	3	37.4–56.9	–	48.3	–	10.0	–
Head appendage lengths							
<i>Cirrus internus</i>	3	10.8–15.4	27.1–30.2	13.8	28.7	2.6	1.6
Cephalic papilla	3	7.8–11.3	19.9–20.9	9.8	20.3	1.8	0.5
<i>Cirrus externus</i>	3	12.3–24.1	32.9–42.4	19.1	38.8	6.1	5.1
Clava	3	5.8–8.8	15.5–16.0	7.6	15.7	1.6	0.3
<i>Cirrus A</i>	3	60.5–85.7	140.9–161.8	72.5	151.1	12.6	10.4
<i>Cirrus A</i> /Body length ratio	3	32%–41%	–	36%	–	4%	–
Body appendage lengths							
Spine on leg I length	3	3.3–4.8	8.1–9.5	4.2	8.8	0.8	0.7
Papilla on leg IV length	3	4.0–5.4	9.5–10.7	4.9	10.2	0.8	0.6
Number of teeth on the collar	3	11–15	–	12.7	–	2.1	–
Claw I heights							
Branch	3	9.9–14.9	26.2–27.5	12.9	26.7	2.6	0.7
Spur	3	2.3–2.9	4.7–6.1	2.5	5.3	0.3	0.7
Spur/branch height ratio	3	17%–23%	–	20%	–	3%	–
Claw II heights							
Branch	3	8.8–14.6	23.5–25.7	12.0	24.7	2.9	1.1
Spur	3	1.8–2.5	4.2–4.9	2.2	4.7	0.4	0.4
Spur/branch height ratio	3	16%–20%	–	19%	–	2%	–
Claw III heights							
Branch	3	9.5–14.7	25.4–26.1	12.5	25.8	2.7	0.3
Spur	3	1.6–2.8	4.3–5.5	2.4	4.9	0.7	0.6
Spur/branch height ratio	3	17%–21%	–	19%	–	2%	–
Claw IV heights							
Branch	3	11.2–17.0	29.4–29.9	14.4	29.8	2.9	0.3
Spur	2	3.2–3.7	6.3–6.5	3.5	6.4	0.4	0.1
Spur/branch height ratio	2	21%–22%	–	22%	–	0%	–

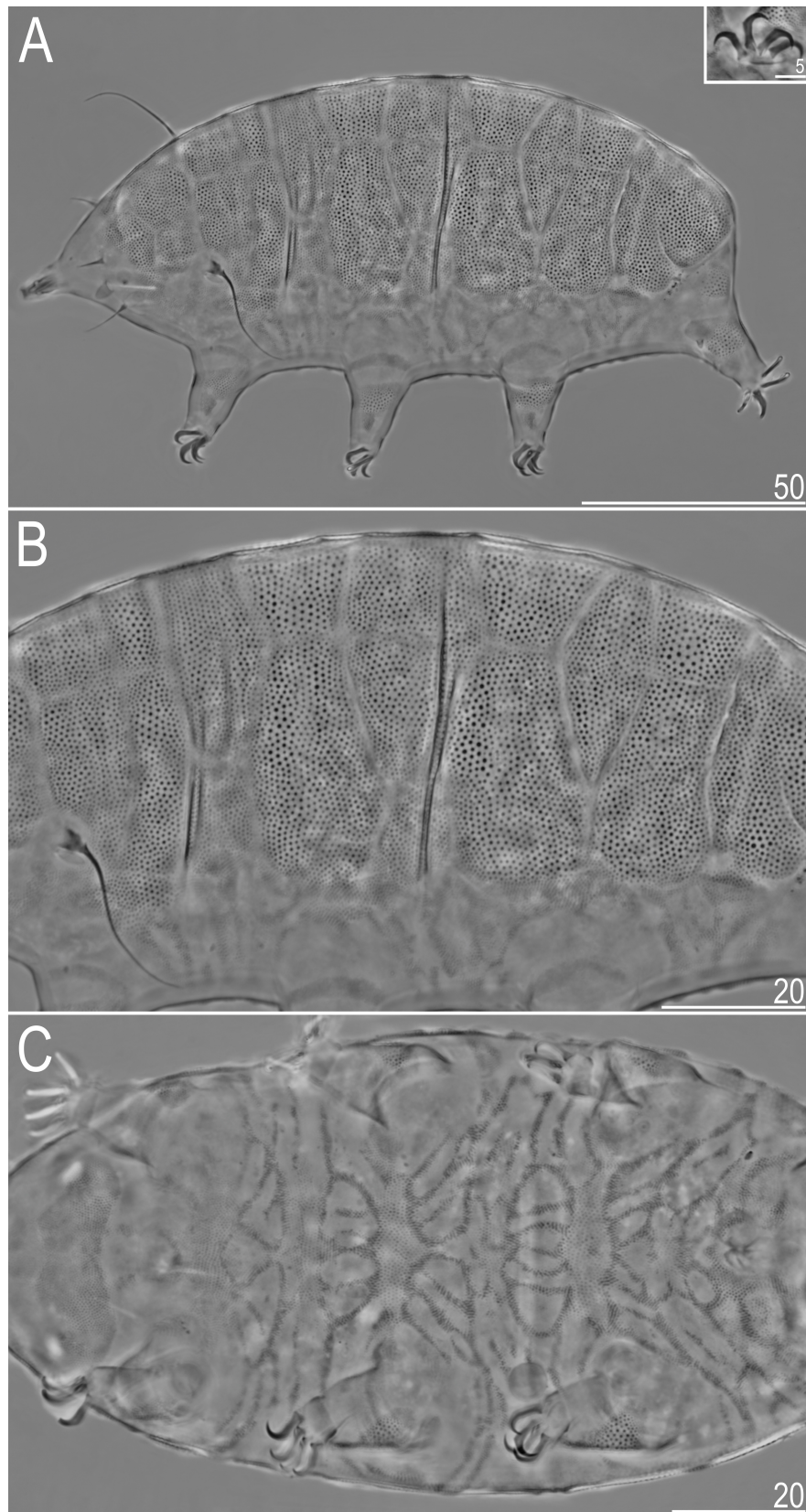


Fig. 24. Morphology of *Pseudechiniscus (Meridioniscus) dreyeri* sp. nov. (PCM): A, holotypic female in dorsolateral view (insert shows claws II); B, dorsal sculpturing; C, ventral sculpturing. Scale bars in µm.

formosus sp. nov. vs brown in *P. (P.) chengi*) and the epicuticular ornamentation on the dorsum (absent in *P. (P.) formosus* sp. nov. vs present in *P. (P.) chengi*).

P. (P.) ehrenbergi Roszkowska et al., 2020, by a longer *cirrus externus* and *cirrus A* (16.6 μm , 32.1 μm in *P. (P.) formosus* sp. nov. vs 9.0–11.7 μm , 21.6–26.8 μm

in *P. (P.) ehrenbergi*).

P. (P.) lacyformis Roszkowska et al., 2020, by the epicuticular ornamentation on the dorsum (absent in *P. (P.) formosus* sp. nov. vs present in *P. (P.) lacyformis*) and shorter *cirrus internus* (9.3 μm in *P. (P.) formosus* sp. nov. vs 10.6–14.0 μm in *P. (P.) lacyformis*).

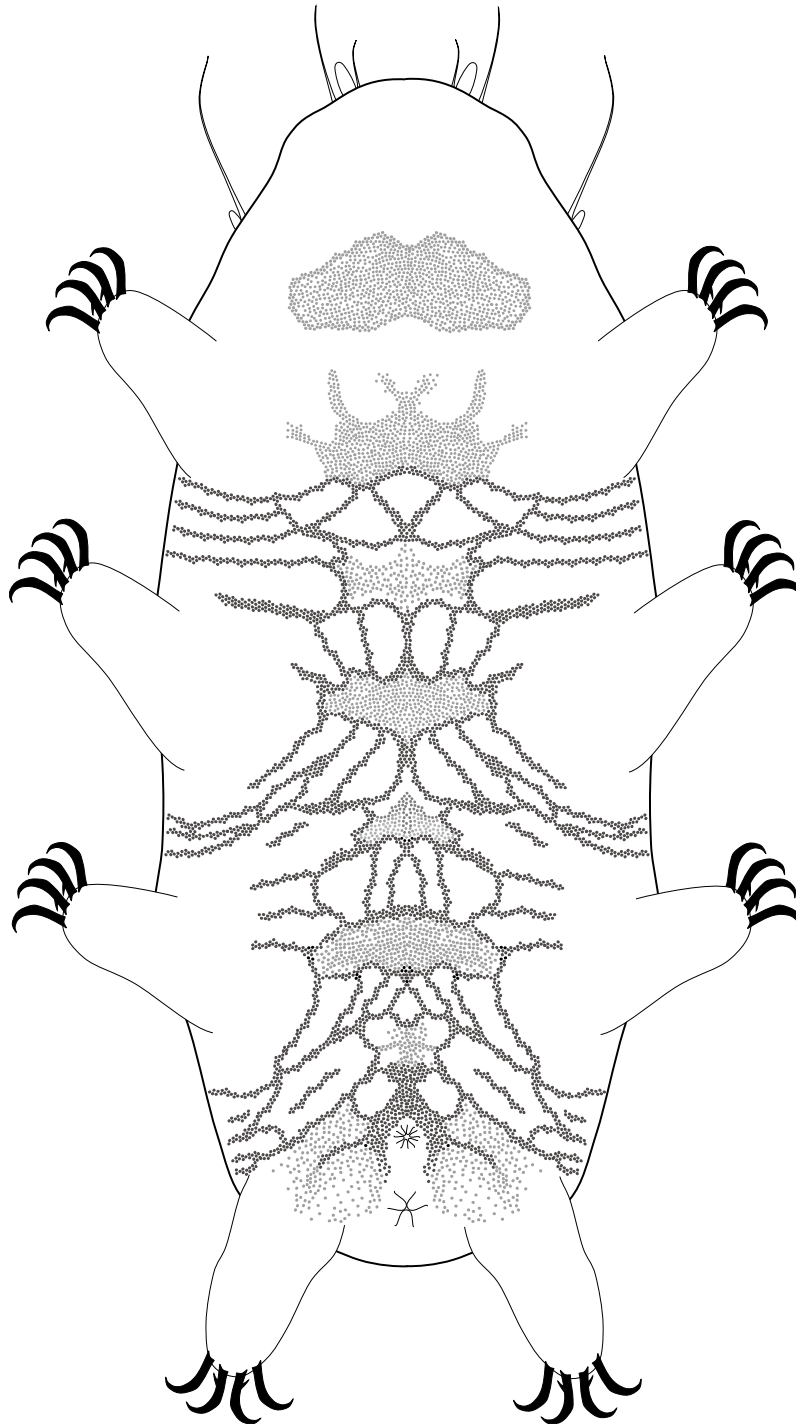


Fig. 25. Schematic depiction of female ventral morphology of *Pseudechiniscus (M.) dreyeri* sp. nov.

P. (P.) shintai Vončina et al., 2020, by body colour (pale yellow in *P. (P.) formosus* sp. nov. vs orange in *P. (P.) shintai*) and the epicuticular ornamentation on the dorsum (absent in *P. (P.) formosus* sp. nov. vs present in *P. (P.) shintai*).

P. (P.) suillus (Ehrenberg, 1853), by relative lengths of some cephalic appendages (*cirrus internus* 37.3, cephalic papilla 15.7, (primary) clava 16.1 in *P. (P.) formosus* sp. nov. vs *cirrus internus* 44.0–49.6, cephalic papilla 19.1–24.3, (primary) clava 20.9–26.8 in *P. (P.) suillus*).

P. (P.) xiai Wang et al., 2018, by body colour (pale yellow in *P. (P.) formosus* sp. nov. vs orange in *P. (P.) xiai*) and the epicuticular ornamentation on the dorsum (absent in *P. (P.) formosus* sp. nov. vs present in *P. (P.) xiai*).

Moreover, *P. (P.) formosus* sp. nov. is also distinguishable from all abovementioned species by the ventral sculpturing pattern.

***Pseudechiniscus (Pseudechiniscus) totoro* sp. nov.**

(Figs. 28–29, Tables 13–14)

urn:lsid:zoobank.org:act:0BA6B1A7-A383-4648-8432-1DCD132D6D75

Tardigrada Register: <http://www.tardigrada.net/register/0114.htm>

Description: Females (i.e., from the third instar onwards; measurements and statistics in table 13): Small, yellow to orange body (Fig. 28A) with minute black eyes; body colour and eyes may dissolve after mounting in Hoyer’s medium. Pseudohemispherical cephalic papillae and elongated (primary) clavae; cirrophores of cephalic cirri merged with *flagellum*. Cirrus *A* short.

Dorsal plate sculpturing of the *Pseudechiniscus* type, with heterogeneous pillars forming patches of

Table 11. Measurements [in µm] of selected morphological structures of the adult females of *P. (M.) dreyeri* sp. nov. mounted in Hoyer’s medium. N, number of specimens/structures measured; Range, refers to the smallest and the largest structure among all measured specimens; SD, standard deviation; *sp*, the proportion between the length of a given structure and the length of the scapular plate

Character	N	Range		Mean		SD		Holotype	
		µm	<i>sp</i>	µm	<i>sp</i>	µm	<i>sp</i>	µm	<i>sp</i>
Body length	15	121–152	609–695	139	655	9	25	151	688
Scapular plate length	15	18.9–23.7	–	21.2	–	1.2	–	21.9	–
Head appendage lengths									
<i>Cirrus internus</i>	14	4.7–7.0	22.0–33.0	6.0	28.4	0.8	3.8	6.1	27.9
Cephalic papilla	15	3.5–5.3	17.9–22.4	4.3	20.3	0.4	1.2	4.6	21.0
<i>Cirrus externus</i>	14	6.8–11.9	31.9–52.2	9.3	43.8	1.6	6.7	10.8	49.3
Clava	14	3.5–4.7	15.2–21.6	4.0	19.1	0.4	1.8	4.2	19.2
<i>Cirrus A</i>	14	21.0–27.0	96.8–126.8	23.1	109.3	2.0	9.3	26.5	121.0
<i>Cirrus A</i> /Body length ratio	14	14%–20%	–	17%	–	1%	–	18%	–
Body appendage lengths									
Papilla on leg IV length	15	1.5–2.3	7.6–10.4	1.9	9.1	0.2	0.7	2.0	9.1
Claw I heights									
Branch	15	5.1–7.5	25.2–34.7	6.7	31.7	0.6	2.3	7.0	32.0
Spur	15	1.4–2.2	6.9–10.3	1.8	8.6	0.2	0.9	1.9	8.7
Spur/branch height ratio	15	23%–31%	–	27%	–	2%	–	27%	–
Claw II heights									
Branch	15	5.5–6.6	26.6–33.3	6.2	29.2	0.3	1.8	6.2	28.3
Spur	15	1.4–2.0	6.6–9.6	1.7	8.1	0.2	0.7	1.8	8.2
Spur/branch height ratio	15	24%–32%	–	28%	–	2%	–	29%	–
Claw III heights									
Branch	15	5.0–6.6	23.9–32.8	6.0	28.5	0.5	2.5	6.5	29.7
Spur	15	1.4–2.1	6.6–9.3	1.6	7.6	0.2	0.7	1.5	6.8
Spur/branch height ratio	15	23%–34%	–	27%	–	4%	–	23%	–
Claw IV heights									
Branch	11	6.6–8.1	31.1–41.5	7.2	34.0	0.5	2.7	7.4	33.8
Spur	11	1.4–2.5	6.7–12.3	2.0	9.5	0.3	1.5	2.0	9.1
Spur/branch height ratio	11	21%–35%	–	28%	–	3%	–	27%	–

similar size (Fig. 28C). *Striae* absent. Pentapartite cephalic plate adjacent to the scapular plate, which is divided into a large anterior portion reaching lateralmost plate margins and two narrow, rectangular posterior portions. Median plates m1–2 bipartite, two pairs of lateral intersegmental plates flanking margins of both m1–2 present; m3 unipartite and rhomboidal. Paired segmental plates I–II and paired pseudosegmental plate IV' present. Caudal plate small and narrow, with short sclerotised incisions (Fig. 28C).

Ventral sculpturing well-developed and reaching lateral body portions (Figs. 28C–D, 29), with larger accumulations of pillars only in the subcephalic and genital areas, and at the level of legs I–III (Fig. 29). A sexpartite gonopore placed anteriorly to legs IV, and a trilobed anus between legs IV. Pedal plates formed as belts of large, widely spaced pillars in the central portions of legs (Fig. 28C). Pulvini absent. Papillae or spines on legs I absent. Papilla IV elongated and small.

Claws minute and isonych; internal claws with delicate, but evident primary spurs positioned at ca. 20–25% of the branch height and divergent from it (Fig. 28A, insert).

Males: Sexual dimorphism evident. Circular gonopore. Body elongated (123–156 µm in length, $sc = 18.2–18.5 \mu\text{m}$, $n = 2$) and slim (Fig. 28B). Cephalic appendages lengths: *cirrus internus* 8.4–9.1 µm, cephalic papilla 3.5–4.0 µm, *cirrus externus* 12.0–13.0 µm, (primary) clava 3.9–5.0 µm, *cirrus A* 25.3–27.5 µm. Clear patches of larger pillars present in the anterior portions of paired segmental plates, in the posterior part of the caudal plate, and on central limb portions. Pulvini clearly marked. Papilla IV length 3.9–4.3 µm. Claws: branch heights 6.4–7.7 µm, spurs 1.8–2.3 µm.

Juveniles (*i.e.*, the second instar; measurements and statistics in table 14): Gonopore absent. Smaller than females, but the body length range overlaps with that of males.

Table 12. Measurements [in µm] of selected morphological structures of the juveniles of *P. (M.) dreyeri* sp. nov. mounted in Hoyer's medium. N, number of specimens/structures measured; Range, refers to the smallest and the largest structure among all measured specimens; SD, standard deviation; *sp*, the proportion between the length of a given structure and the length of the scapular plate

Character	N	Range		Mean		SD	
		µm	<i>sp</i>	µm	<i>sp</i>	µm	<i>sp</i>
Body length	10	100–141	557–732	126	650	11	48
Scapular plate length	10	16.0–23.2	–	19.5	–	2.0	–
Head appendage lengths							
<i>Cirrus internus</i>	10	4.7–7.1	24.1–38.5	5.9	30.7	0.8	4.7
Cephalic papilla	10	2.9–4.9	15.4–25.4	3.9	20.0	0.7	3.2
<i>Cirrus externus</i>	10	7.2–11.4	41.6–55.6	9.6	49.4	1.1	5.1
Clava	10	3.0–4.1	15.7–21.3	3.7	18.8	0.4	1.8
<i>Cirrus A</i>	9	16.4–22.9	96.1–121.8	20.4	107.0	2.2	7.9
<i>Cirrus A</i> /Body length ratio	9	14%–18%	–	16%	–	1%	–
Body appendage lengths							
Papilla on leg IV length	10	1.3–2.0	8.1–10.2	1.8	9.0	0.2	0.8
Claw I heights							
Branch	9	5.0–6.3	26.7–33.1	5.9	30.5	0.5	2.5
Spur	9	1.5–2.0	7.3–11.3	1.8	9.4	0.2	1.3
Spur/branch height ratio	9	27%–34%	–	31%	–	2%	–
Claw II heights							
Branch	9	4.6–6.3	27.2–30.2	5.5	28.6	0.5	1.0
Spur	9	1.4–1.8	6.5–10.0	1.7	8.7	0.1	1.2
Spur/branch height ratio	9	24%–35%	–	30%	–	4%	–
Claw III heights							
Branch	10	4.5–6.2	25.1–31.3	5.5	28.1	0.4	1.7
Spur	10	1.5–1.9	6.5–10.0	1.7	8.6	0.2	1.0
Spur/branch height ratio	10	24%–36%	–	31%	–	4%	–
Claw IV heights							
Branch	10	5.2–7.3	29.9–33.3	6.3	32.1	0.7	1.1
Spur	10	1.7–2.5	9.0–12.6	2.0	10.4	0.3	1.2
Spur/branch height ratio	10	27%–40%	–	33%	–	4%	–

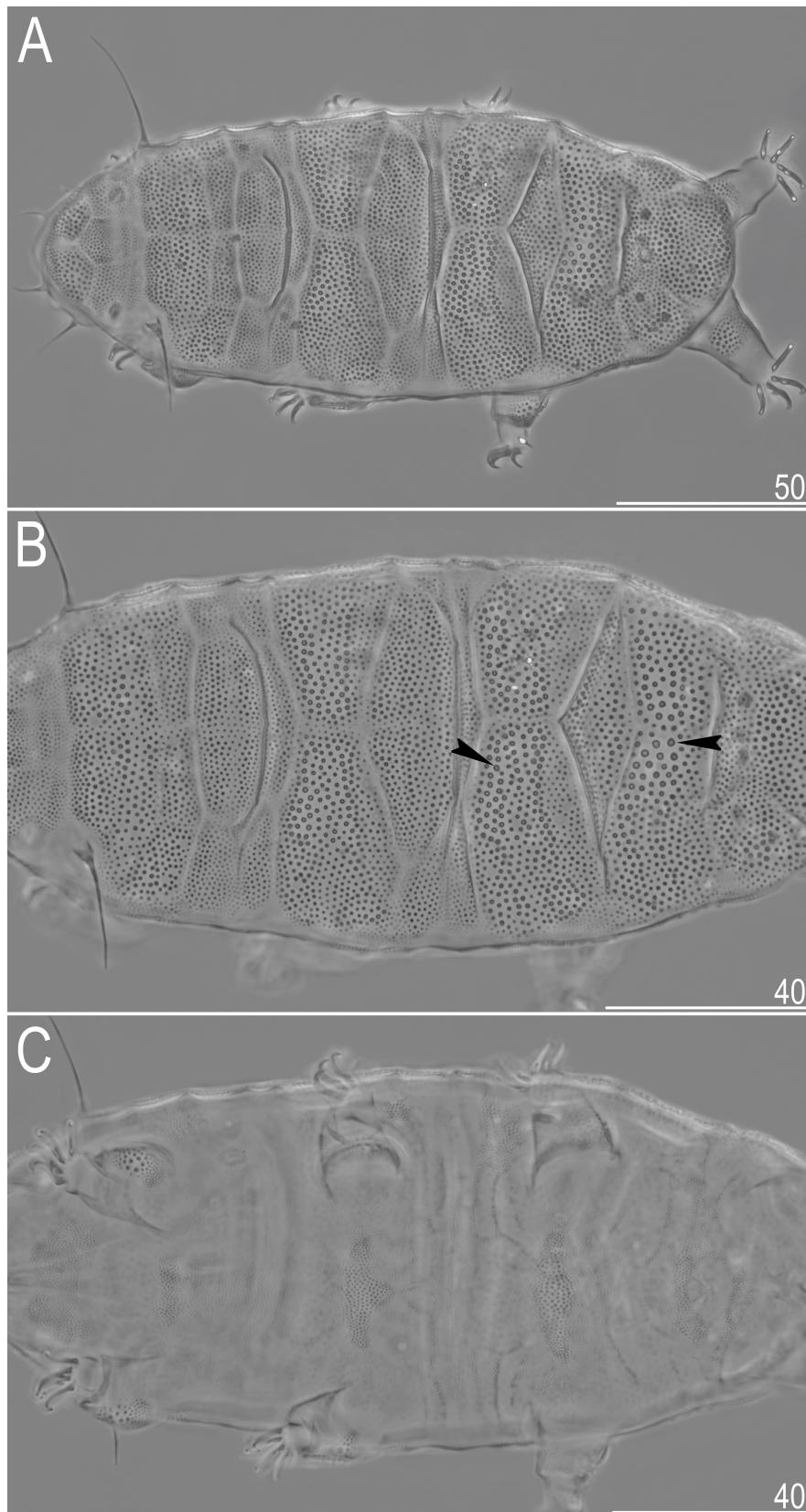


Fig. 26. Morphology of *Pseudechiniscus (Pseudechiniscus) formosus* sp. nov. (PCM): A, holotypic female in dorsal view; B, dorsal sculpturing (arrowheads indicate large *capituli* of pillars); C, ventral sculpturing. Scale bars in μm.

Larvae: Not found.

Eggs: Up to one orange egg per exuvia was found.

Molecular markers and phylogenetic position: Single haplotypes were found in 18S rRNA (OK048616–9) and 28S rRNA (OK048635–8) and four haplotypes were uncovered in ITS-1 (intraspecific

p-distances = 0.2–1.6%; OK048648–51). In the updated phylogeny from Gąsiorek et al. (2021c), the closest relative of *P. (P.) totoro* sp. nov. is *P. (P.) shintai* from Japan (Fig. 30).

Type material: Holotype (adult female on the slide TW.005.11), allotype (adult male on the slide

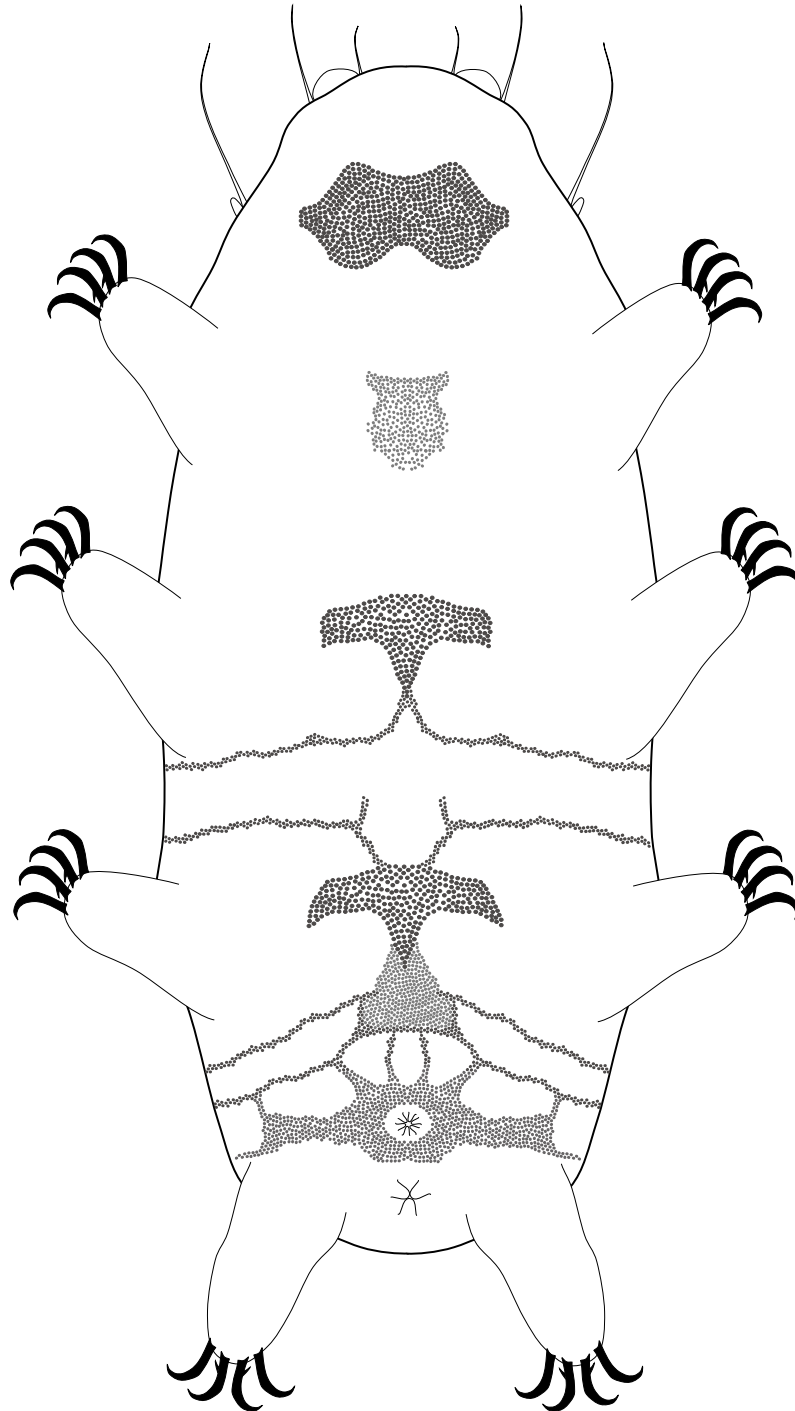


Fig. 27. Schematic depiction of female ventral morphology of *Pseudechiniscus (P.) formosus* sp. nov.

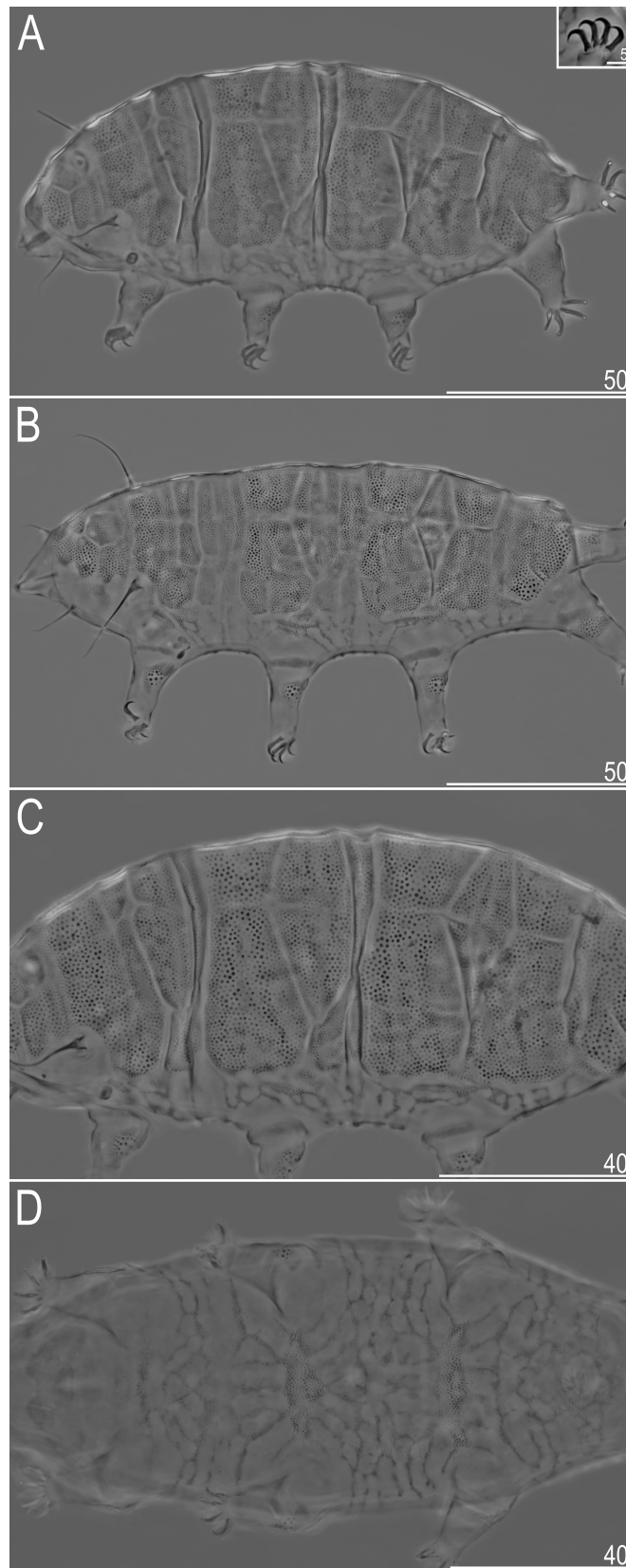


Fig. 28. Morphology of *Pseudechiniscus (Pseudechiniscus) totoro* sp. nov. (PCM): A, holotypic female in dorsolateral view (insert shows claws III); B, allotypic male in dorsolateral view; C, dorsal sculpturing; D, ventral sculpturing. Scale bars in μm.

TW.005.12), 24 paratypes: 13 adult females, 6 adult males, and 5 juveniles on the slides TW.005.08–16. Six specimens were used for DNA sequencing, including two retrieved as hologenophores. Holotype deposited in the Biodiversity Research Center of Academia Sinica (ASIZ01000035), two paratypes (NHMD-915765)

deposited in the Natural History Museum of Denmark, and the remaining material stored at the Jagiellonian University.

Type locality: 24°23'18"N, 121°15'39"E, 3 200 m asl: Taiwan, Snow Mountain (Xueshan), East Peak. Mosses from rocks exposed to sun.

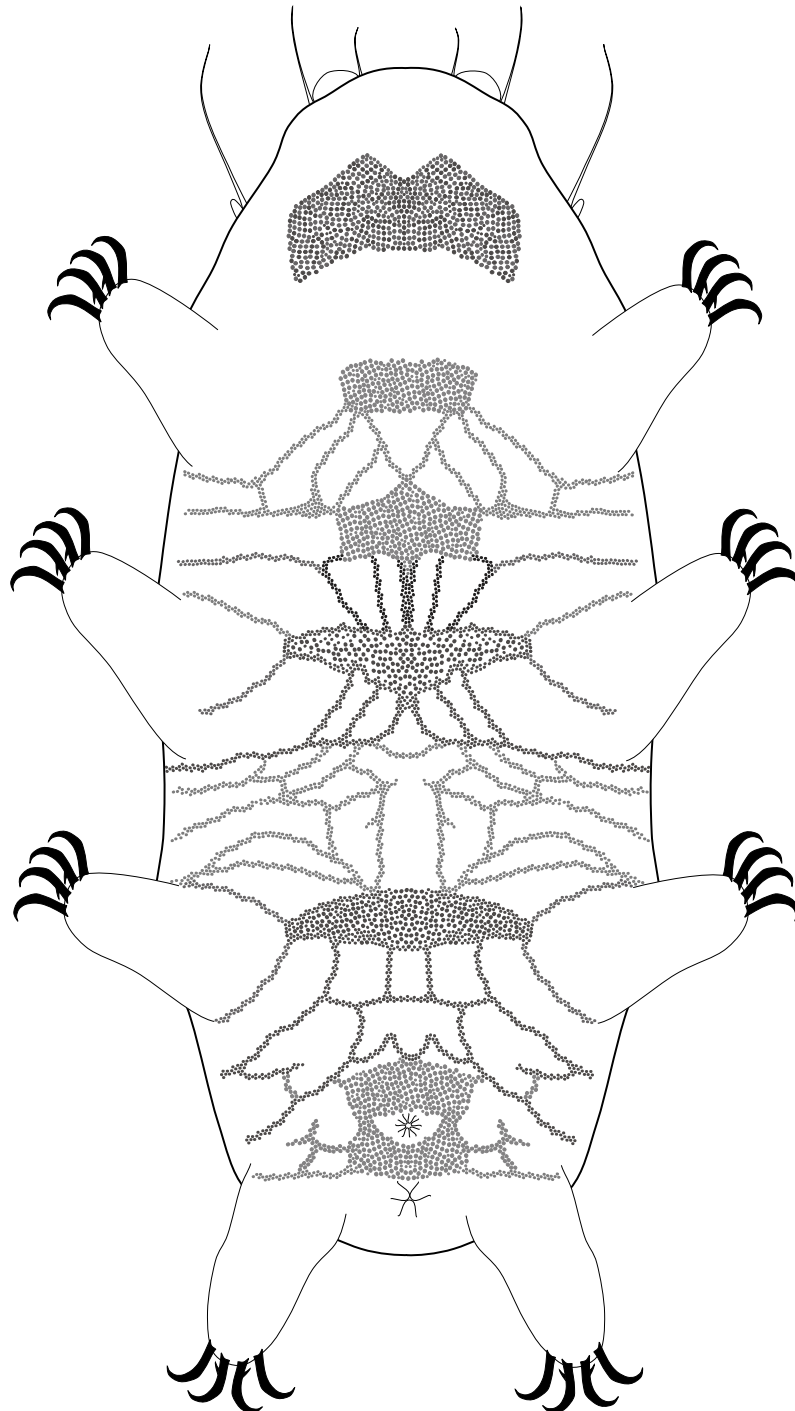


Fig. 29. Schematic depiction of female ventral morphology of *Pseudechiniscus (P.) toloro* sp. nov.

Etymology: The specific epithet is derived from the Japanese animated movie *My Neighbour Totoro* (*Tonari no Totoro*) by Hayao Miyazaki (1988) and commemorates Totoro, the forest spirit and the symbol of Studio Ghibli. Noun in apposition.

Differential diagnosis: Due to the absence of projections/appendages on the posterior margin of the pseudosegmental plate IV', the same species must be compared with *P. (P.) totoro* sp. nov. as for *P. (P.) formosus* sp. nov. Specifically, *Pseudechiniscus (P.) totoro* sp. nov. differs from:

P. (P.) beasleyi, by a different body colour (yellow-orange in *P. (P.) totoro* sp. nov. vs red in *P. (P.) beasleyi*) and shorter claws (6.1–8.0 μm in *P. (P.) totoro* sp. nov. vs 9.1–13.1 μm in *P. (P.) beasleyi*).

P. (P.) chengi, by a different body colour (yellow-orange in *P. (P.) totoro* sp. nov. vs brown in *P. (P.) chengi*) and shorter claws (6.1–8.0 μm in *P. (P.) totoro*

sp. nov. vs 7.9–12.2 μm in *P. (P.) chengi*).

P. (P.) ehrenbergi, by the absence of papilla I (present in *P. (P.) ehrenbergi*).

P. (P.) formosus sp. nov., by the dorsal epicuticular ornamentation (present in *P. (P.) totoro* sp. nov. vs absent in *P. (P.) formosus* sp. nov.) and the spacing of dorsal pillars (widely spaced in *P. (P.) formosus* sp. nov. vs densely arranged in *P. (P.) totoro* sp. nov.).

P. (P.) lacyformis, by the lengths of peribuccal cirri (*cirrus internus* 5.8–11.0 μm, *cirrus externus* 7.8–14.0 μm in *P. (P.) totoro* sp. nov. vs *cirrus internus* 10.6–14.0 μm, *cirrus externus* 14.1–19.4 μm in *P. (P.) lacyformis*).

P. (P.)shintai, by the density and size of pillars present in leg patches (dense and large in *P. (P.) totoro* sp. nov. vs more widely spaced and smaller in *P. (P.)shintai*).

P. (P.) suillus, by the morphology and position

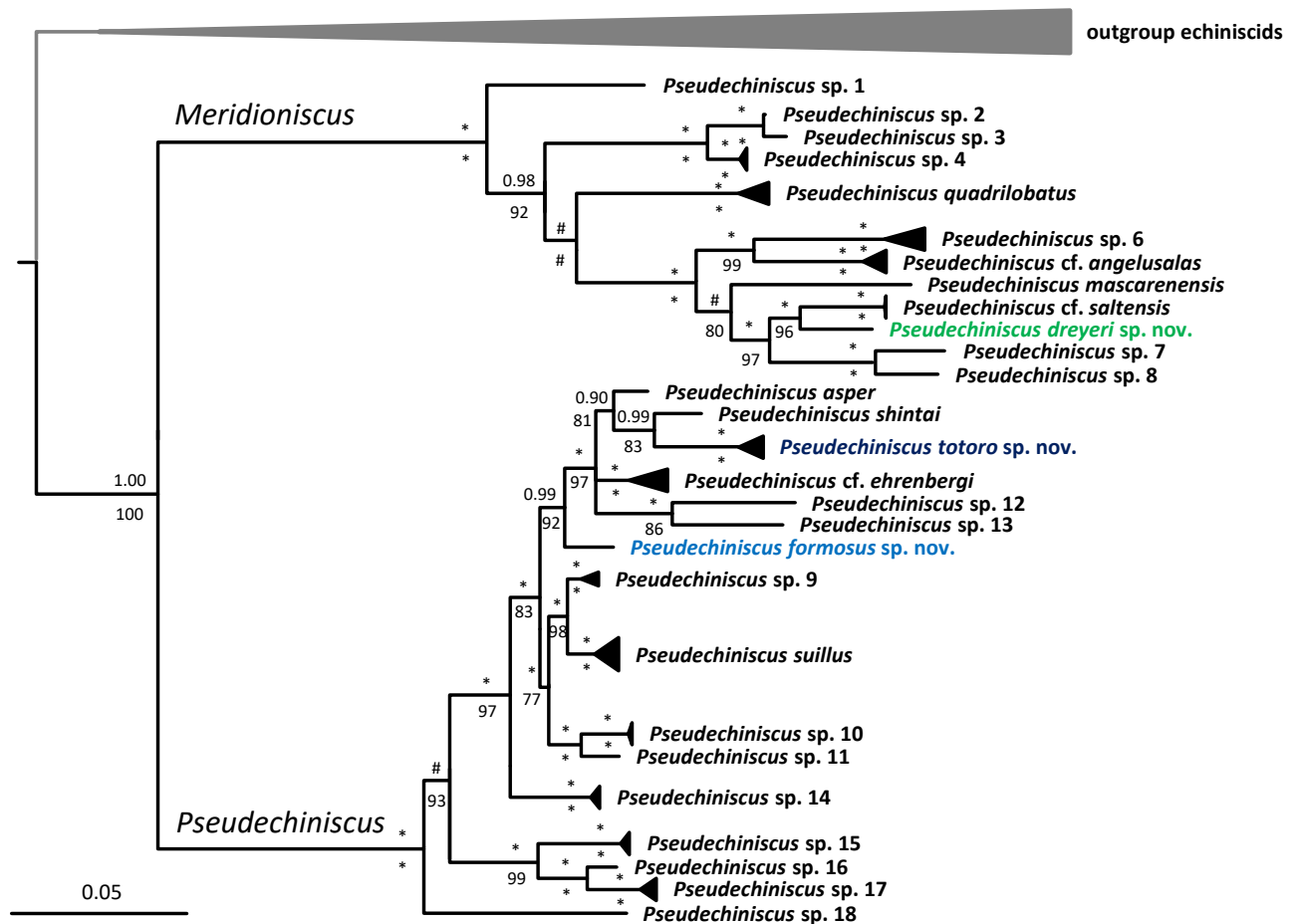


Fig. 30. Position of the Taiwanese species on the phylogenetic tree of the genus *Pseudechiniscus* based on the concatenated matrix (18S rRNA+28S rRNA+ITS-1). Values at nodes separated by forward slashes signify Bayesian posterior probability and bootstrap values (ML), respectively. Maximum supports, i.e., 1.00 for BI and 100 for ML, are indicated by asterisks (*), whereas nodes unsupported in either analysis are marked by hashtags (#). The scale refers to the Bayesian consensus tree and represents substitutions per site. Species numbering preserved from Gąsiorek et al. (2021c).

of primary spurs on internal claws (delicate spurs positioned lower on claw branches in *P. (P.) toloro* sp. nov. vs robust spurs positioned higher on claw branches in *P. (P.) suillus*, see Grobys et al. 2020).

P. (P.) xiai, by the division of the pseudosegmental plate IV' (divided by a median longitudinal suture in *P. (P.) toloro* sp. nov. vs uniform in *P. (P.) xiai*) and slightly shorter claws I–III (6.1–7.5 μm in *P. (P.) toloro* sp. nov. vs 7.6–10.5 μm in *P. (P.) xiai*).

Moreover, *P. (P.) toloro* sp. nov. is distinguishable from all abovementioned species by the ventral sculpturing pattern.

DISCUSSION

The composition of the Taiwanese tardigrade fauna is of particular interest from the biogeographic point of view, as the island constitutes a transient zone,

where the Oriental and Palaearctic elements mix and form a unique fauna with a high fraction of endemics (He et al. 2018). Many animal endemics evolved in isolation among high mountain ranges of Taiwan (Shih et al. 2006), which also exhibit habitats suitable for cold stenothermic species that are widespread in the Palaearctic. In parallel, subtropical evergreen forests growing in the lowlands create favourable conditions for species widely distributed in the tropics. Thus, three kinds of species with broad geographic ranges can be distinguished in the Taiwanese tardigrade fauna: (1) widely distributed species, typically associated with colder habitats (probably cosmopolitan *E. blumi* and Palaearctic *N. reticulatus*), (2) pantropical species or species widely distributed in the Pacific area (*E. lineatus*, *Kristenseniscus tessellatus*; see Suzuki et al. 2018 and Gąsiorek et al. 2019a b), and (3) probable allochthons/ecdemics introduced by humans (*V. perviridis*; see Kaczmarek and Michalczyk 2010).

Table 13. Measurements [in μm] of selected morphological structures of the adult females of *P. (P.) toloro* sp. nov. mounted in Hoyer's medium. N, number of specimens/structures measured; Range, refers to the smallest and the largest structure among all measured specimens; SD, standard deviation; *sp*, the proportion between the length of a given structure and the length of the scapular plate

Character	N	Range		Mean		SD		Holotype	
		μm	<i>sp</i>	μm	<i>sp</i>	μm	<i>sp</i>	μm	<i>sp</i>
Body length	8	141–170	701–809	158	747	9	35	155	752
Scapular plate length	8	18.9–23.4	–	21.2	–	1.7	–	20.6	–
Head appendage lengths									
Cirrus <i>internus</i>	8	5.8–11.0	25.6–50.7	8.2	39.1	1.5	8.4	8.9	43.2
Cephalic papilla	8	2.4–4.0	11.5–20.6	3.3	15.6	0.6	3.2	2.4	11.7
Cirrus <i>externus</i>	8	7.8–14.0	41.1–71.4	12.2	57.8	2.0	9.8	13.8	67.0
Clava	8	4.0–5.5	19.9–23.8	4.6	21.6	0.6	1.5	4.1	19.9
Cirrus <i>A</i>	8	23.7–30.8	108.8–150.8	27.1	128.8	2.3	16.4	26.9	130.6
Cirrus <i>A</i> /Body length ratio	8	14%–20%	–	17%	–	2%	–	17%	–
Body appendage lengths									
Papilla on leg IV length	8	3.2–4.5	15.9–22.2	3.9	18.4	0.4	2.0	3.9	18.9
Claw I heights									
Branch	6	6.4–7.5	29.5–34.7	6.8	32.6	0.4	2.1	7.1	34.5
Spur	6	1.4–2.3	6.5–11.2	2.0	9.5	0.3	1.7	2.3	11.2
Spur/branch height ratio	6	22%–32%	–	29%	–	4%	–	32%	–
Claw II heights									
Branch	6	6.1–6.6	27.4–32.8	6.4	30.8	0.2	2.1	6.5	31.6
Spur	6	1.7–2.0	7.9–10.5	1.8	8.9	0.1	1.0	1.8	8.7
Spur/branch height ratio	6	26%–33%	–	29%	–	2%	–	28%	–
Claw III heights									
Branch	7	6.1–7.0	27.8–34.0	6.4	30.9	0.3	2.7	7.0	34.0
Spur	7	1.3–1.9	6.0–10.1	1.7	8.3	0.2	1.4	1.8	8.7
Spur/branch height ratio	7	21%–30%	–	27%	–	3%	–	26%	–
Claw IV heights									
Branch	5	6.9–8.0	33.5–38.0	7.5	35.8	0.5	1.9	?	?
Spur	5	2.2–2.8	10.7–12.3	2.4	11.6	0.2	0.7	?	?
Spur/branch height ratio	5	29%–37%	–	32%	–	3%	–	?	–

Given that species endemic to Taiwan have been identified in other invertebrate groups, it is possible that also tardigrades exhibiting geographic distributions limited to the island may be uncovered with intensified sampling. Lastly, several Taiwanese echiniscid species can be defined as elements distinct for the Eastern Palaearctic (*E. clevelandi*, *E. hoonsooi*, *E. semifoveolatus*, *N. crebraclava*, and likely *Stellariscus pseudelegans* not found in our samples; Fig. 31); this set of taxa is supplemented by *Echiniscus cheonyoungi* Moon & Kim, 1994, *Echiniscus laterosetosus* Ito, 1993, *Echiniscus polygonalis* Ito, 1993, *Hypechiniscus geminus* Gąsiorek et al., 2021, *H. flavus* Gąsiorek et al., 2021, and *Stellariscus elegans* (Richters, 1907).

There is evidence for close phylogenetic relationships between some of the Taiwanese echiniscids and their continental Palaearctic relatives. The sister relationship between *E. clevelandi* and *E. hoonsooi* within the *E. virginicus* complex (Fig. 11)

supports the hypothesis that these two taxa evolved from a common ancestor in the Far East Palaearctic. This also suggests that *E. cheonyoungi*, described from the Korean Peninsula, is related to this clade. Gąsiorek et al. (2019b) hypothesised allopatric distributions of two other representatives of the complex, *E. lineatus* and *E. virginicus*, thus it would be desirable to verify whether sympatry occurs between the Asian members of this group or if they are separated in space by topographic factors, such as elevation (both *E. clevelandi* and *E. lineatus* inhabit China and Taiwan, and *E. hoonsooi* and *E. cf. virginicus* were reported from Japan (Suzuki 2017; Sato and Suzuki 2020). Moreover, many old Japanese tardigrade reports should be considered dubious, as they represent species with common *Echiniscus* chaetotaxy morphotypes, and chaetotaxy is usually unreliable when considered without the dorsal sculpturing (see records of *E. dreyfusi* de Barros, 1942, *E. fischeri* Richters, 1911, *E. spiniger* Richters, 1904, or

Table 14. Measurements [in μm] of selected morphological structures of the juveniles of *P. (P.) totoro* sp. nov. mounted in Hoyer’s medium. N, number of specimens/structures measured; Range, refers to the smallest and the largest structure among all measured specimens; SD, standard deviation; *sp*, the proportion between the length of a given structure and the length of the scapular plate

Character	N	Range		Mean		SD	
		μm	<i>sp</i>	μm	<i>sp</i>	μm	<i>sp</i>
Body length	5	94–138	602–810	128	703	19	74
Scapular plate length	5	11.6–22.3	–	18.6	–	4.1	–
Head appendage lengths							
Cirrus <i>internus</i>	4	5.7–6.3	25.6–32.0	6.1	30.1	0.3	3.0
Cephalic papilla	5	2.5–3.4	11.2–24.1	3.0	16.8	0.4	4.7
Cirrus <i>externus</i>	4	9.8–12.4	49.7–57.9	11.0	53.9	1.2	3.6
Clava	5	3.4–4.6	17.9–29.3	4.0	22.1	0.5	4.7
Cirrus <i>A</i>	4	14.1–22.1	106.6–121.6	19.8	113.3	3.8	6.2
Cirrus <i>A</i> /Body length ratio	4	15%–16%	–	16%	–	0%	–
Body appendage lengths							
Papilla on leg IV length	5	1.5–3.4	10.2–17.3	2.5	13.3	0.7	2.6
Claw I heights							
Branch	4	6.1–7.3	31.3–33.0	6.5	32.1	0.5	0.9
Spur	4	1.8–2.3	9.1–10.8	2.0	10.0	0.2	0.7
Spur/branch height ratio	4	29%–34%	–	31%	–	3%	–
Claw II heights							
Branch	5	4.5–6.4	28.4–38.8	5.6	31.0	0.7	4.4
Spur	5	1.0–2.0	7.1–10.3	1.5	8.3	0.4	1.2
Spur/branch height ratio	5	22%–36%	–	27%	–	5%	–
Claw III heights							
Branch	4	4.1–7.0	27.9–35.3	5.7	31.4	1.2	3.0
Spur	4	0.8–1.9	6.9–8.6	1.5	8.2	0.5	0.8
Spur/branch height ratio	4	20%–31%	–	26%	–	5%	–
Claw IV heights							
Branch	3	5.1–7.5	33.6–44.0	6.6	38.2	1.3	5.3
Spur	3	1.0–2.0	8.6–10.3	1.7	9.3	0.6	0.9
Spur/branch height ratio	3	20%–28%	–	25%	–	4%	–

E. spinulosus (Doyère, 1840) in Suzuki (2017) that were most probably misidentified with different members of the *E. spinulosus* and the *E. virginicus* complexes). This suggests a putative presence of other autochthonous/endemic echiniscid species in the Far East Asia.

The second argument for the Palaearctic origin of some Taiwanese species is the sister relationship between *N. crebraclava* and *N. reticulatus* (Fig. 23). The latter taxon is a widespread, but not frequently encountered echiniscid (Gąsiorek et al. 2019c 2021b), whereas *N. crebraclava* is known only from two Asian locales (Fig. 31). We do not exclude the possibility that some of numerous Asian records of *N. reticulatus* predating its redescription (Gąsiorek et al. 2019c) represent in fact other *Nebularmis* species, but testing this hypothesis necessitates further sampling. Generally, analogously to what was found for the Japanese fauna up to date (Suzuki 2017), the current data imply a predominantly Palaearctic character of the Taiwanese echiniscid fauna, with the influence of Oriental/tropical elements in the locations with subtropical warm climate.

Similar results were recently presented for the Japanese Milnesiidae: Palaearctic *Milnesium tardigradum* Doyère, 1840 was reported from Honshu, while *M. pacificum* was described from subtropical Japanese islands, and its closest relatives originate from the Neotropics (Sugiura et al. 2020; Morek and Michalczyk 2020). Altogether, these data suggest that both the Taiwanese and Japanese tardigrade faunae deserve much more attention, as they represent a conglomerate of taxa with various biogeographic origins.

CONCLUSIONS

Four new echiniscid species are described by means of integrative taxonomy from the alpine zone of Taiwanese mountains, including a representative of the rare genus *Hypechiniscus*. Furthermore, we reported 11 species that constitute new records for Taiwan. These increase the number of confidently identified echiniscid species known in Taiwan from four to 15.

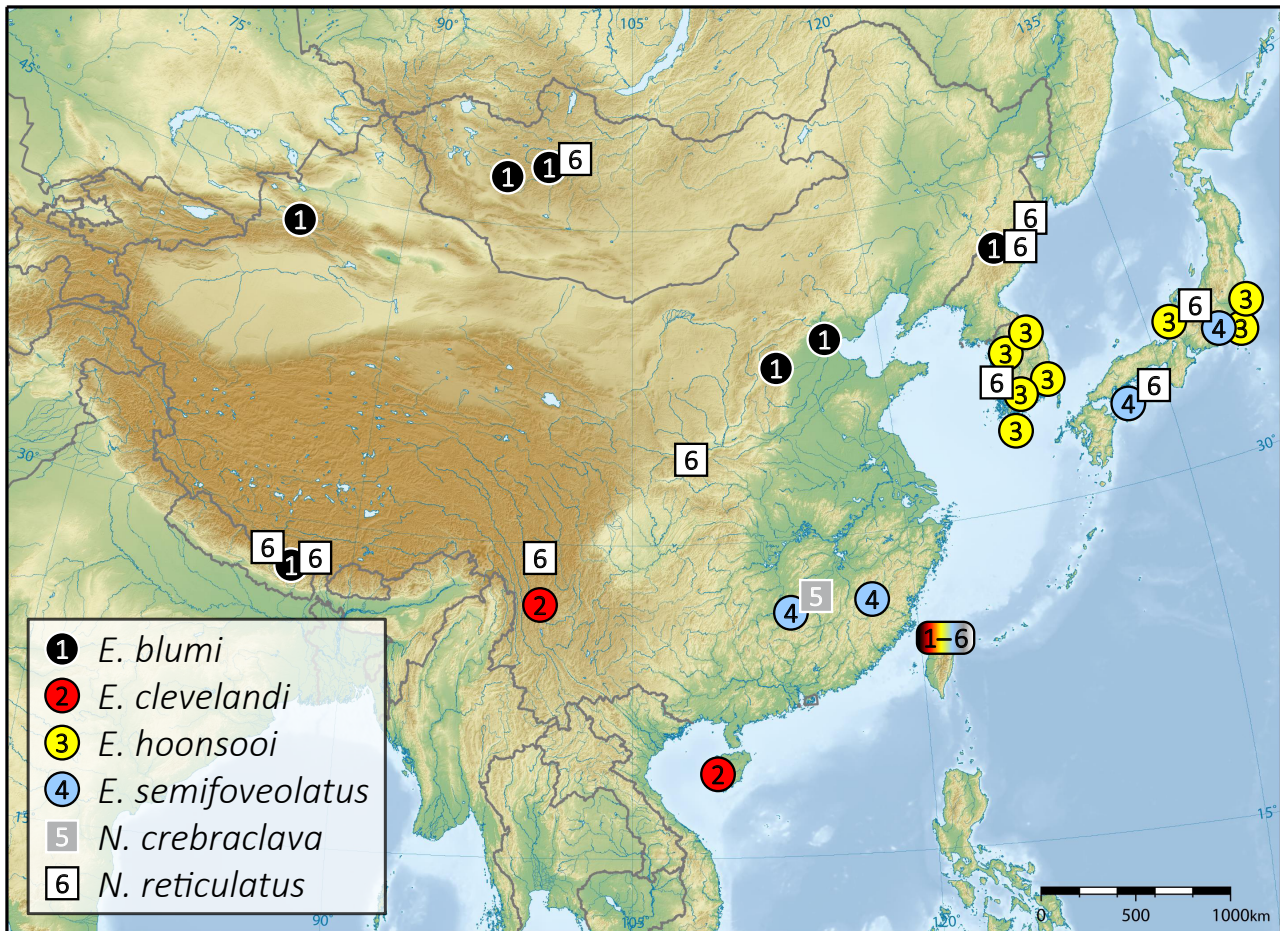


Fig. 31. Distributions of *Echiniscus* and *Nebularmis* species addressed in the present study.

The fact that as many as eleven species have been found in as few as seven moss samples, suggests that the Taiwanese tardigrade fauna may be very diverse. Novel morphological and genetic data for *Echiniscus clevelandi* and *Nebularmis crebraclava* allowed us to amend the descriptions of these species. We hypothesise that the Taiwanese and Japanese tardigrade faunas have transient features of the Oriental-tropical and the Palaearctic region.

Acknowledgments: This work and the four new species names were registered with ZooBank under urn:lsid:zoobank.org:pub:DDF334F9-E702-4B5A-AAE3-C4C57F9EB51E. We are grateful to Niklas Dreyer and Szymon Bacher for the material collected in Asia. Two Reviewers improved this manuscript with their suggestions. The samples were collected with permits from local Taiwanese governments granted to Jen-Pan Huang. The study was supported by the Polish National Science Centre via the ‘Preludium’ (grant no. 2019/33/N/NZ8/02777 to PG, supervised by ŁM) and ‘Sonata Bis’ programmes (grant no. 2016/22/E/NZ8/00417 to ŁM). PG is a recipient of the ‘Etiuda’ (2020/36/T/NZ8/00360, funded by the National Science Centre) and ‘Start’ stipends (START 28.2020, funded by the Foundation for Polish Science).

Authors’ contributions: RMK and PG conceived the study; KV and PG isolated tardigrades from the samples, prepared permanent slides, extracted DNA and Sanger-sequenced individuals, performed qualitative and quantitative morphological analyses, and assembled the figures; PG performed phylogenies and historical biogeography analyses and delineated the new species; PG and ŁM provided funding, interpreted the data and wrote the manuscript; all authors read, corrected and approved the final version of the manuscript.

Competing interests: The authors declare no conflict of interest.

Availability of data and materials: The key datasets from the manuscript are available as additional supplementary files. Sequences are available in GenBank.

Consent for publication: The authors give their consent to publish.

Ethics approval consent to participate: Ethics approval is not necessary.

REFERENCES

- Abe W, Ito M, Takeda M. 2000. First record of *Echiniscus hoonsooi* (Tardigrada: Echiniscidae) from Japan. *Spec Divers* **5**:103–110. doi:10.12782/specdiv.5.103.
- Beasley CW. 1999. A new species of *Echiniscus* (Tardigrada, Echiniscidae) from Northern Yunnan Province, China. *Zool Anz* **238**:135–138.
- Casquet JT, Thebaud C, Gillespie RG. 2012. Chelex without boiling, a rapid and easy technique to obtain stable amplifiable DNA from small amounts of ethanol-stored spiders. *Mol Ecol Resour* **12**:136–141. doi:10.1111/j.1755-0998.2011.03073.x.
- Cesari M, Montanari M, Kristensen RM, Bertolani R, Guidetti R, Rebecchi L. 2020. An integrated study of the biodiversity within the *Pseudechiniscus suillus–facettalis* group (Heterotardigrada: Echiniscidae). *Zool J Linn Soc* **188**:717–732. doi:10.1093/zoolinnean/zlz045.
- Dastyh H. 1980. Niesporczaki (Tardigrada) Tatrzńskiego Parku Narodowego. *Monogr Faun Pol* **9**:1–232.
- Dastyh H. 1999. A new species of the genus *Mopsechiniscus* Du Bois-Reymond Marcus, 1944 (Tardigrada) from the Venezuelan Andes. *Acta Biol Benrod* **10**:91–101.
- de Barros R. 1942. Tardígrados do estado de São Paulo, Brasil. I. Introdução. Gêneros '*Echiniscus*' e '*Pseudechiniscus*'. *Rev Bras Biol* **2**:257–269.
- Degma P, Bertolani R, Guidetti R. 2021. Actual checklist of Tardigrada species. doi:10.25431/11380_1178608. Accessed 22 July 2021.
- Degma P, Meyer HA, Hinton JG. 2021. *Claxtonia goni*, a new species of Tardigrada (Heterotardigrada, Echiniscidae) from the island of Maui (Hawaiian Islands, U.S.A., North Pacific Ocean), with notes to the genus *Claxtonia* Gąsiorek & Michalczyk, 2019. *Zootaxa* **4933**:527–542. doi:10.11646/zootaxa.4933.4.4.
- Degma P, Schill RO. 2015. *Echiniscus pardalis* n. sp., a new species of Tardigrada (Heterotardigrada, Echiniscidae, *arctomys* group) from the Parco Naturale delle Alpi Marittime (NW Italy). *Zoosystema* **37**:239–249. doi:10.5252/z2015n1a12.
- Doyère M. 1840. Mémoire sur les Tardigrades. *Annal Sci Nat Zool Paris* **2**:269–362.
- Drummond AJ, Rambaut A. 2007. BEAST: Bayesian evolutionary analysis by sampling trees. *BMC Evol Biol* **7**:214. doi:10.1186/1471-2148-7-214.
- Drummond AJ, Suchard MA. 2010. Bayesian random local clocks, or one rate to rule them all. *BMC Biol* **8**:114. doi:10.1186/1741-7007-8-114.
- Ehrenberg CG. 1853. Diagnoses novarum formarum. *Ber Bekanntm geeign Verhandl Königl Preuß Akad Wissensch Berlin* **1853**:526–533.
- Ferreira MAR, Suchard MA. 2008. Bayesian analysis of elapsed times in continuous time Markov chains. *Can J Stat* **36**:355–68. doi:10.1002/cjs.5550360302.
- Ficetola GF, Mazel F, Wilfried T. 2017. Global determinants of zoogeographical boundaries. *Nat Ecol Evol* **1**:0089. doi:10.1038/s41559-017-0089.
- Fontoura P, Pilato G, Lisi O. 2010. First record of Tardigrada from São Tomé (Gulf of Guinea, Western Equatorial Africa) and description of *Pseudechiniscus santomensis* sp. nov. (Heterotardigrada: Echiniscidae). *Zootaxa* **2564**:31–42. doi:10.11646/zootaxa.2564.1.2.
- Gąsiorek P, Blagden B, Michalczyk Ł. 2019c. Towards a better understanding of echiniscid intraspecific variability: A redescription of *Nebularmis reticulatus* (Murray, 1905) (Heterotardigrada: Echiniscoidea). *Zool Anz* **283**:242–255. doi:10.1016/j.jcz.2019.08.003.

- Gąsiorek P, Jackson K, Meyer H, Zajac K, Kristensen RM, Nelson DR, Michalczyk Ł. 2019b. *Echiniscus virginicus* complex: the first case of pseudocryptic allopatry and pantropical distribution in tardigrades. *Biol J Linn Soc* **128**:789–805. doi:10.1093/biolinnean/blz147.
- Gąsiorek P, Morek W, Stec D, Michalczyk Ł. 2019a. Untangling the *Echiniscus* Gordian knot: paraphyly of the “*arctomys* group” (Heterotardigrada: Echiniscidae). *Cladistics* **35**:633–653. doi:10.1111/cla.12377.
- Gąsiorek P, Oczkowski A, Blagden B, Kristensen RM, Bartels PJ, Nelson DR, Suzuki AC, Michalczyk Ł. 2021a. New Asian and Nearctic *Hypechiniscus* species (Heterotardigrada: Echiniscidae) signalize a pseudocryptic horn of plenty. *Zool J Linn Soc* **192**:794–852. doi:10.1093/zoolinnean/zlaa110.
- Gąsiorek P, Vončina K, Ciosek J, Veloso M, Fontoura P, Michalczyk Ł. 2021b. New Indomalayan *Nebularmis* species (Heterotardigrada: Echiniscidae) provoke a discussion on its intrageneric diversity. *Zool Lett* **7**:6. doi:10.1186/s40851-021-00172-0.
- Gąsiorek P, Vončina K, Michalczyk Ł. 2020. An overview of the sexual dimorphism in *Echiniscus* (Heterotardigrada, Echiniscoidea), with the description of *Echiniscus masculinus* sp. nov. (the *virginicus* complex) from Borneo. *Zoosyst Evol* **96**:103–113. doi:10.3897/zse.96.49989.
- Gąsiorek P, Vončina K, Zajac K, Michalczyk Ł. 2021c. Phylogeography and morphological evolution of *Pseudechiniscus* (Heterotardigrada: Echiniscidae). *Sci Rep* **11**:7606. doi:10.1038/s41598-021-84910-6.
- Grobys D, Roszkowska M, Gawlak M, Kmita H, Kepel A, Kepel M, Parnikoza I, Bartylak T, Kaczmarek Ł. 2020. High diversity in the *Pseudechiniscus suillus-facettalis* complex (Heterotardigrada: Echiniscidae) with remarks on the morphology of the genus *Pseudechiniscus*. *Zool J Linn Soc* **188**:733–752. doi:10.1093/zoolinnean/zlzl71.
- Guil N, Giribet G. 2009. Fine scale population structure in the *Echiniscus blumi-canadensis* series (Heterotardigrada, Tardigrada) in an Iberian mountain range—When morphology fails to explain genetic structure. *Mol Phyl Evol* **51**:606–613. doi:10.1016/j.ympev.2009.02.019.
- Hall TA. 1999. BioEdit: a user-friendly biological sequence alignment editor and analysis program for Windows 95/98/NT. *Nucleic Acids Symp Ser* **41**:95–98.
- He J, Gao Z, Su Y, Lin S, Jiang H. 2018. Geographical and temporal origins of terrestrial vertebrates endemic to Taiwan. *J Biogeogr* **45**:2458–2470. doi:10.1111/jbi.13438.
- Hoang DT, Chernomor O, von Haeseler A, Minh BQ, Vinh LS. 2018. UFBoot2: Improving the ultrafast bootstrap approximation. *Mol Biol Evol* **35**:518–522. doi:10.1093/molbev/msx281.
- Ito M. 1990. A new species of the genus *Itaquascon* (Eutardigrada: Hypsibiidae) from Taiwan. *Edaphologia* **43**:1–4.
- Ito M. 1993. Taxonomic study on the class Heterotardigrada (Tardigrada) from the northern slope of Mt. Fuji, Central Japan. *Edaphologia* **50**:1–13.
- Kaczmarek Ł, Michalczyk Ł. 2010. The genus *Echiniscus* Schultze 1840 (Tardigrada) in Costa Rican (Central America) rain forests with descriptions of two new species. *Trop Zool* **23**:91–106.
- Kalyaanamoorthy S, Minh BQ, Wong TKF, von Haeseler A, Jermini LS. 2017. ModelFinder: Fast model selection for accurate phylogenetic estimates. *Nat Methods* **14**:587–589. doi:10.1038/nmeth.4285.
- Katoh K, Misawa K, Kuma K, Miyata T. 2002. MAFFT: a novel method for rapid multiple sequence alignment based on fast Fourier transform. *Nucleic Acids Res* **30**:3059–3066. doi:10.1093/nar/gkf436.
- Katoh K, Toh H. 2008. Recent developments in the MAFFT multiple sequence alignment program. *Brief Bioinform* **9**:286–298. doi:10.1093/bib/bbn013.
- Kiosya Y, Vončina K, Gąsiorek P. 2021. Echiniscidae in the Mascarenes: the wonders of Mauritius. *Evol Syst* **5**:93–120. doi:10.3897/evolsyst.5.59997.
- Kristensen RM. 1987. Generic revision of the Echiniscidae (Heterotardigrada), with a discussion of the origin of the family. *In: Bertolani R (ed) Biology of tardigrades. Selected Symposia and Monographs U.Z.I., Modena, Italy, pp. 261–335.*
- Kumar S, Stecher G, Tamura K. 2016. MEGA7: molecular evolutionary genetics analysis version 7.0 for bigger datasets. *Mol Biol Evol* **33**:1870–1874. doi:10.1093/molbev/msw054.
- Lanfear R, Frandsen PB, Wright AM, Senfeld T, Calcott B. 2017. PartitionFinder 2: new methods for selecting partitioned models of evolution for molecular and morphological phylogenetic analyses. *Mol Biol Evol* **34**:772–773. doi:10.1093/molbev/msw260.
- Li X, Li H. 2008. Tardigrades from Taiwan, with the description of a new species of *Doryphoribius* (Tardigrada, Hypsibiidae). *Zool Sci* **25**:554–559. doi:10.2108/zsj.25.554.
- Li X, Wang D-Y, Wang L-Z. 2008. The Tardigrada fauna of Hainan Island (Asia: China) with descriptions of two new species. *Raff Bull Zool* **56**:293–305.
- Li X, Wang L-Z, Yu D. 2007. The Tardigrada fauna of China with descriptions of three new species of Echiniscidae. *Zool Stud* **46**:135–147.
- Marcus E. 1927. Zur Anatomie und Ökologie mariner Tardigraden. *Zool Jahr Abt System* **53**:487–558.
- Mathews GB. 1936–37. Tardigrada from Japan. *Peking Nat Hist Bull* **11**:411–412.
- McInnes SJ. 1994. Zoogeographic distribution of terrestrial/freshwater tardigrades from current literature. *J Nat Hist* **28**:257–352. doi:10.1080/00222939400770131.
- Michalczyk Ł, Kaczmarek Ł. 2013. The Tardigrada Register: a comprehensive online data repository for tardigrade taxonomy. *J Limnol* **72**:175–181. doi:10.4081/jlimnol.2013.s1.e22.
- Mihelčič F. 1951. Beitrag zur Systematik der Tardigraden. *Arch Zool Ital* **36**:57–103.
- Mihelčič F. 1955. Zwei neue Tardigradenarten aus Spanien. *Zool Anz* **155**:309–311.
- Moon SY, Kim W. 1990. A new species of *Echiniscus* (Tardigrada: Echiniscidae) from Korea. *Korean J Syst Zool* **6**:231–234.
- Moon SY, Kim W. 1994. New species of *Echiniscus* (Heterotardigrada: Echiniscoidea: Echiniscidae) from Korea. *Proc Biol Soc Wash* **107**:511–513.
- Morek W, Michalczyk Ł. 2020. First extensive multilocus phylogeny of the genus *Milnesium* (Tardigrada) reveals no congruence between genetic markers and morphological traits. *Zool J Linn Soc* **188**:681–693. doi:10.1093/zoolinnean/zlz040.
- Murray J. 1905. The Tardigrada of the Scottish Lochs. *Trans Roy Soc Edinburgh* **41**:677–698. doi:10.1017/S0080456800035547.
- Murray J. 1907. Scottish Tardigrada, collected by the lake survey. *Trans Roy Soc Edinburgh* **45**:641–668. doi:10.1017/S0080456800011777.
- Murray J. 1910. Part V. Tardigrada. Reports on the Scientific Investigations **1**:83–187.
- Nguyen L-T, Schmidt HA, von Haeseler A, Minh BQ. 2015. IQ-TREE: A fast and effective stochastic algorithm for estimating maximum likelihood phylogenies. *Mol Biol Evol* **32**:268–274. doi:10.1093/molbev/msu300.
- Päckert M, Martens J, Sun Y-H, Severinghaus LL, Nazarenko AA, Ting J, Töpfer T, Tietze DT. 2012. Horizontal and elevational phylogeographic patterns of Himalayan and Southeast Asian forest passerines (Aves: Passeriformes). *J Biogeogr* **39**:556–573. doi:10.1111/j.1365-2699.2011.02606.x.
- Petersen B. 1951. The tardigrade fauna of Greenland. *Medd Grøn*

- 150:1–94.
- Pilato G, Fontoura P, Lisi O. 2008b. New description of *Echiniscus viridis* Murray, 1910 and remarks on the *viridis* group. *New Zeal J Zool* **35**:85–92. doi:10.1080/03014220809510105.
- Pilato G, Fontoura P, Lisi O, Beasley C. 2008a. New description of *Echiniscus scabrospinosus* Fontoura, 1982, and description of a new species of *Echiniscus* (Heterotardigrada) from China. *Zootaxa* **1856**:41–54. doi:10.11646/zootaxa.1856.1.4.
- Pleijel F, Jondelius U, Norlinder E, Nygren A, Oxelman B, Schander C, Sundberg P, Thollesson M. 2008. Phylogenies without roots? A plea for the use of vouchers in molecular phylogenetic studies. *Mol Phyl Evol* **48**:369–371. doi:10.1016/j.ympev.2008.03.024.
- Qiao P, Zhang P, Sun X, Li X. 2013. *Echiniscus semifoveolatus* (Heterotardigrada: Echiniscidae), a newly recorded species from China. *Zootaxa* **3718**:183–192. doi:10.11646/zootaxa.3718.2.6.
- Ramazzotti G. 1959. Il gruppo dell'*Echiniscus viridis* con la nuova specie *E. perviridis* e *Macrobotus pustulatus* altra nuova specie (Tardigrada). *Atti Soc Ital Sci Nat Mus Civ Stor Nat Milano* **98**:303–309.
- Rambaut A, Suchard MA, Xie D, Drummond AJ. 2014. Tracer v.1.6. Available at: <http://beast.bio.ed.ac.uk/Tracer>. Accessed 17 May 2021.
- Richters F. 1903. Nordische Tardigraden. *Zool Anz* **27**:168–172.
- Richters F. 1904. Beitrag zur Verbreitung der Tardigraden im südlichen Skandinavien und an der mecklenburgischen Küste. *Zool Anz* **28**:347–352.
- Richters F. 1907. Zwei neue *Echiniscus*-Arten. *Zool Anz* **31**:197–202.
- Richters F. 1911. Südamerikanische Tardigraden. *Zool Anz* **38**:273–277.
- Richters F. 1926. Tardigrada. In: Kükenthal W & Krumbach T (eds) *Handbuch der Zoologie*. Vol. 3. Walter de Gruyter & Co., Berlin and Leipzig, pp. 58–61.
- Riggin GT. 1962. Tardigrada of Southwest Virginia: with the addition of a description of a new marine species from Florida. Virginia Agricultural Experimental Station, Technical Bulletin **152**:1–145.
- Ronquist F. 1997. Dispersal-vicariance analysis: A new approach to the quantification of historical biogeography. *Syst Biol* **46**:195–203. doi:10.1093/sysbio/46.1.195.
- Ronquist F, Huelsenbeck JP. 2003. MrBayes 3: Bayesian phylogenetic inference under mixed models. *Bioinformatics* **19**:1572–1574. doi:10.1093/bioinformatics/btg180.
- Roszkowska M, Grobys D, Bartylak T, Gawlak M, Kmita H, Kepel A, Kepel M, Parnikoza I, Kaczmarek Ł. 2020. Integrative description of five *Pseudechiniscus* species (Heterotardigrada: Echiniscidae: the *suillus-facettalis* complex). *Zootaxa* **4763**:451–484. doi:10.11646/zootaxa.4763.4.1.
- Sato T, Suzuki AC. 2020. Two interesting records of genus *Echiniscus* (Heterotardigrada) from Mt. Hodosan, Nagatoro, Japan. *Hiyoshi Rev Nat Sci* **67**:35–41.
- Schultze CAS. 1840. *Echiniscus Bellermanni*; animal crustaceum, *Macroboto Hufelandii* affine. Apud G. Reimer, Berolini, 8 pp.
- Séméria Y. 1994. Une espèce nouvelle de tardigrade de Taiwan: *Echiniscus pseudelegans*, n. sp. (Heterotardigrada Echiniscidae). *Bull Mens Soc Linn Lyon* **63**:28–30.
- Shih H-T, Hung H-C, Schubart CD, Chen CA, Chang H-W. 2006. Intraspecific genetic diversity of the endemic freshwater crab *Candidiopotamon rathbunae* (Decapoda, Brachyura, Potamidae) reflects five million years of the geological history of Taiwan. *J Biogeogr* **33**:980–989. doi:10.1111/j.1365-2699.2006.01472.x.
- Stec D, Kristensen RM, Michalczyk Ł. 2020. An integrative description of *Minibiotus ioculator* sp. nov. from the Republic of South Africa with notes on *Minibiotus pentannulatus* Londoño et al., 2017 (Tardigrada: Macrobiotidae). *Zool Anz* **286**:117–134. doi:10.1016/j.jcz.2020.03.007.
- Stec D, Smolak R, Kaczmarek Ł, Michalczyk Ł. 2015. An integrative description of *Macrobotus paulinae* sp. nov. (Tardigrada: Eutardigrada: Macrobiotidae: *hufelandi* group) from Kenya. *Zootaxa* **4052**:501–526. doi:10.11646/zootaxa.4052.5.1.
- Sugiura K, Minato H, Matsumoto M, Suzuki AC. 2020. *Milnesium* (Tardigrada: Apochela) in Japan: The first confirmed record of *Milnesium tardigradum* s.s. and description of *Milnesium pacificum* sp. nov. *Zool Sci* **37**:476–495. doi:10.2108/zs190154.
- Sun X, Li X, Feng W. 2014. Two new species of Tardigrada (Echiniscidae, Hypsibiidae) from China. *Proc Biol Soc Wash* **126**:323–328. doi:10.2988/0006-324X-126.4.323.
- Suzuki AC. 2017. Tardigrade research in Japan. In: Motokawa M & Kajihara H (eds) Chapter 10. Species diversity of animals in Japan. Diversity and commonality in animals, Springer, Tokyo, pp. 267–284. doi:10.1007/978-4-431-56432-4_10.
- Suzuki AC, Heard L, Sugiura K. 2018. Terrestrial tardigrades from Mikurajima Island (the first report). *Mikurensis* **7**:3–8.
- Thulin G. 1911. Beiträge zur Kenntnis der Tardigradenfauna Schwedens. *Ark Zool* **7**:1–60. doi:10.5962/bhl.part.1270.
- Thulin G. 1928. Über die Phylogenie und das System der Tardigraden. *Hereditas* **11**:207–266. doi:10.1111/j.1601-5223.1928.tb02488.x.
- Trifinopoulos J, Nguyen L-T, von Haeseler A, Minh BQ. 2016. W-IQ-TREE: a fast online phylogenetic tool for maximum likelihood analysis. *Nucleic Acids Res* **44**:232–235. doi:10.1093/nar/gkw256.
- Tumanov DV. 2020. Analysis of non-morphometric morphological characters used in the taxonomy of the genus *Pseudechiniscus* (Tardigrada: Echiniscidae). *Zool J Linn Soc* **188**:753–775. doi:10.1093/zoolinnean/zlzo97.
- Vaidya G, Lohman DJ, Meier R. 2011. SequenceMatrix: concatenation software for the fast assembly of multi-gene datasets with character set and codon information. *Cladistics* **27**:171–180. doi:10.1111/j.1096-0031.2010.00329.x.
- Vončina K, Kristensen RM, Gąsiorek P. 2020. *Pseudechiniscus* in Japan: re-description of *Pseudechiniscus asper* Abe et al., 1998 and description of *Pseudechiniscusshintai* sp. nov. *Zoosyst Evol* **96**:527–536. doi:10.3897/zse.96.53324.
- Wang L, Xue J, Li X. 2018. A description of *Pseudechiniscus xiai* sp. nov., with a key to genus *Pseudechiniscus* in China. *Zootaxa* **4388**:255–264. doi:10.11646/zootaxa.4388.2.7.
- Xue J, Li X, Wang L, Xian P, Chen H. 2017. *Bryochoerus liupanensis* sp. nov. and *Pseudechiniscus chengi* sp. nov. (Tardigrada: Heterotardigrada: Echiniscidae) from China. *Zootaxa* **4291**:324–334. doi:10.11646/zootaxa.4291.2.5.
- Yin H, Li X. 2011. New records of tardigrades (Tardigrada) from Taiwan. *J Shaanxi Normal Univ Nat Sci Ed* **39**:55–59.
- Yu H-T. 1995. Patterns of diversification and genetic population structure of small mammals in Taiwan. *Biol J Linn Soc* **55**:69–89. doi:10.1016/0024-4066(95)90029-2.
- Yu Y, Blair C, He XJ. 2020. RASP 4: Ancestral state reconstruction tool for multiple genes and characters. *Mol Biol Evol* **37**:604–606. doi:10.1093/molbev/msz257.
- Yu Y, Harris AJ, Blair C, He XJ. 2015. RASP (Reconstruct Ancestral State in Phylogenies): a tool for historical biogeography. *Mol Phyl Evol* **87**:46–49. doi:10.1016/j.ympev.2015.03.008.